ISTANBUL TECHNICAL UNIVERSITY ★ GRADUATE SCHOOL

RIDE QUALITY EVALUATION METHODS FOR OFF-ROAD VEHICLES

M.Sc. THESIS

Hande TÜTÜNCÜ ÇALKAN

Department of Mechanical Engineering

Automotive Engineering Programme

FEBRUARY 2022

ISTANBUL TECHNICAL UNIVERSITY ★ GRADUATE SCHOOL

RIDE QUALITY EVALUATION METHODS FOR OFF-ROAD VEHICLES

M.Sc. THESIS

Hande TÜTÜNCÜ ÇALKAN
(503181717)

Department of Mechanical Engineering

Automotive Engineering Programme

Thesis Advisor: Prof. Dr. Özgen AKALIN

FEBRUARY 2022

ISTANBUL TEKNİK ÜNİVERSİTESİ ★ LİSANSÜSTÜ EĞİTİM ENSTİTÜSÜ

YOL DIŞI TAŞITLAR İÇİN SÜRÜŞ KALİTESİ DEĞERLENDİRME YÖNTEMLERİ

YÜKSEK LİSANS TEZİ

Hande TÜTÜNCÜ ÇALKAN
(503181717)

Makina Mühendisliği Anabilim Dalı

Otomotiv Programı

Tez Danışmanı: Prof. Dr. Özgen AKALIN

ŞUBAT 2022

Hande TÜTÜNCÜ ÇALKAN, a M.Sc student of ITU Graduate School student ID 503181717, successfully defended the thesis entitled "RIDE QUALITY EVALUATION METHODS FOR OFF-ROAD VEHICLES", which she prepared after fulfilling the requirements specified in the associated legislations, before the jury whose signatures are below.

Thesis Advisor :	**Prof. Dr. Özgen AKALIN** İstanbul Technical University	....
Jury Members :	**Assis. Prof. Dr. Osman Taha ŞEN** Istanbul Technical University	....
	Assis. Prof. Dr. Erdem UZUNSOY Bursa Technical University	....

Date of Submission : 14 January 2022
Date of Defense : 10 February 2022

To my family,

FOREWORD

I would like to thank my thesis advisor Prof. Dr. Özgen Akalın for his constant support and encouragement in the course of this study. Also, I would like to thank Research Assistant Halil Yahya Yeşilyurt for his contributions to developing MATLAB scripts to calculate the ride quality metrics.

This study was a part of "Vehicle Ride Quality Performance Specification" effort in "AVT-308 Cooperative Demonstration of Technology (CDT) for Next-Generation NATO Reference Mobility Model (NG-NRMM)" led by Dr. Xiaobo Yang of Oshkosh Corporation. His guidance throughout this work is greatfully acknowledged.

The MSC Software Corporation kindly provided the MSC ADAMS Car model for the FED-Alpha vehicle. In addition, I would like to thank BİAS Mühendislik and Hexagon for offering MSC software academic licenses.

Last but not least, I would like to thank my beloved family who has always supported me.

February 2022

Hande TÜTÜNCÜ ÇALKAN
Mechanical Engineer

TABLE OF CONTENTS

Page

ABBREVIATIONS

AAP	: Average Absorbed Power
Acc	: Acceleration
BS	: British Standard
CDT	: Cooperative Demonstration of Technology
EC	: European Commission
eVDV	: Estimated Vibration Dose Value
FFT	: Fast Fourier Transform
GPS	: Global Positioning System
ISO	: International Organization for Standardization
TOP	: Test Operations Procedure
Rms	: Root Mean Square
RMQ	: Root Mean Quad
IRI	: International Roughness Index
MTVV	: Maximum Transient Vibration Value
NATO	: North Atlantic Treaty Organization
NG-NRMM	: Next-Generation NATO Reference Mobility Model
ORV	: Overall Ride Value
PSD	: Power Spectral Density
SAE	: Society of Automotive Engineers
UTACV	: Urban Tracked Air Cushion Vehicle
VDV	: Vibration Dose Value
WL	: Wavelength

SYMBOLS

a_w	: Weighted acceleration (translational or rotational) as a function of time (time history), in m/s2 or rad/s2, respectively
A_i	: Rms acceleration in ft/sec^2 within the ith spectral band
c	: Damping coefficient
f_i	: Frequency weighting factors
g_{rms}	: The overall root-mean-square value of acceleration for a selected frequency band
Gd(n), Gd(Ω)	: Displacement power spectral density, m^3
G_1(.)	: PSD of track 1
G_2(.)	: PSD of track 2
G_{12}(.)	: Cross spectrum between tracks 1 and 2
k_s	: Suspension stiffness
k_t	: Tire stiffness
N	: Spatial frequency, cycles/m
m_s	: Sprung mass
m_u	: Unsprung mass
Hz	: Hertz
P	: Absorbed Power, Watt
t	: Time
W_i	: Frequency, radians/second
w	: Waviness
y_0(t)	: Displacement come from ground
y_1(t)	: Unsprung mass displacement
y_2(t)	: Sprung mass displacement
Ω	: Angular spatial frequency, rad/m, wavenumber
λ	: Wavelength, m
γ^2	: Coherence function

LIST OF TABLES

LIST OF FIGURES

Page

RIDE QUALITY EVALUATION METHODS FOR OFF-ROAD VEHICLES

SUMMARY

Analyses were made on the FED-Alpha vehicle model using the ADAMS Car program to observe the effect of road characteristics on ride quality. The vehicle was developed by Ricardo Inc. as a fuel-efficient all-terrain military vehicle. The FED-Alpha is a 4x4 wheeled vehicle and the front and rear axles have an independent double-wishbone suspension system. The suspension system has air bellows and titanium helical springs and dampers. The dampers give different damping characteristics at low and high frequencies.

In the ride quality evaluation standards, the constraints of analysis or test have been determined. The constraints mentioned were discussed and analysis studies were performed with these constraints. For example, speed deviation, which is one of the absorbed power method constraints, is examined and the effect of this value on ride quality is examined by exceeding the restricted value. Analyses were made by collecting data on three axes at three different vehicle locations.

Waviness, phase angle, wavenumber, wavelength and roughness were chosen as the road parameters to examine ride quality effects.

Synthetic roads were created by changing the road parameter to be examined. Synthetic roadways were modeled in a format that could be analyzed with ADAMS Car.

Absorbed power, vibration dose value, and frequency weighted rms acceleration methods were used for ride quality evaluation in the scope of this thesis. Absorbed power was calculated with the transfer function and the FFT method, and the different results between the two methods were examined. Since the difference in results was negligible, the calculations continued with the transfer function. MATLAB and SIMULINK software were used simultaneously in the ride quality evaluation method calculations. The acceleration data was collected from the driver seat base, passenger seat base, and middle point of the rear passenger seat base. Acceleration data were exported from the ADAMS Car. With the help of MATLAB code, the tab files were imported to SIMULINK and the acceleration data was passed through transfer functions. Obtained results are converted into graphics with the help of MATLAB.

Analyses were made between the speed of 8,05 km/h and 24 km/h to determine vehicle 6-Watt speed in the z-axis on synthetic roads. First, the found absorbed power values are plotted in the speed domain. Then, 6-Watt speed was determined by fitting a second-degree polynomial to the plotted graph in the speed domain. Finally, using the fitted second-degree polynomial, 6-Watt speed was calculated. Using the same second-degree polynomial calculation model, the vibration dose value and frequency weighted rms acceleration values corresponding to the 6-watt speed were calculated. The purpose of comparing these values is to determine how other methods evaluate the 6-watt ride quality limit defined in the absorbed power method. A higher correlation rate was detected with frequency weighted rms acceleration and a slightly lower correlation with vibration dose value.

Ride quality result graphs were plotted in three axes by analyzing four rms roughness values. As the road rms roughness value increases, all vibration evaluation values in the z-axis increase. This result means that ride quality deteriorated in the z-axis due to

roughness. It has been determined that the ride quality decreases depending on the increasing speed. It has been observed that the absorbed power values are most affected by the change of vehicle speed in the z-axis. It has been determined that with the increase of the road rms roughness, the ride quality decreases in the x and y axes. But the change is not continuously increasing depending on the speed.

Analyses were made at three different waviness values and ride quality graphs were plotted for each axis. As the waviness increase, the ride quality increase in the z-axis. The ride quality decrease depending on the speed increase. No change was detected in the ride quality in the y-axis depending on the waviness change. The decrease in the waviness led to a decrease in the ride quality in the x-axis. Still, no correlation could be observed in the change depending on the speed in the x-axis.

Analyses were made on roads with four different wavenumber bandwidths. It is observed that the ride quality change as the wavenumber bandwidth change in the z-axis. The ride quality increase on wider bandwidth at low wavenumber range. The ride quality increase on narrow bandwidth at high wavenumber range at low speed. The ride quality increase on narrow bandwidth at high wavenumber range at high speed. As the speed increases, the ride quality in the z-axis decrease, but it has been observed that the slope of the speed-related increases differs on the roads with different wavenumber bandwidths. It was determined that one of the parameters affecting the ride quality in the x and y axes is the wavenumber bandwidth, but no correlation could be detected.

Analyzes were made on the road with four different phase angles. It has been determined that as the phase angle increases, the ride quality in the z-axis increase. As the speed increases, the ride quality values in the z-axis decrease. As the phase angle increases, the ride quality on the y-axis decrease. It is evaluated that the ride quality decrease is the roll motion caused by the opposite movement of the right and left wheel. It was observed that the phase angle change in the x-axis did not have much effect on the ride quality.

Analyzes were made at different speed profiles on the 5,08 cm rms roughness road. As a result, it has been determined that even if the speed deviation factor specified in the standard is exceeded and the average speed is maintained and driven for approximately 300 meters, the absorbed power values in the z-axis will not change. However, this result needs to be supported by the results of the analysis to be made in different vehicles.

When the ride quality evaluation methods are compared, it has been determined that the absorbed power will give the most sensitive results changing by vehicle speed. It is considered that the absorbed power, vibration dose value and frequency weighted rms acceleration methods will be sufficient for the evaluation of the ride quality in the z-axis. However, it is thought that it is necessary to include the suspension and wheel parameters in the x and y-axis evaluations.

YOL DIŞI TAŞITLAR İÇİN SÜRÜŞ KALİTESİ DEĞERLENDİRME YÖNTEMLERİ

ÖZET

Yol parametrelerinin sürüş konforuna etkisini incelemek amacıyla ADAMS Car programı kullanılarak yol dışı taşıt olan FED-Alpha araç modeli ile analizler yapılmıştır. FED-Alpha aracı ön ve arka akslarında çift salıncaklı süspansiyon kolları bulunan 4 tekerlekli arazi aracıdır. Süspansiyon sisteminde yaylanma görevi için hava körükleri ile titanyum helisel yay beraber kullanılmış, sönümleme için düşük ve yüksek frekanslarda farklı tepkiler veren damper kullanılmıştır. Araç yakıt verimliliği yüksek arazi askeri aracı olarak geliştirilmiştir. Süspansiyon hava körükleri aracın sürüş yüksekliğinin korunmasında önemli role sahiptir. Damper özellikle zorlu arazi koşullarında aracın sürüş kalitesini iyileştirilmesi konusunda önemli role sahiptir.

Araç sürüş kalitesi geliştirilmesi aşamasında tasarımcılar karşılaştırılabilir analizlere ihtiyaç duymaktadır. Bu analizler günümüzde tasarım aşamasında ADAMS Car gibi programlarla yapılabilmektedir. Tekrarlanabilir analizlerin yapılabilmesi tasarım optimizasyonunda hızlı sonuçlar elde edilmesine yaramaktadır. Tekrarlanan analizlerin karşılaştırılabilir olması için metotlarının yeterli kısıtlar ile kısıtlanmış olması gerekmektedir. Benzer araçlar ile performans kıyaslamasında yapılmasında yapılan analizlerin aynı tanımlanmış yollarda yapılması gerekmektedir. Bunu sağlayabilmek için standartlarda yol ile ilgili sürüş kalitesini değiştirecek parametrelerin kısıtlanması gerekmektedir.

Etkisini incelemek istenen yol parametreleri olarak dalgalılık (waviness), faz açısı (phase angle), dalga sayısı (wavenumber), dalga boyu (wavelength) ve pürüzlülük (roughness) seçilmiştir. Sürüş kalitesi değerlendirmek amacıyla standartlarında bahsi geçen kısıtlar incelenmiş ve analiz çalışmaları bu kısıtlar çerçevesinde oluşturulmuştur ve bu kısıtların etkisi encilenmiştir. Bu kısıtlardan biri olan hız profili, standartta tarif edilen ortalama hızın değişimi değeri 0,1 limitlerinin dışarına çıkarılıp 0,15 değerinde analiz edilmiş ve sonuçları değerlendirilmiştir. Analizler aracın üç farklı konumunda üç eksende data toplanarak yapılmıştır.

İncelenmek istenen yol parametresinin incelenmek istenen değeri değiştirilip diğer yol parametreleri sabit tutularak sentetik yollar oluşturulmuştur. Sentetik yollar ADAMS Car ile analiz yapılabilecek formata getirilmiştir. ADAMS Car modelinin düzgün çalıştığından emin olunabilmek için FED-Alpha aracının daha önce yapılmış test sonuçları incelenerek karşılaştırılmıştır. Karşılaştırma sonucunda sonuçların birbirine yeterince yakın olduğundan emin olunduğunda sentetik yol analizlerine geçilmiştir.

Sürüş konforu değerlendirme metodu olarak absorbe edilen güç (absorbed power), titreşim doz değeri (vibration dose value) ve ağırlıklandırılmış frekans rms ivmelenme (frequency weighted rms acceleration) metodu kullanılmıştır. Absorbe edilen güç hem transfer fonksiyonu hem hızlı Fourier dönüşümü (FFT, Fast Fourier Transform) metodu ile hesaplanarak, iki metodun arasındaki korelasyon incelenmiştir. İnceleme sonucunda korelasyon üç eksen için yüksek çıktığı için transfer fonksiyonu ile hesaplama çalışmaları devam etmiştir. Değerlendirme metodu hesaplarında eş zamanlı olarak MATLAB ve SIMULINK yazılımları kullanılmıştır. Analizler ile aracın sürücü koltuğu bağlantı bölgesinden, ön yolcu koltuğu bağlantı bölgesinden ve arka yolcu koltuğu bağlantı bölgesi orta konumlarından toplanan ivme dataları tab dosyası

şeklinde ADAMS Car analiz ortamından dışarıya çıkarılmıştır. MATLAB kodu yardımıyla tab dosyası SIMULINK'e aktarılarak ivme datası belli TARADCOM transfer fonksiyonlarından geçirilir. Üç eksen için elde edilen sonuçlar MATLAB yardımıyla grafiklere dönüştürülmektedir.

Analiz sonuçlarının irdelenmesine yardımcı olması için eş zamanlı olarak ADAMS Car modelinden araç hızı, direksiyon açısı, aracın ağırlık merkezinin y ve z eksenindeki yer değiştirmesi, şasi yunuslama ve yuvarlanma açıları ve ivme dataları kayıt altına alınmıştır.

ADAMS Car'dan toplanan zaman eksenindeki ivme değerleri her yöntemin tarif edildiği standarttaki ağırlıklandırma değerleri ile ağırlıklandırılmıştır. Bu değerlerin etkisi sentetik yolları analizlerinde değerlendirilmiştir.

Absorbe edilen güç değerlendirme yöntemi standardında maksimum insan vücudunun dayanabileceği gücün 6-Watt olduğu tariflenmektedir. Aracın sentetik yollarda z ekseninde hangi hızda 6-Watta ulaştığını tespit etmek amacıyla 8,05 km/h ile 24 km/h hızları arasında analizler yapılmıştır. Bulunan sonuçlar hız eksenindeki grafiği çizilmiştir. Çizilen grafiğe ikinci dereceden polinom uydurularak 6-Watta geldiği hız değeri tespit edilmiştir. 6-Watt değeri ile diğer değerlendirme metotlarında tanımlanan konfor parametreleri arasındaki korelasyonu incelemek için aynı işlem titreşim doz değeri ve ağırlıklandırılmış frekans rms ivmelenme metoduna da uygulanmıştır. 6-Watt değerine karşıklık gelen titreşim doz değeri ve ağırlıklandırılmış frekans rms ivmelenme değerleri ilgili standartta tariflenen konfor limitleri ile değerlendirilmiştir. Değerlendirme sonucunda ağırlıklandırılmış frekans rms ivmelenme ile yüksek oranda titreşim doz değeri ile kısmen daha düşük oranda korelasyon tespit edilmiştir.

Dört farklı rms pürüzlülük değerinde analizler yapılarak her eksen için grafikler oluşturulmuştur. Yolun rms pürüzlülük değerine arttıkça z ekseni için tüm değerlendirme metotlarının da değeri artmaktadır. Bu da sürüş konforunun z ekseninde bozulduğu anlamına gelmektedir. Grafiklerde artan hıza bağlı olarak sürüş konforunun azaldığı tüm değerlendirme metotlarında tespit edilmiştir. Hızın değişiminden en fazla etkilenen değerlendirme metodunun absorbe edilen güç olduğu görülmüştür. Yolun rms pürüzlülük değerinin artması ile x ve y eksenlerinde sürüş konforunun azaldığı tespit edilmiştir. Fakat hıza bağlı olarak değişim her zaman artış eğiliminde değildir.

Dalgalılık değeri PSD grafiğinin ters eğimidir. Üç farklı dalgalılık değerlerinde analizler yapılarak her eksen için grafikler oluşturulmuştur. Dalgalılık değeri arttıkça z ekseninde tüm değerlendirme metotlarının da değeri azalmakta yani konfor artmaktadır. Hızın artışına bağlı olarak tüm konfor parametrelerinin değeri artmakta, konfor düşmektedir. Dalgalılık değişimine bağlı olarak y eksenindeki konforda bir değişiklik tespit edilememiştir. Dalgalılık değerinin azalması ile x eksenindeki tüm değerlendirme metotların değerinde artış gözlenmiştir fakat hıza bağlı değişimde korelasyon kurulamamıştır. Temel olarak dalgalılık değerinin değişikliği ile en fazla etkilenen eksenin z olması beklenmektedir. Analiz sonuçları bu öngörüyü doğrular niteliktedir.

Dört farklı dalga sayısı bant genişliğine sahip yollarda analizler yapılmıştır. Dalga sayısı bant genişliği değiştikçe z eksenindeki konforun etkilendiği gözlemlenmektedir. Hız arttıkça z eksenindeki konfor düşmektedir fakat farklı dalga sayısı bant genişliğine sahip yollarda hıza bağlı artışların eğimi farklılık gösterdiği görülmüştür. x ve y eksenlerindeki konforu etkileyen parametrelerden birinin dalga boyu bant genişliği olduğu tespit edilmiş ancak korelasyon tespit edilememiştir.

Dalga sayısı bant genişliğinin hız ekseninde incelenmesi çok kolay görülmemektedir. Z ekseninde yapılan analizler sonucunda düşük dalga sayısı bant bölgesinde konfor hissindeki etkisinin az olduğu tespit edilmiştir. Yüksek dalga sayısı bant bölgesindeki güç etkisinin konfor parametrelerine etkisinin yüksek olduğu gözlemlenmiştir. Yolun PSD datası düşük dalga sayısı bant aralığındaki komponentleri kapsadığı durumda sürüş konforu değerlendirme metotları değerleri azalmaktadır. Bunun nedeninin düşük dalga sayısı bant aralığındaki komponentlerin yolun sertliğini azalması olarak değerlendirilebilir. Yolun PSD datası yüksek dalga boyu bant aralığındaki komponentleri kapsamadığı durumda düşük hızlarda sürüş konforu değerlendirme metotları değerleri düşüktür fakat aracın hızına karşı daha sürüş konforu değerlendirme metotları değerleri daha yüksek artış trendine sahiptir. Yüksek dalga sayısı bant bölgesinde güç etkisi az olan yolların hıza bağlı değişimden daha fazla etkilendiği gözlenmiştir. Aracın hızı arttıkça sürücüye gelen ivmelerin en yüksek tepe nokta değeri daha düşük frekans bandına kaymaktadır.

Dört farklı faz açısına sahip yolda analizler yapılmıştır. Faz açısı değeri arttıkça x eksenindeki konfor parametrelerinin iyileştiği tespit edilmiştir. Hız arttıkça z eksenindeki konfor hissi azalmaktadır. Faz açısı arttıkça y eksenindeki değerlendirme metotlarının değeri artmakta konfor hissi kötüleşmektedir. Bunun sebebinin sürücünün aracı düz bir çizgide sürmeye çalışırken ortaya çıkan yanal kuvvetler olduğu değerlendirilmiştir. x yönündeki konfora faz açısı değişiminin çok etkisi olmadığı gözlemlenmiştir.

Faz açısının etkisi aracın farklı bölgelerinden toplanan değerlerle incelenmiş ve karşılaştırılmıştır. Düşük faz açısına sahip sentetik yollarda aracın arka yolcu koltuğundaki konfor değerinin en düşük olduğu, en yüksek konforun ön yolcu koltuğundan olduğu tespit edilmiştir. Yolun faz farkı arttıkça arka yolcu koltuğunun konforu iyileşmektedir. Faz açısı 180° olan yani sağ ve sol tekerlerin birbiri ile zıt hareket ettiği yolda arka sürüvü koltuğundaki konfor çok yüksektir. Bunun sebebinin ivme toplanan konumun arka koltuğun tam ortası olmasıdır. İki lastiğin birbirine zıt hareketi buraya gelen kuvveti ve yer değiştirmeyi azaltmaktadır.

5,08 cm rms pürüzlülüğe sahip yolda farklı hız profillerinde analizler yapılmıştır. Standartta belirtilen ortalama hızdan sapma faktörü aşıldığı durumda bile eğer ortalama hız korunur ve yaklaşık 300 metre sürülürse z eksenindeki absorbe edilen güç değerlerinin değişmeyeceği tespit edilmiştir. Fakat farklı araç modellerinde bu analizler yapılmalı sonuç doğrulanmalıdır. Bu durumda bile test şartlarını kolaylaştırılamayacağı düşünülmektedir.

Metotlar birbiri ile karşılaştırıldığında absorbe edilen güç, aracın hız değişimine karşı en hassas sonuçları vereceği tespit edilmiştir. z ekseninde yapılacak sürüş dinamiği değerlendirilmesinde absorbe edilen güç, titreşim doz değeri ve ağırlıklandırılmış frekans rms ivmelenme metodunun yeterli olacağı değerlendirilmektedir. Ağırlıklandırma fonksiyonunun farklılığından dolayı sonuçların artış eğiminde farklılıklar görülmektedir.

X ve y ekseni değerlendirilmelerinde süspansiyon ve tekerlek parametrelerini de dahil ederek frekans ekseninde değerlendirmeler yapılması gerektiği düşünülmektedir. X ve y eksenindeki konfor parametrelerin aracın süspansiyon ve tekerlek karakteri ile daha çok ilişkili olduğu öngörülmektedir.

Yapılan çalışmaların sonucu olarak olarak dalgalılık, faz açısı, dalga sayısı, dalga boyu ve pürüzlülük değerlerinin sürüş kalitesi analizlerinde limitlenmesi ve raporlanması gerektiği tespit edilmiştir. Özellikle z ekseninde yapılacak olan değerlendirilmesinde yol parametrelerinin sürüş kalitesini direk etkilediği değerlendirilmektedir. Yolun PSD grafiğinin oluşturulması analiz sonuçlarının değerlendirilmesinde çok faydalı olmaktadır. Sürüş kalitesi değerlendirilmesinde PSD grafiğinin faydalı olacağı düşünülmektedir.

1. INTRODUCTION

Ride quality is one of the most crucial challenges in vehicle design. Vehicle manufacturers need to measure and evaluate ride quality to compare the comfort and health status of the driver and passengers and optimize it during the vehicle design stage. Ride quality is about drivers' and passengers' feeling of well-being against the disturbing effect from the road while driving. At the same time, ride quality is defined as a measure of vehicle mobility. Ride quality relates to the limits for drivers and passengers to control the vehicle without losing driving stability. Also, this is related to the definitions regarding the vibration affecting the human body and health problems resulting from exposure to vibration [1].

Vibrations transmitted to the driver and passengers while driving are caused by road roughness and the vehicle's vibration-producing components (engine, transmission, gearboxes, etc.). Ride quality studies are concerned with the transmitted vibrations caused by the disruptive effects from the road to the human body by damping with damping factors such as wheels, suspension and seat. To reduce vibration from the road, vehicle manufacturers improve damping factors. However, the critical and challenging thing here is defining the vibration limits that disturb drivers and passengers. Two different basic methods were used to find the vibration limits, subjective evaluation and objective evaluation. Many researchers have tried to determine the limits by using different methods. Within the scope of this thesis, objective evaluation methods will be examined in detail and subjective evaluation methods will be mentioned.

This thesis discusses three objective evaluation methods: Absorbed power, vibration dose value, and rms acceleration methods. And, It is discussed how these methods are affected by changing road parameters such as roughness, wavelength, wave number, phase angle and driving parameters such as speed derivation. In the study, analyzes were performed on the speed coefficient of variation defined and limited in the TOP-01-1-014A standard. In addition, there are examples in the literature in which vibrations from the seat pad, waist, foot and steering wheel are evaluated.

Analysis studies were carried out with the help of the FED-Alpha (Fuel Efficiency Demonstrator) vehicle developed by Ricardo company and using the ADAMS Car analysis program. The test results of the FED-Alpha vehicle on the KRC road will be compared with the analysis results to ensure the accuracy of the ADAMS Car model. The model will then be analyzed on different synthetic roads and the effect of road parameters on ride quality will be examined.

2. RIDE QUALITY EVALUATION METHODS

2.1 Subjective Evaluation Method

The subjective evaluation method is based on ratings regarding ride quality performance based on the experience of the driver or passengers. In the subjective evaluation method, subjects are asked to describe how it feels by performing repeated tests under test conditions. This rating is highly influenced by environmental and personal factors such as the subject’s physical and healthy conditions, mood, noise, the weather, experience of the subject, whether he or she knows the ride quality parameters, and the subject's gender. Therefore, it is always preferable to examine a large number of subjects in this method.

In the subjective evaluation method, minimizing the subject's influence from environmental conditions is critical. Because, for example, the subjects can easily confuse the discomfort caused by the noise level of the environment and the discomfort caused by the vibration effect from the road. It is necessary to compose the questions to focus on the ride quality to minimize the environmental impact while driving and prevent the subject from being affected by the environment. For this reason, the grading of the subject should be according to precise criteria that are understandable by everyone. The SAE standard [2] aimed to standardize the subjective grading method using a 1 to 10 scoring system. Under vibration, the subject must first decide whether the ride quality effect is acceptable, borderline or unacceptable, as seen in the chart described in the standard [2]. The next step is to calculate the average score based on the assessment given by the subjects. Finally, it is to evaluate considering the chart in Figure 2.1 according to the numerical value of the average taken [2].

1	2	3	4	5	6	7	8	9	10
UNACCEPTABLE				BORDER LINE	ACCEPTABLE				
CONDITION NOTED BY									
ALL OBSERVERS		MOST OBSERVERS		SOME OBSERVERS	CRITICAL OBSERVERS		TRAINED OBSERVERS		NOT OBSERVED
INTOLER-ABLE	SE-VERE	VERY POOR	POOR	MARGINAL	BARELY ACCEPT.	FAIR	GOOD	VERY GOOD	EXCELLENT
1	2	3	4	5	6	7	8	9	10

Figure 2.1 : Subjective evaluation chart [2].

The subjective evaluation method cannot ultimately ensure understanding the cumulative effect of vibration in three directions [3]. At the same time, determining the direction in which the discomfort originates is not possible. With an expert evaluation, it is only possible to understand whether discomfort comes from the vertical, lateral, or longitudinal directions. Even so, it is impossible to be sure of the accuracy of the evaluation.

Testing is mandatory in the subjective evaluation method. The test can be a road test or a simulator test. In addition, to have an accurate assessment, it is necessary to test on many subjects with different physical and experience conditions, which requires enormous organization and an enormous budget.

Early research focused on how the human body responds faced to sinusoidal vibration. These studies have also led to misinterpretations as they do not directly simulate the actual road condition of vehicles. The main reason is that vehicles are not exposed to sinusoidal vibration in real road conditions. Deusen et al. included the studies of different researchers using shake tables in their research [4]. Each researcher defined the acceleration limit value for discomfort at different levels. Jacklin and Liddell conducted experiments between 1-7 Hz and classified the vibration as perceptible, disturbing and uncomfortable. Meister conducted experiments with 15 subjects between 1-70 Hz and divided discomfort characteristics into five different categories, as seen in Figure 2.2. Dieckmann developed a more advanced way, defined the K coefficient, and changed the calculation method of the K coefficient in different frequency ranges. Goldman divided the ride quality assessment into three categories: perceptible, unpleasant and intolerable. Janeway defined the J limit and described a different calculation method for frequency ranges like Reither's method. Since it is not easy to evaluate the subjects' responses against the frequency band, the researchers could not reach a consensus. In addition, since the parameters such as suspension and tire properties of the examined vehicle will change the feeling in the frequency band, the results made with the simulator are far from the impact that will reach a general evaluation [4]. These ride quality evaluation methods are no longer being used.

When the graphics were examined, it was determined by all researchers that the feeling of discomfort increased and decreased in specific regions. However, each researcher has predicted the acceleration value of this discomfort value differently. In addition, the ride sensation had a different rating, probably because the questions and the subjective evaluation chart were different.

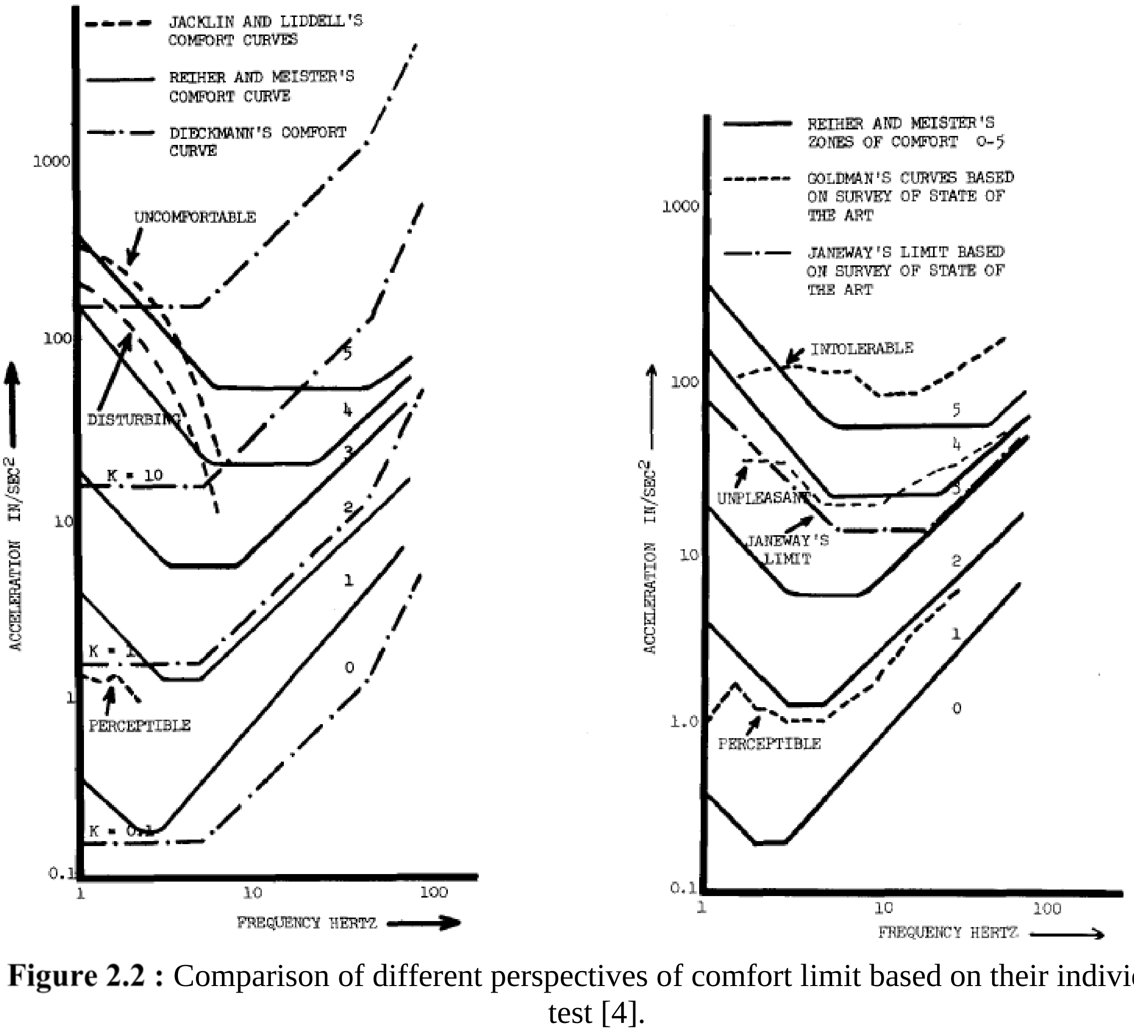

Figure 2.2 : Comparison of different perspectives of comfort limit based on their individual test [4].

Metha et al. conducted tests lasting 45 minutes in 3 different vehicles. They asked their subjects to rate the ride quality from 1 to 10 according to the criteria of overall ride quality, whole-body vibration, harshness, impact harshness and seat comfort. The main reason for choosing particular characters of the scoring titles is to prevent the subjects from the influence of the environment and to focus on the ride quality characteristic. Another aim of the study is to compare the subjective evaluation method used with the objective evaluation method available in the literature. They argue that it is more accurate to use overlapping methods to interpret the ride quality effect of the vehicle. Therefore, the correlation between subjective evaluation and weighted rms, unweighted rms, absorbed power, weighted histogram, unweighted histogram and ISO fatigue decreased productivity boundary methods were investigated. A correlation factor was found greater than 0,91 between the subjective and all objective evaluation methods [5].

Because the subjective evaluation is very dependent on the subject's physical condition, it is difficult to obtain very reliable results. Mansfied et al. showed that females' responses under average 1,0 m/s^2 rms vibration are more significant than the males' under average 1,5 m/s^2 rms vibration. At the same time, male and female subjects gave different responses to the frequency of the disturbing shock factor found in the vibration profile. Males rated unequally spaced shocks as more severe than equally spaced ones, while females rated unequally spaced shocks as less potent than equally spaced ones [6].

One of the main reasons for the inadequacy of the subjective evaluation method is that the method cannot give input for ride quality improvement in the vehicle design phase. Any ride quality assessment will greatly benefit design improvement and a cost-save solution during the design phase. Another disadvantage of the subjective evaluation method is that feedback can be given after the vehicle is produced. Therefore, improvement can be made after the prototype phase. Also, after the design improvement, it is almost impossible to repeat the test under the same conditions since it is desired to see the effect of the modification on the ride quality. Since it is not a repeatable method, it can be done as a supportive study rather than a primary method in design optimization.

2.2 Objective Evaluation Method

Emphasis is placed on the importance of repeatable analysis and test methods to improve ride quality assessment. For this reason, computational methods developed correlating subjective evaluation methods.

Stephens and David thought that to examine the ride quality of the driver and passengers, it was necessary to explore the vibration in all axes, so they studied with this perspective. It was emphasized that the acceleration time history, vibration amplitude, power spectral density, and frequency characteristic are essential for the evaluation methods. Their analysis determined that the maximum vertical acceleration level was always more than lateral. Stephens and David determined that the maximum rms acceleration in the 1/3 octave frequency band according to ISO standard is adequate to detect the vehicle's vibration band. The acceleration values of the vehicle in the 1/3 octave frequency range are plotted and it is shown that the accelerations reach the maximum accelerations at specific frequencies (Figure 2.3). Even though maximum rms acceleration values vary according to the vehicle type, it is seen that they reach the maximum at values that are close to each other [7].

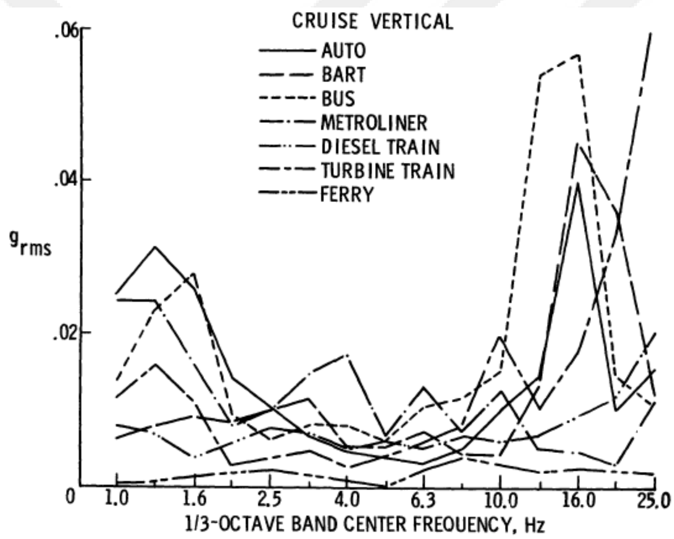

Figure 2.3 : Vertical rms acceleration on different road vehicles 1/3 octave band center frequency [7].

Stephens and David's research results were showed that maximum resonance response is seen in the 1,4 Hz region of the vertical direction and 1,5 Hz region of the lateral direction. These values are similar to ISO reference values [7]. It is necessary to pay attention to future vibrations in these regions in the analysis. At the same time, it is seen that vertical and lateral directions should be examined differently.

As the g_{rms} value increases, the driver and passenger's acceptable percent decrease. Acceptable percent is visibly falling in the specific frequency band range. According to the evaluation made using the maximum weighted rms acceleration method given in ISO, the maximum acceleration rms value should be less than 0,035 g_{rms} for acceptable ride quality (Figure 2.4). If the maximum acceleration value is less than 0,035 g_{rms} , the driver and passenger withstand the vibration band sensitive to the human body [7].

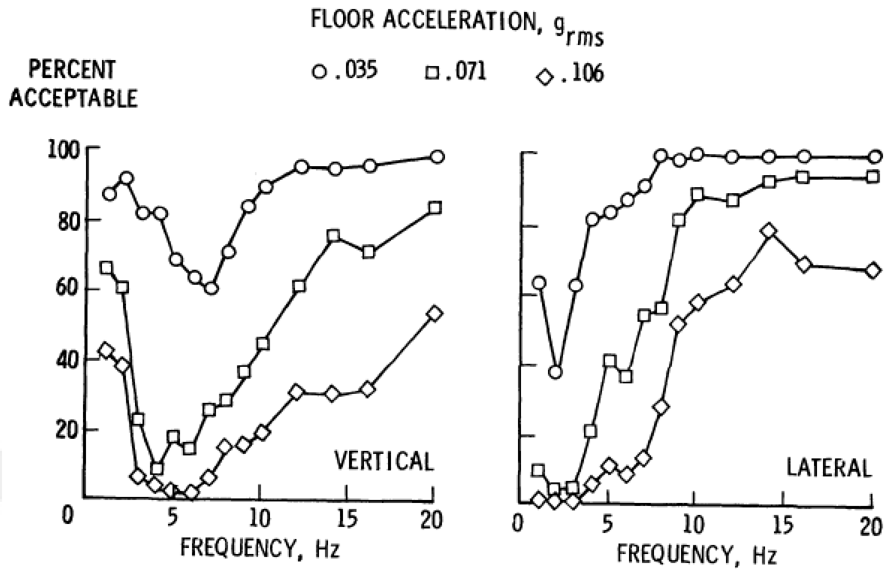

Figure 2.4 : Test subject acceptability in different acceleration [7].

Dr. Versace aimed to develop a method to correlate the subjective and objective evaluation methods together. For this purpose, he primarily focused on developing the subjective evaluation method reliability. By using the "Null meter" device, the subjects were set to decrease or increase the noise value according to the discomfort of the road. He thought it would be much easier to express ride quality severity with the definition of noise. Acceleration data was collected from the vehicle at the same time. The noise value adjusted with the “null meter” was digitized with a potentiometer and its correlation with mean square speed, acceleration and jerk were compared. According to the analysis results, human responses have a low correlation with mean square velocity and acceleration and a high correlation with the jerk method [4].

Kumar et al. analyzed the ride quality effect on two different vehicles to evaluate different road conditions, different driving speeds and different loading conditions. They were able to find comparable results for vehicle ride quality by evaluating the overall ride value (rms weighted acceleration). They observed that the overall ride value (ORV) increases as the average speed of the vehicle increases while the ride comfort decreases. It has also been observed to have better ride quality in the loaded condition than in the unloaded condition. According to Kumar’s study, it is seen that the lateral vibration in the vehicle's rotation axis can be ignored in the ride quality evaluation. The lateral vibration effect is very minimal relative to the vertical axis. In addition, it can be said that the effect of discomfort on ride quality is caused by dominant frequencies. The dominant frequency changes according to the road's quality and the vehicle's load condition [8].

Holmlund researched to obtain comparable ride quality evaluation results for all axes of absorbed power and mechanical impedance (Z). For the mechanical impedance calculation, it is necessary to collect force, acceleration and velocity data simultaneously. It has been explained in the research that it is tough to collect simultaneous force and acceleration data. When the results were examined, it was seen that the similarity between the acceleration and force values was very high on the z-axis. On the other hand, it was low in the x and y-axis, especially between 2-12 Hz. It has been observed that the absorbed power value is higher in the relaxed position, but the maximum frequency is lower. When the test and laboratory data were encountered in absorbed power and mechanical impedance measurements, it showed high consistency for the z-axis. Still, no consistency was found for the x and y-axis [9].

Mansfied et al. examined the correlation with the subjective evaluation using rms acceleration, VDV, MTVV, absorbed power objective evaluation methods in his study. They made their analyzes with five different vibration profiles lasting 20 seconds in a laboratory environment. 11 male and 13 female subjects evaluated the five different vibration conditions with ride quality perspective. When the acceleration-based measurements are examined, the highest correlation coefficient with the ride quality evaluation is the VDV calculation method. It was also found that MTVV had the worst correlation coefficient compared to other methods. Absorbed power resulted in the highest median correlation between subjective evaluation and vibration magnitude. However, absorbed power and VDV were evaluated as the methods with the best correlation coefficient [6].

Spasng and Arnberg found a strong correlation between VDV, MTVV, rms acceleration and absorbed power methods when subjected to single shocks. It has been concluded that the rms acceleration method is an easy method to measure and calculate. However, Howarth and Griffin found that the VDV had a higher correlation coefficient with the subjective evaluation on the road, which included high shock amplitude characters because VDV used the fourth power of acceleration in its calculation [6].

As defined in Whole-Body Vibration, the human body is sensitive to vibrations at some frequencies and cannot perceive vibrations at some frequencies. For this reason, researchers and standards use the weighting factors in the calculations. The primary purpose is to use weighting factors to increase the effects of vibrations where the human body is more sensitive and decrease the ones the human body cannot perceive. Therefore, within the scope of this study, frequency weighting factors will be used in the objective evaluation methods.

Healey et al. examined different frequency weighting factors used in the calculations of Janeway, Dieckmann, UTACV, ISO weighted rms, unweighted rms and absorbed power. Study analyses results showed that the unweighted rms method values have a sufficient correlation coefficient as the weighted rms values. It is seen that absorbed power has a high correlation coefficient in the vertical direction but a low correlation coefficient in the lateral direction. When all methods are compared, it is seen that the correlation coefficients in the vertical direction are higher than the correlation coefficients in the lateral and magnitude [10].

Strandemar, in his thesis, processes the signals he collects from the road data as phase equivalent signals and time combined signals and generates data by making small changes in the maximum amplitudes of these signals to use them in the simulator. In the study, a total of 4 subjects, one experienced, one inexperienced, and two trained, were asked to answer yes or no questions of whether they could perceive these signals. The primary purpose is to determine which analysis method and subject's perception had similar results. At the same time, rms acceleration compares PSD data with subjective data as a frequency domain method. It was determined that the calculations made with the time domain, regardless of the signal type, were more compatible with the subjective evaluation. Frequency domain analyses performed with phase equivalent signals resulted in poor correlation with subjective evaluation. Strandemar says that using the time domain method will give more successful results in analyzing the human body response from the signal change [11].

Within the scope of this study, absorbed power, rms weighting acceleration and vibration dose value methods, which have a high correlation with subjective evaluation in the literature, will be used.

2.2.1 Absorbed power

The absorbed power method was first introduced by Pradko et al. as the power spent to maintain ride stability by relaxing and stretching the muscles in the body against the disruptive effect on the road [12].

The absorbed power method has advantages in understanding the limits of the human body against random and sinusoidal vibration [13].

According to Pradko and A. Lee, the human body can behave in elastic or inelastic ways under vibration. The human body applies a reaction to protect its state against vibration and this reaction can be measured based on distance. The human body spends energy to create the reaction force until the vibration disappears. The ratio of the total energy to the applied time is called absorbed power. In the study they published, they explained that the correlation coefficient between subjective methods and absorbed power was high. They clarified that it is a critical estimation method, especially for making estimations in a random environment [13].

According to Pradko et al.'s work, absorbed power can be analyzed in time and frequency domains. The absorbed power can be calculated using the transfer function when analyzing the time domain. According to Pradko et al.'s work, absorbed power is a scalar quantity, and the magnitude of absorbed power is calculated by adding three axes values. At the same time, they reported that the absorbed power limit determined the conditions of use of the vehicle. For example, a passenger car's acceptable limit is 0,2-0,3 Watt, but a military vehicle's acceptable limit is between 6-10 Watt [14].

Keenan and Robert used the absorbed power method in their studies. They claimed that 6-Watt was a low value even if everyone accepted it. Despite their claim, they used it in their analysis because the best available approach was 6-Watt [12].

The absorbed power calculation method is used to find 6-Watt speed, defined as a comfort limit at the vertical axis. The absorbed power is a scalar quantity in the frequency domain so that reason only the maximum value makes sense at the time domain. Absorbed power can also be applied to the lateral and longitudinal axes, but different weighting factors from the vertical axis are used.

The absorbed power calculation method and its constraints are defined in ITOP-01-1-014A. To collect the acceleration data used in the calculation, road and record parameters are restricted, such as road profile, output sensor data resolution and sensor range. The purpose of the restriction is to make 6-Watt speed and vehicles' performance comparable for all vehicles. In the standard, it is defined that the acceleration sensor should be used in the acceleration measurement band from 0,1 Hz to 100 Hz and that the sensor should take 400 samples per second. At the same time, the analysis parameters should be selected with a frequency domain resolution of 0,2 Hz or less. Another parameter is the analysis time or the road length. The standard limited the analysis to be recorded for at least one second. (The minimum distance is determined depending on the vehicle's speed.) The other restricted parameter is the speed deviation during the test or analysis. It is requested that the aimed average speed and the achieved average speed be the same as possible. For this purpose, the speed coefficient of variation value was defined and requested to be at most 0,1. The speed coefficient of variation value calculated the speed deviation divided by the average vehicle speed. The standard also mentions the parameters of the road to be analyzed. Road parameters are defined such that the waviness should be approximately 2, and the wavenumber spectrum is defined between 0,5 feet and 64 feet wavelength. These parameters will be examined in depth within the scope of the thesis and their effects on absorbed power will be discussed. In addition, it is recommended that analysis or test is started with 1-Watt speed and finished 15-Watt speed limit.

The absorbed power is calculated with the formulation given below. Narrowband frequency is used in calculations.

$$P = \sum_{1}^{n} (C_i) {A_i}^2 \tag{2.1}$$

P: Absorbed power, Watt

A_i: rms acceleration in ft/sec^2 within the ith spectral band.

$$C_i = K_1 K_0 (F_1 F_4 - F_2 F_3) / \, ({F_3}^2 + {W_i}^2 {F_4}^2) \tag{2.2}$$

$W_i = 2\pi f_i$ Frequency, radians/second

f_i= frequency weighting factors

F and K= Different calculated values for X, Y and Z axes

In the standard, functions are used for weighting the acceleration data. Using the weighting functions increases the acceleration values that the body is sensitive to and filters the acceleration values that the body is not sensitive to. Frequency weighting factors vary according to the directions (Figure 2.5).

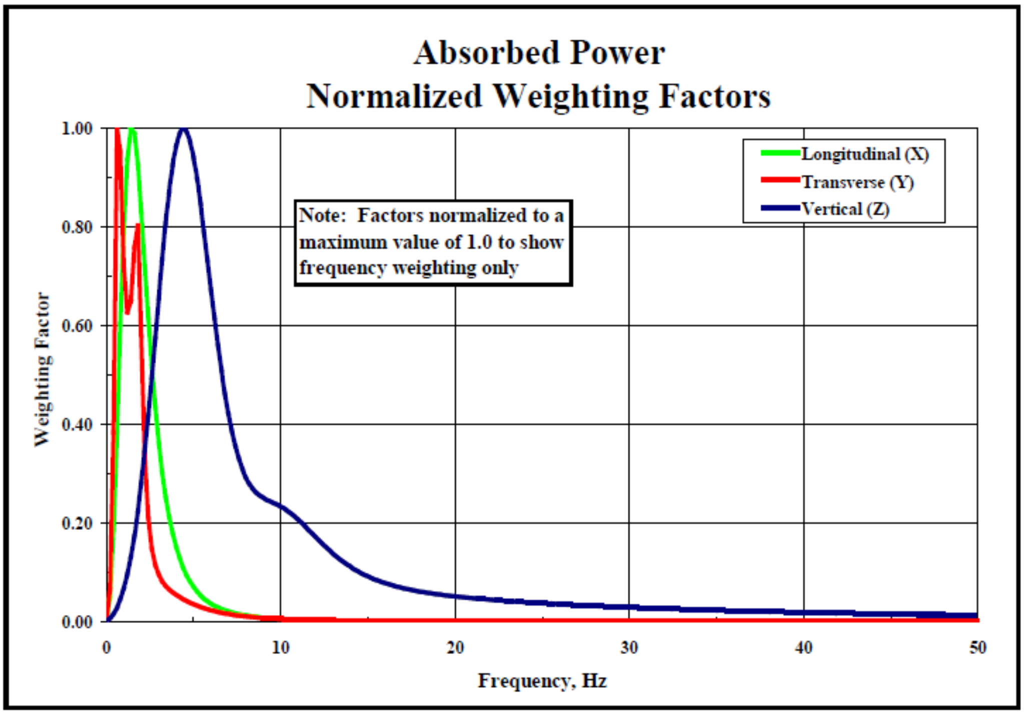

Figure 2.5 : Absorbed power weighting factors in three axes [1].

To find the 6-Watt speed value, an analysis/testing activity is carried out to cover the speeds between 1-Watt and 10-Watt. First, these values are plotted on the graph as a speed function. Then, the speed corresponding to 6-Watt is calculated by fitting the second-order polynomial curve to this graph. The calculated speed is the speed limit for comfort on the road conditions performed by the analysis or test.

Absorbed power measures the intensity of the vibration input. According to Pradko et al., PSD definitions and the absorbed power measurement are required for random road analyzes. Pradko et al. analyzed 26 different roads and calculated absorbed power, rms acceleration and measured acceleration values. Then results were compared with the subjective evaluation results obtained with ten different subjects. As a result, rms acceleration and absorbed power showed similar results. As the roughness of the road increases, rms acceleration and absorbed power increase [15].

2.2.2 ISO method frequency weighted rms acceleration

Another method that defines the ride quality and the maximum vibration that the human body can withstand is the rms weighted acceleration method which is defined in ISO 2631-1 [16]. The rms weighted acceleration method has wider frequency band limits than absorbed power. Absorbed power limits will be used in this study.

Because the standard is not explicitly created for the land vehicle, it covers the acceleration data in the 0 to 400 Hz band. However, it will be used between 0 and 80 Hz frequency range, which are essential for the land vehicle in our analysis.

Frequency weighted rms acceleration is calculated with the formulation given below. 1/3 Octave band frequency is used in calculations.

$$a_w = [\frac{1}{T}\int_0^T a_w^2(t)dt\,]^{1/2} \tag{2.3}$$

a_W: weighted acceleration (translational or rotational) as a function of time (time history), in m/s^2 or rad/s^2, respectively

T= duration of the measurement, in seconds.

Similarly, frequency weighting factors are used in the absorbed power method to weight certain frequency ranges and filter specific frequency ranges (Figure 2.5).

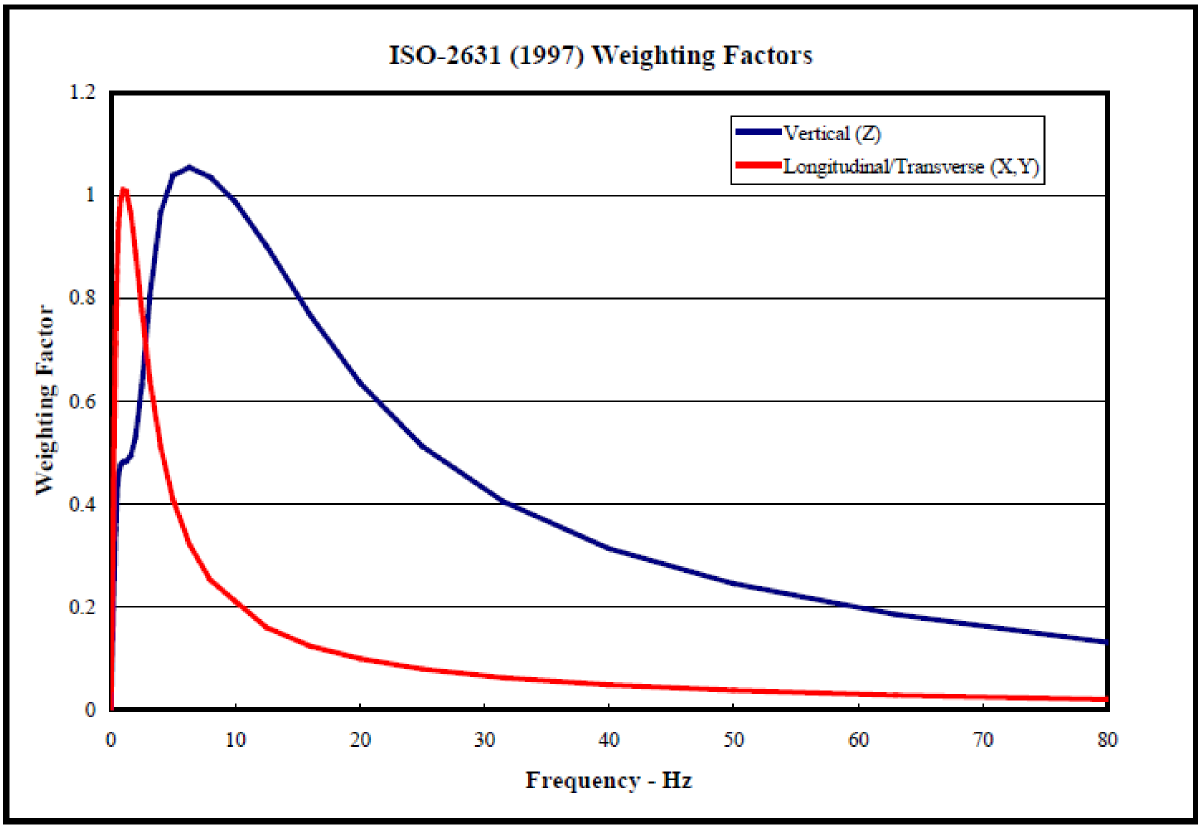

Figure 2.6 : ISO 2631 weighting factors for vibration dose value and frequency weighted rms acceleration methods [16].

In the ISO 2361-1 standard, criteria are shared about how rms weighted acceleration values feel by humans. Greater than 2 m/s^2 is defined as “extremely uncomfortable”, less than 0,315 m/s^2 is defined as “not uncomfortable”. Between “extremely uncomfortable” and not uncomfortable, a different range is defined as a comfortable level in the Table 2.1 [16]. In this study, rms weighted acceleration value will be found by reference to 6-Watt speed value and compared with predictive values in the standard.

Table 2.1 : Frequency weighted rms acceleration method comfort limits [16].

Rms Acceleration Result	Feeling
Less than 0,315 m/s^2	Not uncomfortable
0,315 m/s^2 to 0,63 m/s^2	A little uncomfortable
0,5 m/s^2 to 1 m/s^2	Fairly uncomfortable
0,8 m/s^2 to 1,6 m/s^2	Uncomfortable
1,25 m/s^2 to 2,5 m/s^2	Very uncomfortable
Greater than 2 m/s^2	Extremely uncomfortable

2.2.3 Vibration dose value

Another measurement method used in this study is vibration dose value. Unlike rms weighted acceleration for the calculation method, it uses the fourth power of acceleration. Therefore, it is possible to make more precise calculations, mainly if the road profile contains shock effects with high acceleration amplitude [1].

The vibration dose value is calculated with the formulation given below. 1/3 Octave band frequency is used in calculations. It also uses the same frequency weighting factors as frequency weighted rms acceleration.

$$VDV = \left\{ \int_{0}^{T} [a_w(t)]^4 dt \right\}^{1/4} \tag{2.4}$$

a_w (t) = instantaneous frequency-weighted acceleration.

T= duration of the measurement, in seconds.

Since the 4th power of the acceleration is taken in the equation, the time-dependent effect is emphasized when it is met with high accelerations in extreme conditions. In the analyzes made on the roads with transient characteristics, it was determined that there was a greater consistency between the VDV evaluation method and the subjective evaluations of the subjects compared to the rms acceleration method [17].

2.2.4 Comparison of different objective evaluation methods

Objective evaluation analysis methods differ from each other due to frequency weighting factors difference, frequency band difference, and calculation method.

Bao et al. compare the results of ISO 2631 frequency weighted rms acceleration and absorbed power analysis in their research. If it is a road with a random roughness surface, they found that the rms acceleration value corresponding to 6-Watt is 2,07 m/s^2 [18]. In this study, frequency weighted rms acceleration and vibration dose value, which corresponds to 6-Watt of absorbed power, will be compared.

The Department of Mechanical and Aeronautical Engineering in South Africa has determined which method is suitable to measure their vehicles' ride quality. They collected acceleration data from the driver and all passenger seats by testing in 7 different driving scenarios. At the same time, Els made a subjective evaluation with 61 subjects from different physical, age, gender and occupational groups and compared the results. As a result of the tests and analyzes, it was seen that the rms, VDV and eVDV values had an excellent correlation coefficient with the subjective evaluation in the vertical direction. This correlation is in a linear trend. Absorbed power analysis results did not increase the linear trend even though absorbed power has a good correlation coefficient with the subjective evaluation. As the terrain roughness increases, a large increase in absorbed power has little effect on the driver. The study shows that the pitch and roll acceleration values are weakly correlated with the subjective evaluation and have no effect on ride quality at low speeds. In the study, only 50% of the subjects expressed that they found the 6-Watt value comfortable, and the study suggests that vibrations up to 12-Watt for a short time can be tolerated. The following table shows the results of the objective evaluation methods. As seen in the table, the unweighted rms acceleration value corresponding to 6,3-Watt is 2,8 m/s^2, the frequency weighted rms value is 2,0 m/s^2, the rms value according to BS 6841 is 1,8 m/s^2 and the VDV value is 26 $m/s^{1.75}$ (Table 2.2) [19].

Table 2.2 : Values of objective evaluation methods corresponded to subjective value [19].

Subjective value from present study (%)	Unweighted RMSz (m/s^2)	ISO 2631 RMSz (m/s^2)	BS 6841 RMSz (m/s^2)	AAP (W)	VDI 2057 (-)	BS 6841 VDV ($m/s^{1.75}$)
10	0.8	0.2	0.2	0.2	12	6
20	1.3	0.75	0.6	0.9	31	11
30	1.9	1.1	1.0	2.1	50	16
40	2.4	1.55	1.4	3.9	69	21
50	2.8	2.0	1.8	6.3	88	26
60	3.4	2.5	2.2	9.3	107	32
70	4.0	2.9	2.6	13	126	36
80	-	-	-	17.1	-	41

3. ROAD PROFILE DESCRIPTION

Mathematical methods have been used to define the road profile. The most widely used method for defining the road profile is the Power Spectral Density (PSD) method defined in ISO 8608. There are many parameters that come out of the PSD graphs that help us define the road. This study will examine waviness, wavelength, and wavenumber parameters derived from PSD graphics. In addition, the phase difference related to the wave graph of the road will also be examined.

3.1 Power Spectral Density PSD

PSD is defined as the limiting mean-square value of a signal per unit frequency bandwidth in ISO 8608 [3].

It is possible to express the road as PSD in three ways: displacement PSD, velocity PSD and acceleration PSD. According to ISO 8606 definitions, displacement PSD is expressed as vertical road profile displacement and velocity PSD is the rate of change of the vertical road profile displacement per unit distance traveled. Acceleration PSD is the rate of change of the slope of the vertical road profile per unit distance traveled.

The power spectral density (PSD) method defines the road surface and understands the road's characteristics. Within the scope of the study, the values used to define the road’s character will be detailed. Previous studies on these characteristics will also be examined within the scope of this thesis.

3.2 Roughness

Roughness can be expressed as the surface irregularity on the road that will adversely affect the vehicle's ride quality. There are many road roughness calculation methods: rms, IRI, PSD etc. The roughness value of the roads used in this study is defined in centimeter units with the rms calculation method. In this thesis, the effect of ride quality is examined by analyzing the roads with different rms roughness values. At the same time, previous research about relations between road rms roughness and ride quality will also be mentioned. However, the rms calculation method is not the scope of this thesis.

Durst et al. examined the relationship between the road's root-mean-square (rms) roughness value and the absorbed power. They determined the vehicle's maximum speed on different rms roughness roads, referring to the 6-Watt absorbed power limit. As a result of the study, as the road rms roughness value increases, the vehicle limit speed decreases (Figure 3.1) [20].

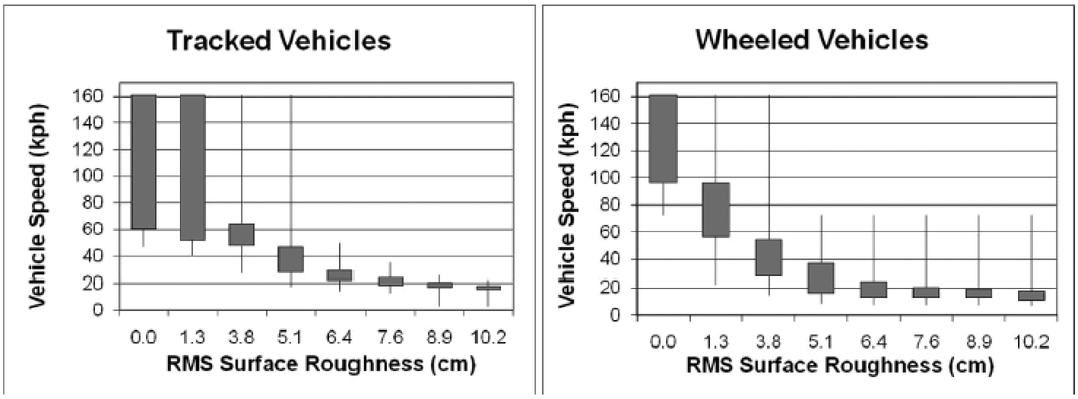

Figure 3.1 : 6-Watt speed on different rms surface roughness [20].

3.3 Waviness

The displacement PSD data plotted on the logarithmic axis is curved according to the rules described in ISO 8606. The negative slope of this line is defined as waviness.

The waviness value is expected to be 2 for human-made roads [12]. The general analysis approach is made with the assumption that the waviness value is 2. Within the scope of this thesis, the effect of waviness values in terms of ride quality will be examined.

Keenan and Robert performed simulations on approximately 12-meter-long roads with PSD slope values ranging from -0,6 to -2,3 (-0,6 -1,2 -1,85 -2,0 -2,15 -2,3) (Figure 3.2) to determine the critical speed by taking the 6-Watt absorbed power limit into account. The critical speed is defined as the vehicle speed at which the absorbed power reaches 6-Watt in the study. The critical speed value increases as the PSD slope decreases. For -0,6 and -1,2 PSD slope critical speed is 2 mph, for -1,85 slope critical speed is 4 mph, for -2,0 slope critical speed is 5 mph, for -2,15 slope critical speed is 10 mph, for -2,3 slope critical speed is 17 mph (Table 3.1). The waviness value is defined as the negative slope of the PSD graph in the spectral frequency domain. For this reason, inference can be made over the waviness value with the PSD slope. The base of this inference is that as the PSD slope decreases from -0.6, the high-frequency components decrease while the low-frequency components increase. Analyzes are made with the assumption that the pitch angle was low. However, on roads with PSD slopes of -0,6 and -1,2, it is determined that the pitch and jounce motion of the vehicle is excessive, and it is decided not to use these values. As a result of the analysis, it has been determined that the vehicle's ride quality is directly related to the PSD slope of the road [12].

Table 3.1 : Critical speed according to different PSD slopes [12].

PSD Slope (-Waviness)	Critical Speed (MPH)
-0.6	2
-1.2	2
-1.85	4
-2.0	5
-2.15	10
-2.3	17

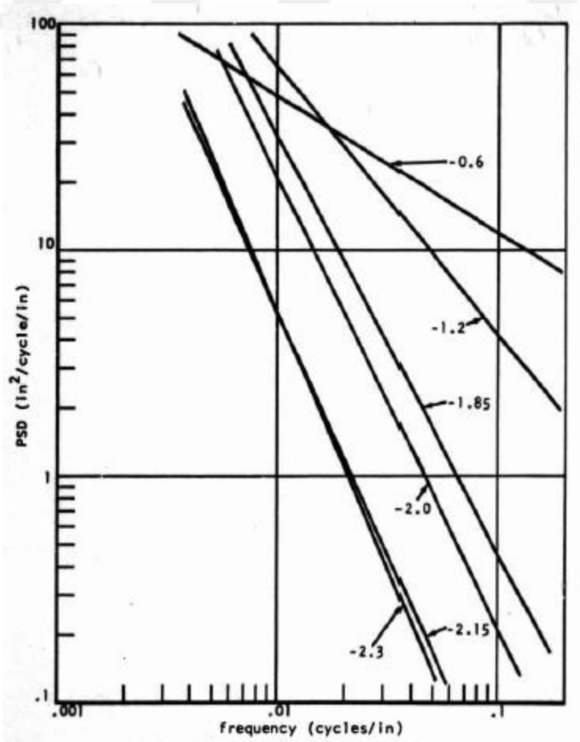

Figure 3.2 : Different slope values on the PSD chart [12].

Mucka analyzed the road data with a PSD slope value between 1,5 and 3,5 and at 36, 54 and 72 km/h speeds using a quarter car model setup. The analysis results show that the vehicle can be driven at higher speeds and comfortably at high PSD slope values [21].

3.4 Wavenumber and Wavelength

Wavelength is the distance between corresponding points of two consecutive waves. Wavenumber is the number of complete cycles in a predefined distance or spectral frequency. Wavenumber is the inverse of wavelength.

The PSD plot shows the distribution of irregularities over the wavelength. The wavenumber and wavelength representations are shown below in Figure 3.3 [3] in the PSD plot.

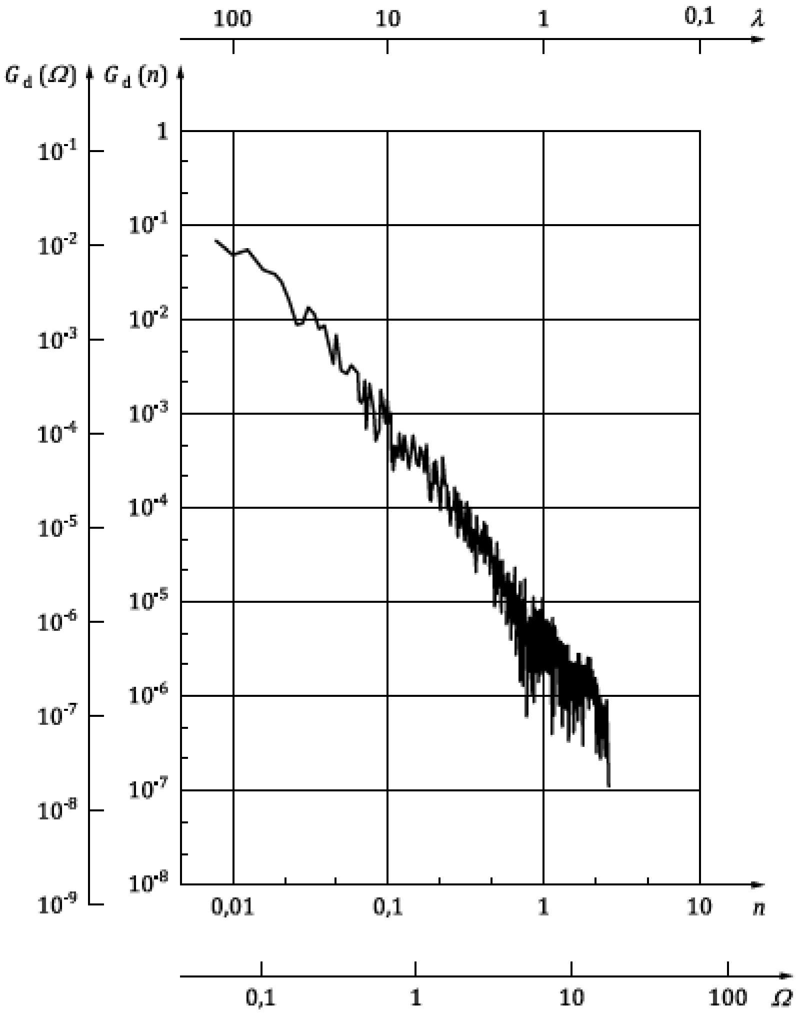

Figure 3.3 : Example of PSD graph [3].

Ω: angular spatial frequency, rad/m, wavenumber

λ: wavelength, m

$G_d(n)$, $G_d(\Omega)$: displacement power spectral density, m^3

N: spatial frequency, cycles/m

In the evaluation method standards, it is recommended to use different wavelength bandwidths. Road data covering 0,35 m and 90,9 m wavelengths are used in ISO 8608, while road data covering 0,78 m - 50 m wavelengths are used in EC standards [20]. In the ITOP 01-1014A standard, where the absorbed power calculation is explained, it is recommended that the road to be analyzed should cover 0,5 feet to 64 feet (0,15 m – 19,5 m) wavelengths [1].

Cenek et al. modeled two different vehicle models with a quarter car and half car methods in their study and analyzed the roads with different wavelength bandwidths at different speeds. In addition, it has been examined whether the vehicle's maximum response is at a particular wavelength if it is a road covering different wavelengths with a specified speed. In the analyzes made at 72 km/h, it was determined that the wavelength at which the vehicle resonates was 15,3 m. When the vehicle speed was increased and analyzed at 108 km/h, the wavelength the vehicle resonated was 17,3 m, which is a further band. When the analysis is performed at different boosted wavelength values on the same International Roughness Index (IRI) road, the sprung mass acceleration value increases as the boosted wavelength increases (Table 3.2). The IRI value is used to define the roughness value of the road. As a result of the analyzes made using the quarter car model, the roughness value of the road at a certain speed is defined. It converts the vehicle's reaction against the road into a coefficient. The sprung mass acceleration value changes depending on whether the vehicle model is a quarter car or half car and according to the type of vehicle being modeled [22].

Table 3.2 : Sprung mass acceleration and dynamic DIF values in different wavelength road [22].

Truck Speed		20 m/s (72 km/h)			32 m/s (108 km/h)		
Boosted Wavelength		2m	None	10m	2m	None	10m
IRI (m/km)		4.05	4.05	4.05	4.05	4.05	4.05
RMS Sprung mass accelerations (%g)	QTF	6.48	7.26	9.58	8.51	10.26	20.02
	QTR	15.67	52.33	19.92	18.74	30.66	63.36
	HT	7.90	12.24	10.00	9.17	14.03	30.55
	Htrac	15.72	19.72	11.76	48.43	30.78	30.30
	Hsemi	5.85	7.79	8.11	15.33	22.95	18.42
Dynamic Pavement Loading DIF Values (%)	QTF	6.40	7.24	9.25	8.91	10.22	19.02
	QTR	14.61	24.06	18.96	17.46	29.10	60.23
	HTF	6.57	7.47	8.13	8.73	9.68	17.29
	HTR	11.96	19.51	14.81	13.19	21.57	49.34
	HtracF	7.31	7.57	8.84	11.91	13.72	18.80
	HtracR1	6.60	7.32	6.65	16.45	18.76	15.09
	HtracR2	9.51	11.86	12.05	29.49	35.97	28.03
	HsemiR1	7.94	9.47	10.80	19.67	24.19	20.27
	HsemiR2	7.29	9.11	11.29	19.56	23.10	19.84

3.5 Phase Angle Difference

One wavelength corresponds to 2π radians or 360 degrees. The surface corresponding to the right and left wheels of the road can be at different phase angle wavelengths. Due to the difference in the phase angle between the right and left of the road, the right and left wheels to make bump and rebound movements at different times. This difference can be seen by comparing the wavelength of the road followed by the two wheels (Figure 3.4).

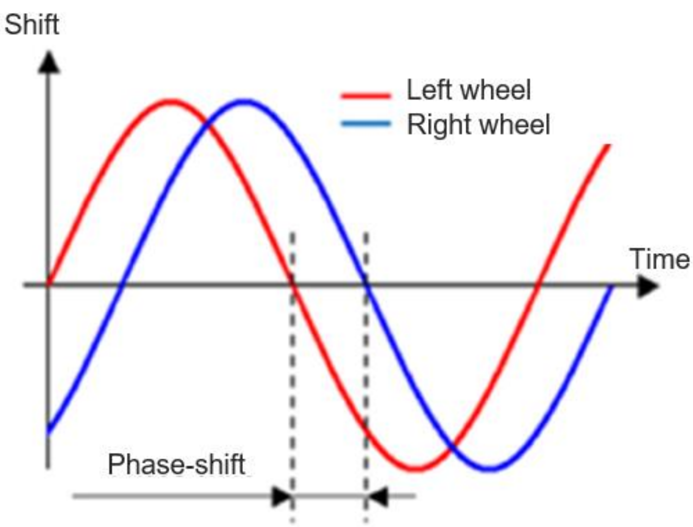

Figure 3.4 : Represented phase angle difference in sinus curve [23].

Within the scope of this study, the effect of ride quality will be examined by analyzing the right and left road track with 0 degrees, 45 degrees, 90 degrees and 180 degrees phase angles. The aim is to determine how much the ride quality is affected by the different jounce and rebound movements of the right and left wheels of the vehicle.

This thesis examined wheel travel values of the front right and left tires to evaluate the phase difference on synthetic roads with different phase angles. For phase 0 road, it can be seen that the right and left wheels move together, leading to the high coherence function value. When the Phase 180 road is examined, it is seen that the right and left wheels move opposite to each other (Figure 3.5).

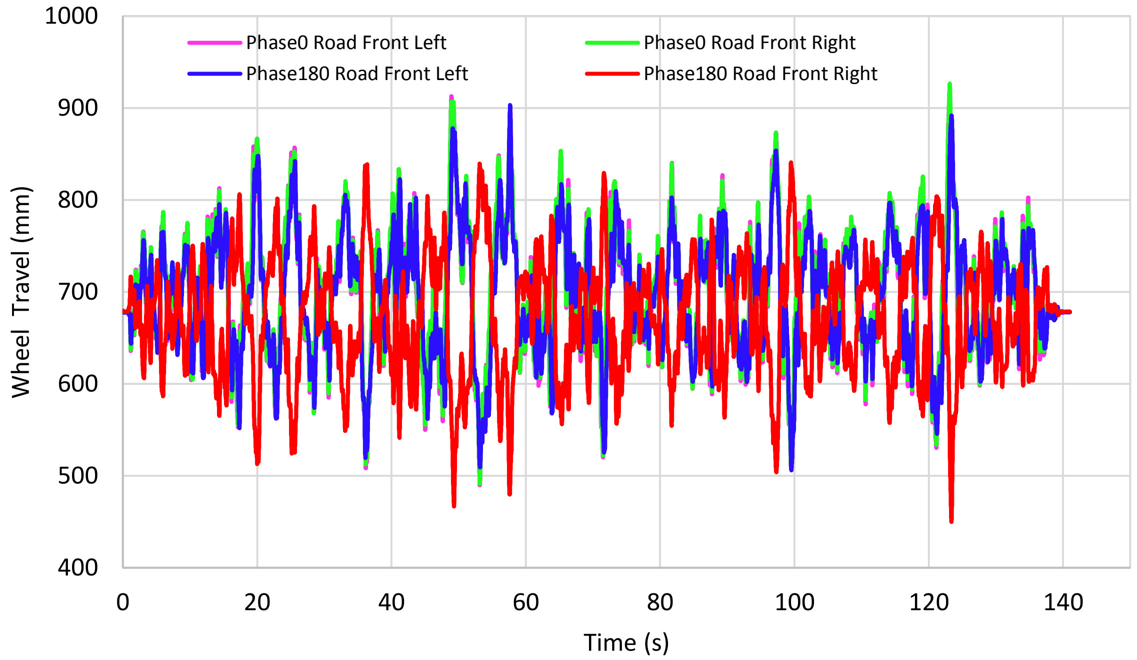

Figure 3.5 : Right and left front tire wheel travel on phase 0° and phase 180° road.

The coherence function (γ^2) describes the relationship between the two measured road PSD plots. The relationship between the PSD graphics of the road followed by the right and left wheels can also be defined with the coherence function. Coherence varies between 1 and 0 values; one indicates no difference in PSD value between the right and left of the road, and zero indicates that the PSD values are inverse of each other. The calculation method is defined in the ISO 8608 standard (Formula 3.1) [3].

$$\gamma^2 = \frac{{G_{12}}^2(.)}{G_1(.).G_2(.)} \tag{3.1}$$

γ^2 : Coherence function

$G_{12}(.)$: Cross spectrum between tracks 1 and 2

$G_1(.)$: PSD of track 1

$G_2(.)$: PSD of track 2

3.6 Road Data Modeling Interval

The more the interval increases for the analysis, the more the input followed by the wheel will increase and a more precise result will be obtained, but this will also affect analysis times and costs. It is expected that the interval effect will be seen much more in random frequency roads and short-wavelength roads.

In their paper, Keenan and Robert examined the effect of different intervals on the absorbed power value. The road model detail decreases as the interval speed increases (Figure 3.6). The analysis was carried out with the M35 truck with the heavy class and long wheelbase and the M151 light class jeep with a narrow wheelbase. The point contact follower tire model was used in the analysis. It has been observed that intervals are essential in light and short vehicles. Because interval has quickly affected absorbed power in light and short vehicles (Table 3.3). At the same time, it has been evaluated that the interval value may increase to shorten the analysis duration in vehicles with heavy and long wheelbases [12].

Table 3.3 : Critical speed according to different intervals at M151 and M35 vehicles [10].

Interval (inches)	Average Absorbed Power (Watt)	
	M151	M35
1,0	7,206	1,328
1,5	7,000	1,207
2,0	7,221	1,298
2,5	6,740	1,276
3,0	7,819	1,377
3,5	6,085	1,234
4,0	8,735	1,318
4,5	7,129	1,404
5,0	5,094	1,254
6,0	6,236	1,186
9,0	4,329	1,082
12,0	4,256	1,016
16,0	-	1,321

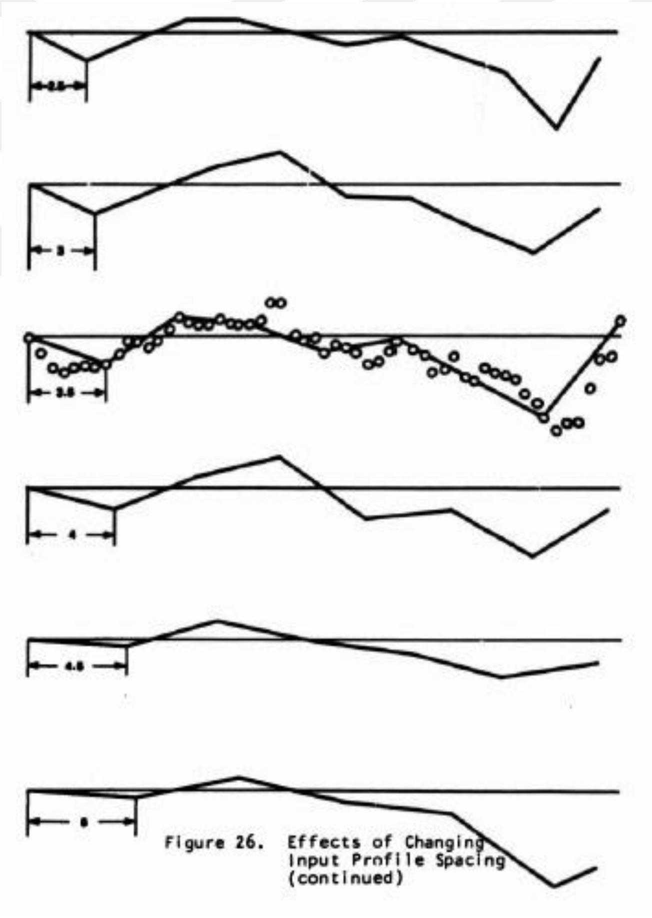

Figure 3.6 : Input profile spacing [10].

Within the scope of this study, the comparison of interval value and ride quality will not be included. Instead, the modeling range of the road data will be specified as the analysis inputs.

4. SIMULATION AND SIMULATION MODEL VALIDATION

4.1 FED-Alpha Vehicle Model

FED-Alpha armored personnel carrier vehicle from the Light Combat Vehicle product family is used in the simulations. The vehicle is an off-road vehicle with a 4x4 wheel configuration and a double-wishbone axle system. Within the scope of the study, the low-pressure configuration of the tire was used as the terrain capabilities of the vehicle will be examined and analyzed in rugged terrain conditions. FED-Alpha vehicle configuration parameters are given in Table 4.1 below.

Table 4.1 : FED-Alpa vehicle configuration.

Parameter	Value
Vehicle mass	5157 kg
Vehicle sprung mass	4093 kg
Height	2088 mm
Length	5156 mm
Widht	2288 mm
Wheelbase	3302 mm
Track width	1953,2 mm
Ground clearance	337,8 mm
Vehicle COG position x	2831 mm
Vehicle COG position y	5,08 mm
Vehicle COG position z	966,5 mm
Approach angle	54°
Departure angle	57°
Tire Type	335 / 65 R 22,5
Tire Pressure	35 psi
Engine Type	Cummins 4.5 L Diesel
Transmission Type	6-Speed Automatic

Figure 4.1 : Picture of FED-Alpha vehicle.

In the suspension system, which is essential in the ride quality effect of the vehicle, titanium coil springs are used with air bellows for spring function and dampers that behave differently at low and high frequencies for damping function. The double-wishbone axle system allows the right and left wheels to move independently. In addition, the suspension allows ±180 mm rebound and jounce movement (Figure 4.2).

With the air bellows and the ride height sensor integrated into the axles, the vehicle's height is kept constant against changing weight and load configurations. The air bellows' stiffness value and the vehicle's spring characteristic change according to the suspension speed. When unloaded condition, only titanium springs determine the spring characteristics of the vehicle. As the load on the suspension increases, the pressure of the air inside the air bellows increases and the stiffness value of the suspension has a stiffer curve.

FED-Alpha's damper has two different damping characteristics: a high frequency and low frequency that damper characteristics are selected depending on affected frequency. Depending on the vehicle's speed, lower damping force affects the loads coming with high frequency. On the other hand, as the speed of the vehicle increases, the low-frequency curve increases with a higher trend. In this case, it can be concluded that the vehicle's movement in the low-frequency band is dampened more.

There is a stabilizer bar in the suspension system to reduce the vehicle's rolling movement. The stabilizer bar is located only on the front axles, not on the rear. As a result, it affects the handling capacity, especially in road conditions where two wheels move relatively.

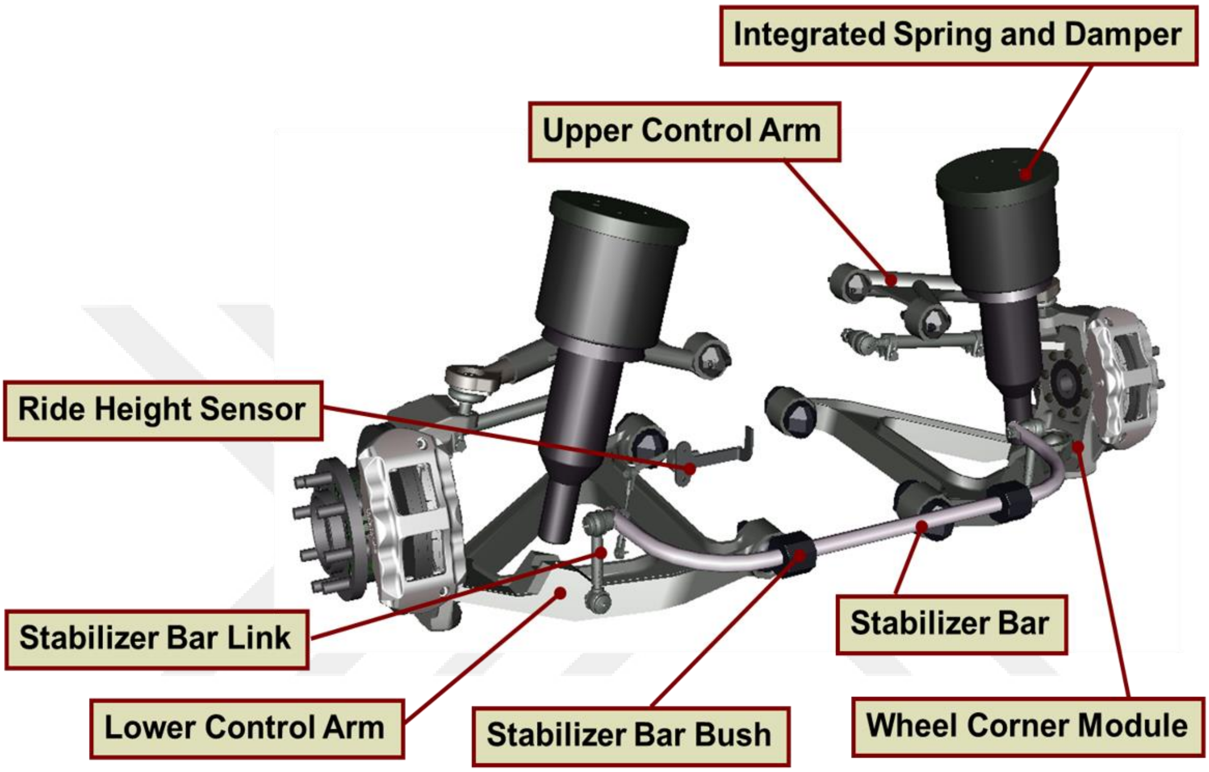

Figure 4.2 : Picture of FED-Alpha suspension system.

4.2 ADAMS Car Simulation

Absorbed power, frequency weighted rms and vibration dose value calculations were made with the help of MATLAB and SIMULINK programs by taking the acceleration data to the driver, the passenger next to the driver and the middle of the seat behind the driver from the FED-Alpha vehicle model using the ADAMS Car program. The vehicle is modeled using the ADAMS Car program and analyses were made on the synthetic road (Figure 4.3).

By the behavior algorithm of the FED-Alpha suspension system, titanium springs and air bellows, stiffness values corresponding to different speeds in particular rebound and bound movements were modeled by creating a look-up table. In addition, the low and high-frequency characteristic in the damper model is modeled as a transfer function.

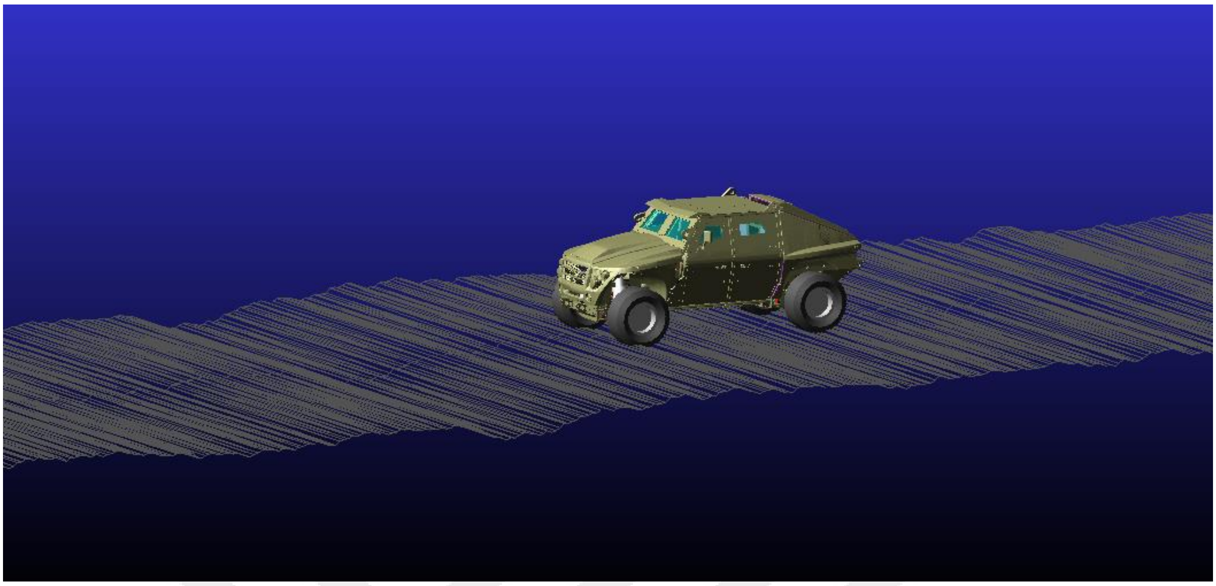

Figure 4.3 : Picture of FED-Alpha in the ADAMS Car program on the synthetic road.

The simulation solver parameter and modeling parameter used in ADAMS Car simulation are given in Table 4.2 below.

Table 4.2 : Simulation solver parameter and modeling parameter in the ADAMS Car.

Parameter	Value
Output Sampling Rate	100 Hz
Tire Contact Model	3D Enveloping Contact
Damper Model	Transfer Function
Suspension Model	Look-up Table
Tire Pressure	35 psi
ADAMS Solver Integrator	HHT
ADAMS Solver Error	$2{,}5E^{-5}$

4.3 Absorbed Power Calculation Method

The absorbed power is calculated by two different methods using MATLAB and SIMULINK programs: FFT Method ve Transfer Function Method. There are studies in the literature using two methods. The primary purpose of this study is to compare two different methods, identify the method that converges most with the test results, and carry out detailed analyses with it.

4.3.1 Fast Fourier transform (FFT) method

The acceleration data obtained in the time domain were transformed into the frequency domain with the help of the Fast Fourier Transform (FFT) method. Then, these accelerations are multiplied by the coefficient C_i according to Equation 2.2 and the absorbed power value is calculated. This calculation is repeated for all three axes.

C is calculated with the coefficients K and F, as shown below. Coefficients are calculated for different formulations in all three axes and are described in the TOP-01-014 [1] standard. The calculation method is as shown below.

Longitudinal / Fore-Aft (X)

$$K_0 = 4{,}3532 \tag{4.1}$$

$$K_1 = 1{,}356 \tag{4.2}$$

$$W_i = 2\pi f_i \tag{4.3}$$

$$F_1 = 1{,}0 \tag{4.4}$$

$$F_2 = 0{,}219106 \tag{4.5}$$

$$F_3 = -0{,}0185308 W_i^2 + 1 \tag{4.6}$$

$$F_4 = -0{,}00061893 W_i^2 + 0{,}219106 \tag{4.7}$$

Transverse / Side-to-Side (Y)

$$K_0 = 4{,}353 \tag{4.8}$$

$$K_1 = 1{,}356 \tag{4.9}$$

$$W_i = 2\pi f_i \tag{4.10}$$

$$F_1 = 0{,}24052124 * 10^{-3} {W_i}^4 - 0{,}066974483 {W_i}^2 + 1 \tag{4.11}$$

$$F_2 = 0{,}57384538 * 10^{-5} {W_i}^4 - 0{,}50170413 * 10^{-2} {W_i}^2 + 0{,}33092592 \tag{4.12}$$

$$F_3 = -0{,}14979958 * 10^{-5} {W_i}^6 + 0{,}0010088882 {W_i}^4 - 0{,}10108617 {W_i}^2 + 1 \tag{4.13}$$

$$F_4 = -0{,}1713749 * 10^{-7} {W_i}^6 + 0{,}53137351 * 10^{-4} {W_i}^4 - 0{,}011096507 {W_i}^2 + 0{,}33092592 \tag{4.14}$$

Vertical (Z)

$$K_0 = 4{,}3537 \tag{4.15}$$

$$K_1 = 1{,}356 \tag{4.16}$$

$$W_i = 2\pi f_i \tag{4.17}$$

$$F_1 = -0{,}10245 * 10^{-9} {W_i}^6 + 0{,}17583 * 10^{-5} {W_i}^4 - 0{,}44601 * 10^{-2} {W_i}^2 + 1 \tag{4.18}$$

$$F_2 = 0{,}12882 * 10^{-7} {W_i}^4 - 0{,}93394 * 10^{-4} {W_i}^2 + 0{,}10543 \tag{4.19}$$

$$F_3 = -0{,}45416 * 10^{-9} W_i^{\,6} + 0{,}37667 * 10^{-5} W_i^{\,4} - 0{,}56104 * 10^{-2} W_i^{\,2} + 1 \tag{4.20}$$

$$F_4 = -0{,}21179 * 10^{-11} W_i^{\,6} + 0{,}51728 * 10^{-7} W_i^{\,4} - 0{,}17947 * 10^{-3} W_i^{\,2} + 0{,}10543 \tag{4.21}$$

W_i : $2\pi f_i$ Frequency, radians/second

f_i: frequency weighting factors

4.3.2 Transfer function method

The accelerations in the time domain taken from the sensors on the vehicle are analyzed in the transfer functions described in the TARADCOM report [24] to calculate the absorbed power. The solution has been found by integrating transfer functions into SIMULINK. Different transfer functions are defined for each axis. The acceleration values in the transfer functions must be converted to ft/sec^2 units. The transfer function acts as a weighting factor.

Longitudinal / Fore-Aft (X)

$$G(S) = \frac{230S}{(S^2 + 16S + 100)(S + 15)} \tag{4.22}$$

Transverse / Side-to-Side (Y)

$$G(S) = \frac{525S(S + 9{,}47)(S + 9{,}8)}{(S^2 + 8{,}8S + 142)(S^2 + 3{,}39S + 14{,}2)(S + 126)} \tag{4.23}$$

Vertical (Z)

$$G(S) = \frac{14{,}5S(S + 44)}{(S^2 + 24S + 750)(S + 63)} \tag{4.24}$$

4.3.3 Compare absorbed power calculation method

Analyzes were made at a speed of 8,05 km/h up to 19,32 km/h and the acceleration data from the driver's seat base were recorded on the 5,08 cm rms synthetic road. Calculations were made with the above-mentioned absorbed power calculation methods using MATLAB and

SIMULINK. It has been determined that the FFT method and the transfer function method created by TRADCOM have very close results for all axes (Figure 5.5, 4.5, 4.6). Therefore, it was decided to continue further studies with the TRADCOM Transfer Function in line with this result.

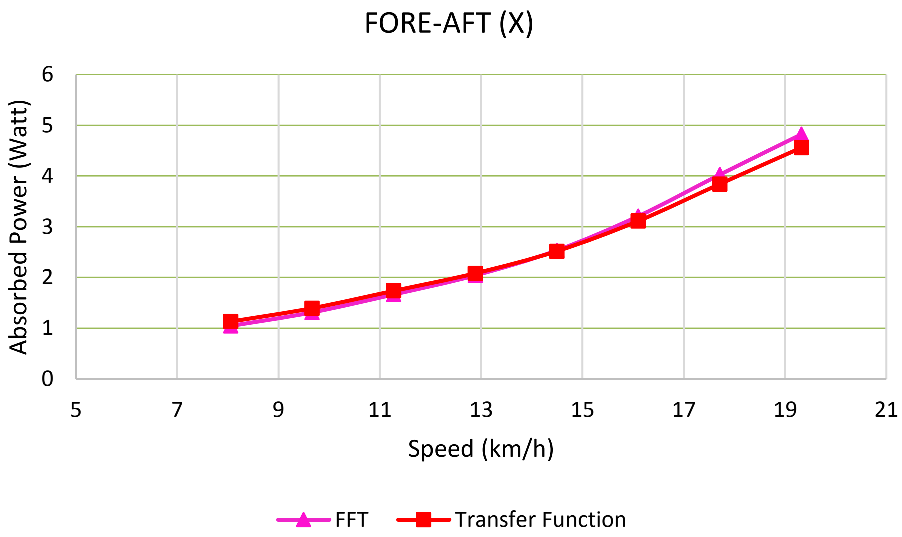

Figure 4.4 : Compare the different calculation methods of the absorbed power results in the fore-aft axis.

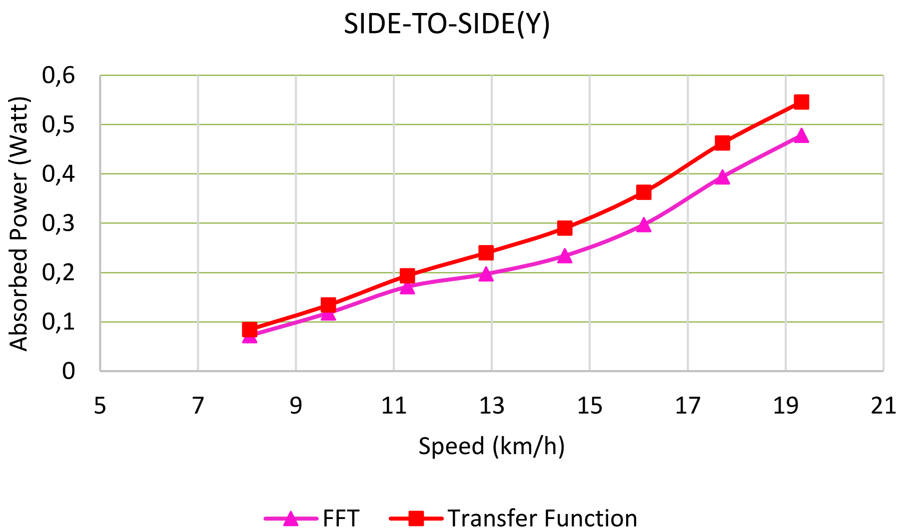

Figure 4.5 : Compare the different calculation methods of the absorbed power results in the side-to-side axis.

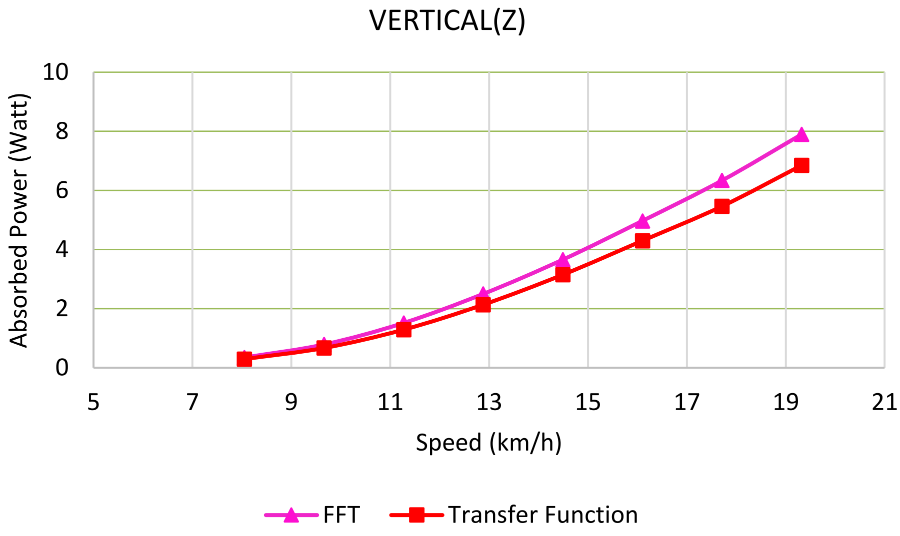

Figure 4.6 : Compare the different calculation methods of the absorbed power results in the vertical axis.

4.4 Comparison Between Test and Simulation Model

Before the analysis studies, it should be ensured that the analysis model is correct, and a validation study should be done to ensure its accuracy.

FED-Alpha vehicle tested on symmetrical roads with rms roughness levels of 2,54 cm, 3,81 cm, 5,08 cm, 7,61 cm and 10,16 cm and asymmetrical roads with a rms level of 2,54 cm – 3,81 and 3,81 cm – 5,08 cm. While testing, the vehicle's acceleration data and GPS coordinates were recorded on the driver's seat base. The coordinates taken from the test were modeled in the virtual environment and converted into a file format used by ADAMS Car.

One of the main issues to be considered when comparing simulation and test results is that the sensor sample rate is equal. The evaluation was made by synchronizing the simulation sample rate with the test.

Simulations and tests were performed between 8,6 km/h and 17,2 km/h speed on the 5,08 rms symmetrical road. The results are graphed as absorbed power, vibration dose value and frequency weighted rms acceleration. As can be seen, the test and analysis methods draw very close graphs to each other. When the methods are compared, it is seen that the highest harmony is achieved in the z-axis with the vibration dose value method. In absorbed power and frequency weighted rms acceleration methods, even if the correlation decreases as the speed of the vehicle increases in the z-axis, it is not at a level that makes the accuracy of the analysis model doubtful. For all methods, correlation in the y-axis is better at high speeds and worse at low speeds. The x-axis results change as the speed with the driver difference between test and analysis in all methods (Figure 4.7, 4.8, 4.9).

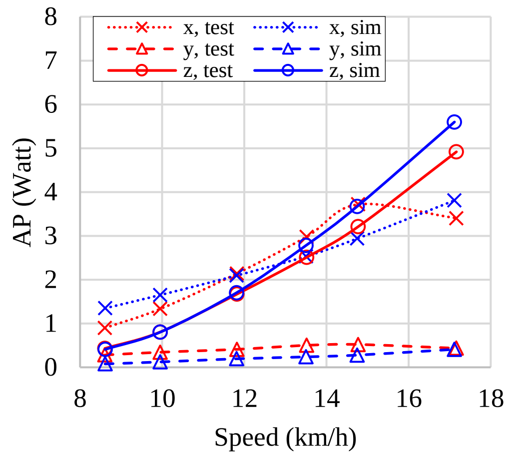

Figure 4.7 : The absorbed power test and simulation results on 5,08 cm rms KRC symmetric road in all axes.

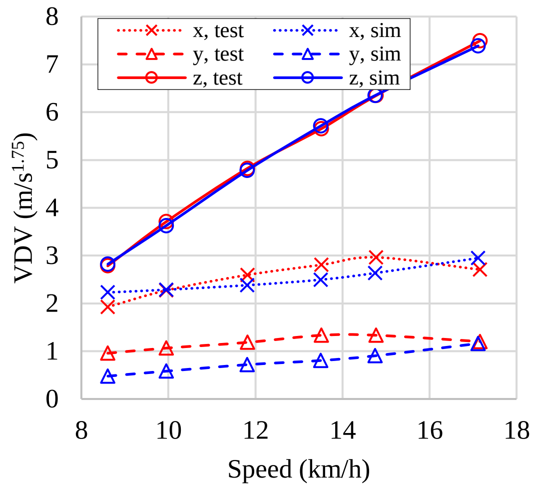

Figure 4.8 : Freq. Weighted rms acc. test and simulation results on 5,08 cm rms KRC symmetric road in all axes.

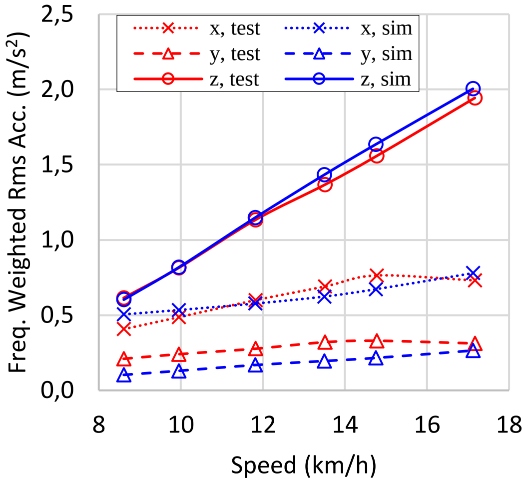

Figure 4.9 : The vibration dose value test and simulation results on 5,08 cm rms KRC symmetric road in all axes.

Simulations and tests performed between 8,6 km/h and 17,2 km/h speed 2,54 cm – 3,81 cm asymmetrical road. The absorbed power comparison graph is presented in Figure 4.7, the vibration dose value comparison graph is presented in Figure 4.8 and the frequency weighted rms acceleration comparison graph is presented in Figure 4.9. As can be seen, in parallel with the result reached in symmetrical roads, test and analysis methods draw very close graphs to each other. On asymmetrical roads, the driver completes the test by keeping the steering of the vehicle stable and keeping the vehicle stable on one side of the road with low rms roughness and one side on the road with high rms roughness. In all calculation methods, the worst correlation was obtained on the y-axis. This result may be occurred due to differences in the driver of test and analysis. The best correlation was obtained on the z-axis for all methods (Figure 4.10, 4.11, 4.12).

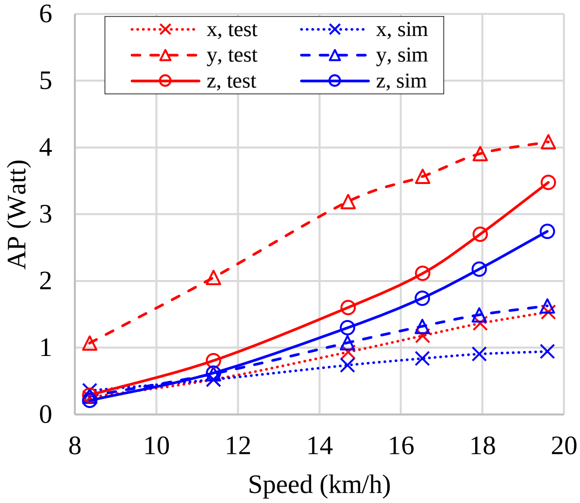

Figure 4.10 : Absorbed power test and simulation results on 3.81 cm – 2.54 cm rms KRC asymmetric road in all axes.

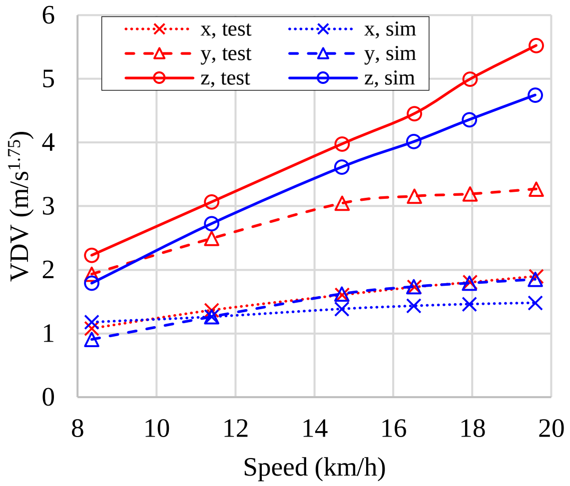

Figure 4.11 : The vibration dose value test and simulation results on 3.81 cm – 2.54 cm rms KRC asymmetric road in all axes.

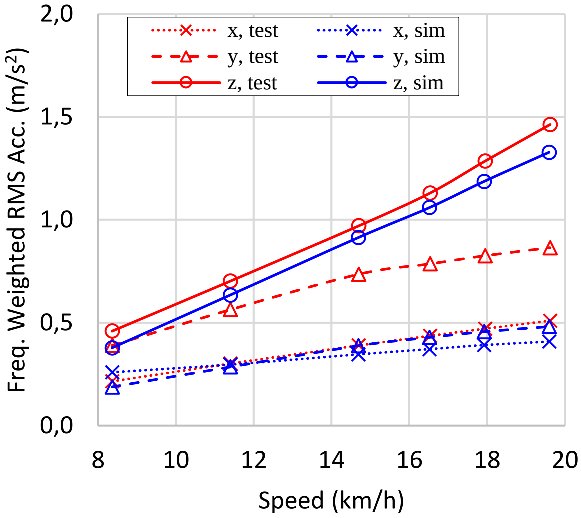

Figure 4.12 : Freq weighted rms acc. test and simulation results on 3.81 cm – 2.54 cm rms KRC asymmetric road in all axes.

As a result of the analyzes and tests performed on all road profiles, the linear correlation factors matrix was created for the z-axis (Table 4.3). In addition to all analysis methods, results for both driver and passenger are given in the matrix. With a very high correlation factor of 0,99, this value shows us that the analysis model of the vehicle is compatible with the actual vehicle.

Table 4.3 : R^2 Correlation factors in the z-axis.

Road Profile	AP		VDV		a_w	
	Driver	Passenger	Driver	Passenger	Driver	Passenger
2,54 cm rms, symmetric	1,00	0,99	0,99	0,99	1,00	1,00
3,81 cm rms, symmetric	1,00	1,00	1,00	1,00	1,00	1,00
5,08 cm rms, symmetric	1,00	1,00	1,00	1,00	1,00	1,00
7,62 cm rms, symmetric	1,00	1,00	1,00	1,00	1,00	1,00
10,16 cm rms, symmetric	1,00	1,00	0,99	1,00	1,00	1,00
3,81 cm – 2,54 cm rms, asymmetric	1,00	1,00	0,99	1,00	1,00	1,00
5,08 cm – 3,81 cm rms, asymmetric	1,00	1,00	1,00	1,00	1,00	1,00

According to the results obtained, it can be deduced that the results of the ADAMS Car analysis model will be close to the results of the actual vehicle tests.

5. SYNTHETIC ROAD SIMULATIONS AND RESULTS

Synthetic roads were created by changing the parameters to see the effect of road parameters on ride quality. Acceleration data will be recorded by driving the vehicle on these roads at various speeds. Data measured from the seat base from three different vehicle positions will be used in all analyses. The effect of ride quality will be examined by calculating absorbed power, frequency weighted rms acceleration and vibration dose value from the acceleration data.

Vehicle speed, steering wheel angle, COG change at z and y directions, chassis roll and pitch angle will be recorded to help interpret the results.

5.1 The Effects of Rms Roughness on Ride Quality

5.1.1 Simulation results of the effects of rms roughness

FED-Alpha vehicle is driven on 2,54 cm, 3,81 cm, 5,08 cm and 6,35 cm rms roughness roads . X, y and z axes acceleration data will be recorded from the driver seat base, passenger seat base and rear passenger seat center.

6-Watt absorbed power speed, frequency weighted rms acceleration and vibration dose value graphs will be examined to observe the ride quality effect of increased rms roughness level.

Change of absorbed power, frequency-weighted rms acceleration and vibration dose values in the z-axis for the driver seat base between 8,05 km/h and 24 km/h are shown in Figure 5.1, 5.2. 5.3. As a result of the increase in the vibration evaluation values, ride quality decreases, with increasing rms value. When compared to frequency weighted rms acceleration and vibration dose value methods, it can be said that the absorbed power method is most affected by the increase in speed. This conclusion can be obtained due to the fact that the increasing slope of the evaluation values against speed is seen in the most absorbed power method.

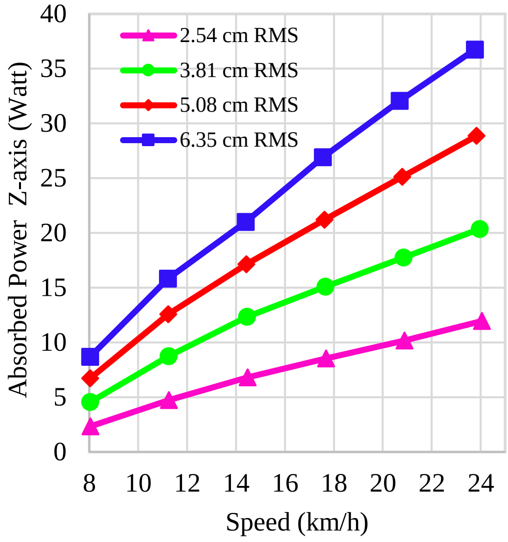

Figure 5.1 : The absorbed power results of the driver seat base as a function of vehicle speed on different roughness roads in the z-axis.

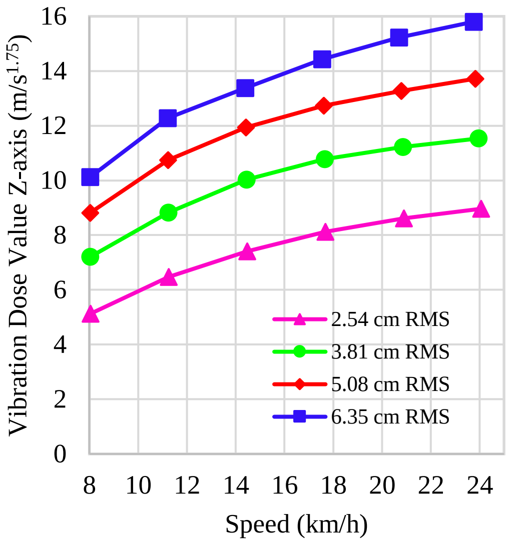

Figure 5.2 : The vibration dose value results of the driver seat base as a function of vehicle speed on different roughness roads in the z-axis.

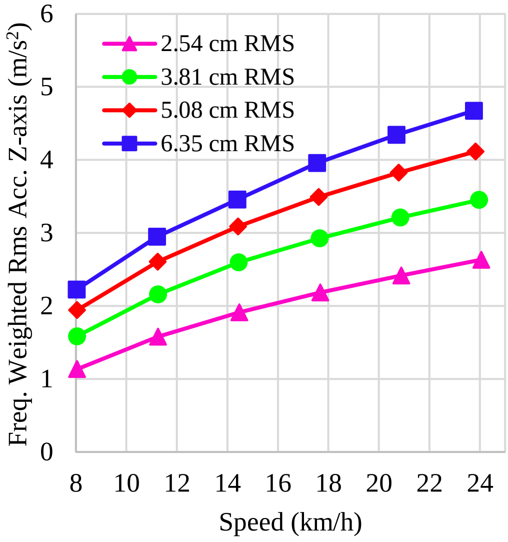

Figure 5.3 : The freq. weighted acc. results of the driver seat base as a function of vehicle speed on different roughness roads in the z-axis.

A second-order polynomial curve is set to the absorbed power curve plotted depending on the speed. According to this polynomial, the vehicle speed corresponding to 6-Watt of absorbed power is calculated. Speed values to reach 6-Watt absorbed power are 13,35 km/h for 2,54 cm rms road, 9,08 km/h for 3,81 cm rms road, 7,33 km/h for 5,08 cm rms road and 6,51 km/h for 6,35 cm rms road (Figure 5.4).

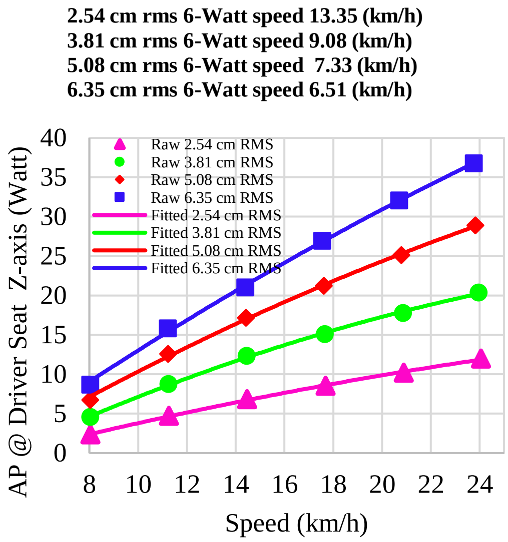

Figure 5.4 : The absorbed power results and the 6-watt speed of the driver seat base as a function of vehicle speed on different roughness roads in the z-axis.

It is evaluated that as the road roughness increases, the decrease in ride quality is due to the increase in the amplitudes of the accelerations transmitted to the vehicle body. The acceleration amplitudes are higher on the 6,35 cm rms road in the time domain (Figure 5.5).

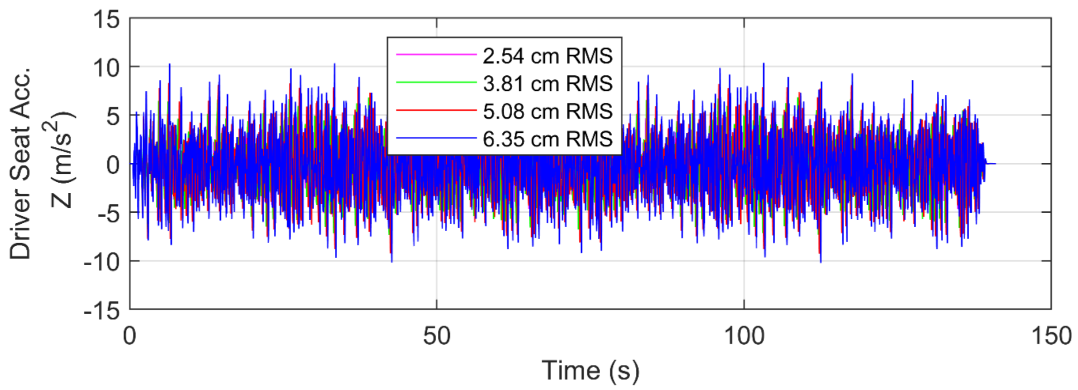

Figure 5.5 : Driver seat acceleration as a function of time on different roughness roads.

The graphs plotted for the x-axis for the absorbed power, frequency weighted rms acceleration and vibration dose value in the vehicle speed domain (Figure 5.6, 5.7, 5.8). It is seen from the graphs that as the rms roughness value increases, the vibration evaluation values in the x-axis increase. When all evaluation methods are compared, the highest seat acceleration values are seen on the 6,35 cm rms road, which is the highest roughness value. Absorbed power and frequency weighted rms acceleration methods seem to change with the same trend against the increasing speed. It is seen that the vibration dose value on the x-axis does not change as the speed increases, except for 20 km/h. Decrease seen in all vibration evaluation values at a speed of 20 km/h on low rms (2,54, 3,81 and 5,08) roads. Also, a decrease was seen at 18 km/h on a high rms road. These decreases are explained by the decrease of the maximum accelerations in the longitudinal direction in the 1,5 Hz region. Since the frequency range of 1.5 Hz is the region where high weighting factors are multiplied, a slight change in acceleration values in this region has a significant effect on the results. This decrease may also be due to the damper function. To better understand the reason, it is necessary to make an evaluation in the frequency domain by including the suspension characteristics into the analysis parameters.

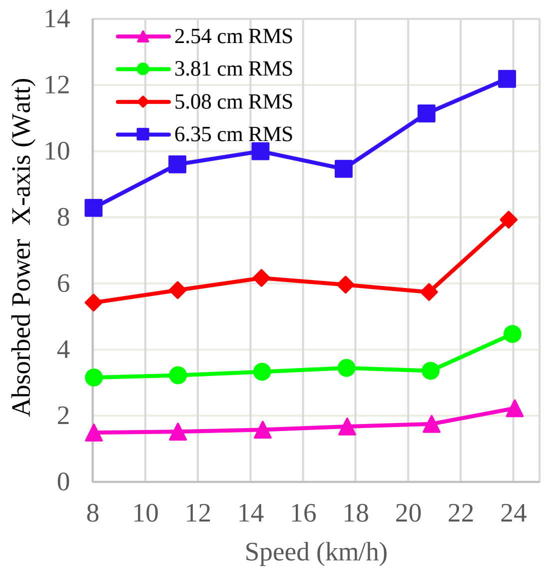

Figure 5.6 : The absorbed power results of the driver seat base as a function of vehicle speed on different roughness roads in the x-axis.

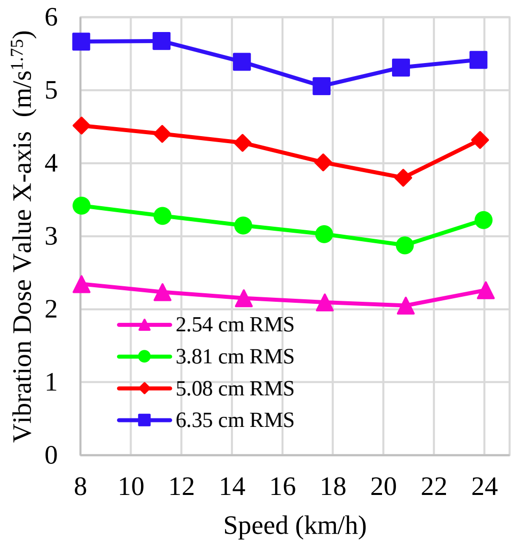

Figure 5.7 : The vibration dose value results of the driver seat base as a function of vehicle speed on different roughness roads in the x-axis.

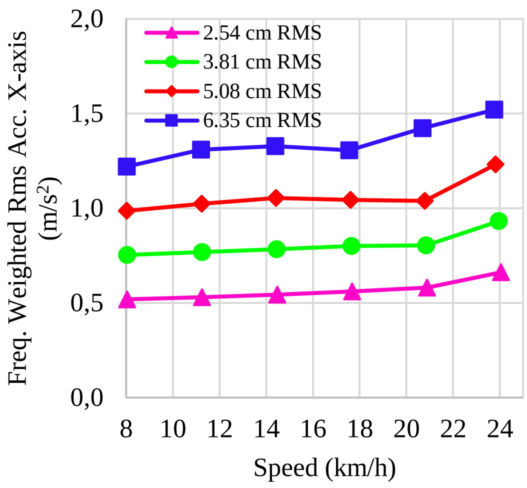

Figure 5.8 : The freq. weighted rms acc. results of the driver seat base as a function of vehicle speed on different roughness roads in the x-axis.

The graphs plotted for the absorbed power, frequency weighted rms acceleration and vibration dose value values in the vehicle speed domain for the y-axis (Figure 5.9, 5.10, 5.11). The graphs show that as the rms roughness value increases, the ride quality in the y-axis decreases. The correlation could not be detected in the vibration evaluation values depending on the speed. As the speed increased up to 18 km/h for each rms, the vibration evaluation values increased and decreased after 18 km/h. When the change in vibration evaluation values is negligible, it is thought that the driving quality does not change with the increase in speed.

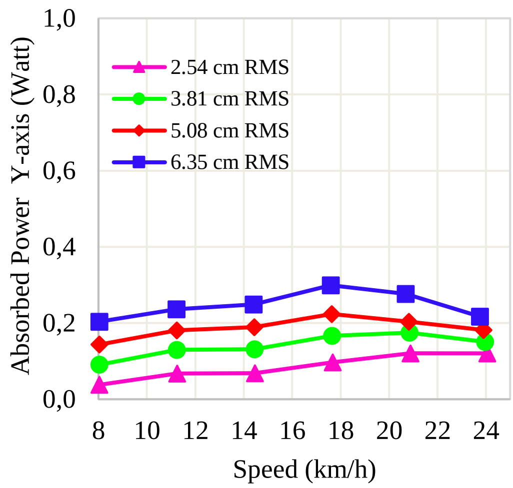

Figure 5.9 : The absorbed power results of the driver seat base as a function of vehicle speed on different roughness roads in the y-axis.

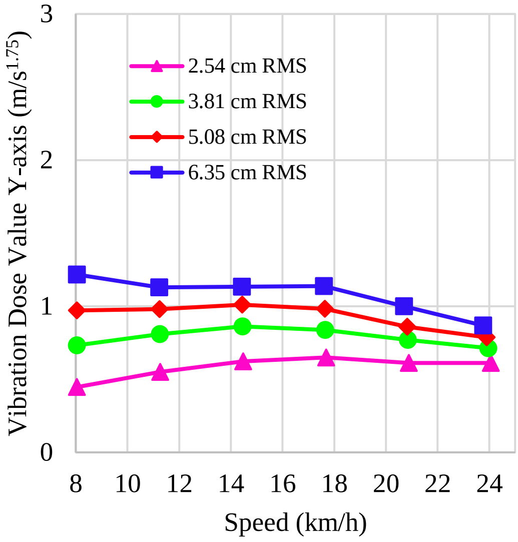

Figure 5.10 : The vibration dose value results of the driver seat base as a function of vehicle speed on different roughness roads in the y-axis.

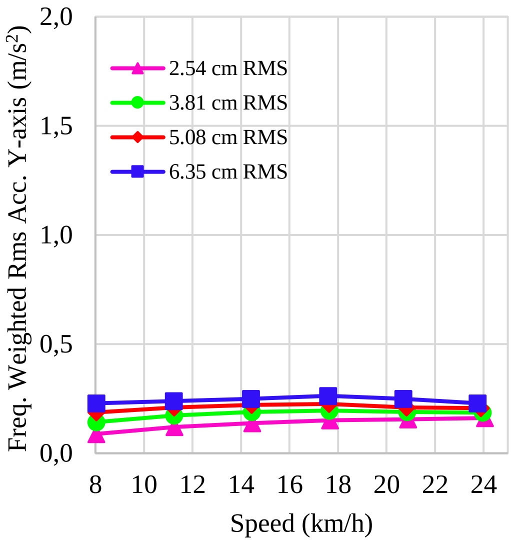

Figure 5.11 : The freq. weighted rms acc. results of the driver seat base as a function of vehicle speed on different roughness roads in the y-axis.

The acceleration was recorded on the seat base at the driver, passenger and rear passenger seat center. Considering that the values of increased vibration evaluation negatively affect comfort, when these values are examined, it is seen that the highest feeling of discomfort is in the rear passenger. It has been determined that the most comfortable is passenger. Examining this relation on the z-axis for FED-Alpha; On the 2,54 cm rms road, the driver reached 6-Watt at a speed of 13,35 km/h, the passenger at 15.28 km/h and the rear passenger at 9,63 km/h. On the 6,35 cm rms road, the driver reached 6-Watt at 6,51 km/h, passenger 7,01 km/h and rear passenger 5,45 km/h. The relation is the same in other axes and other evaluation methods (Figure 5.12, 5.13).

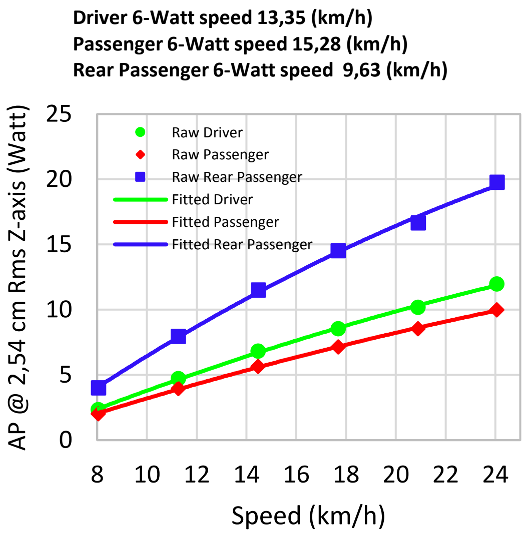

Figure 5.12 : The absorbed power results according to sensor location as a function of the 6-Watt speed at 2,54 rms road in the z-axis.

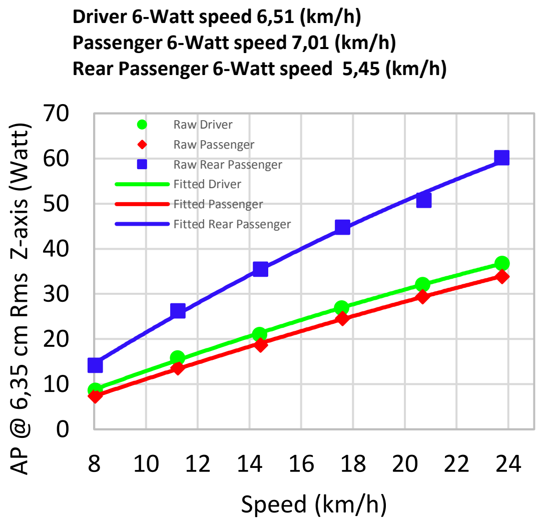

Figure 5.13 : The absorbed power results according to sensor location as a function of the 6-Watt speed at 6,35 rms road in the z-axis.

5.1.2 Discussion on the effects of rms roughness

As a result of the analyses, it has been determined that the ride quality decrease with the increasing rms roughness level, and the vibration evaluation values increase. The ride quality decreases with increasing speed in the z-axis. As the roughness of the road increases, the 6-Watt speed decreases in the z-axis. When the accelerations from the driver's seat are examined, 6-Watt speed is 13,35 km/h at 2,54 cm roughness, 9,08 km/h at 3,81 cm roughness, 7,33 km/h at 5,08 cm roughness and 6,51 km/h at 6,35 cm roughness road (Figure 5.14).

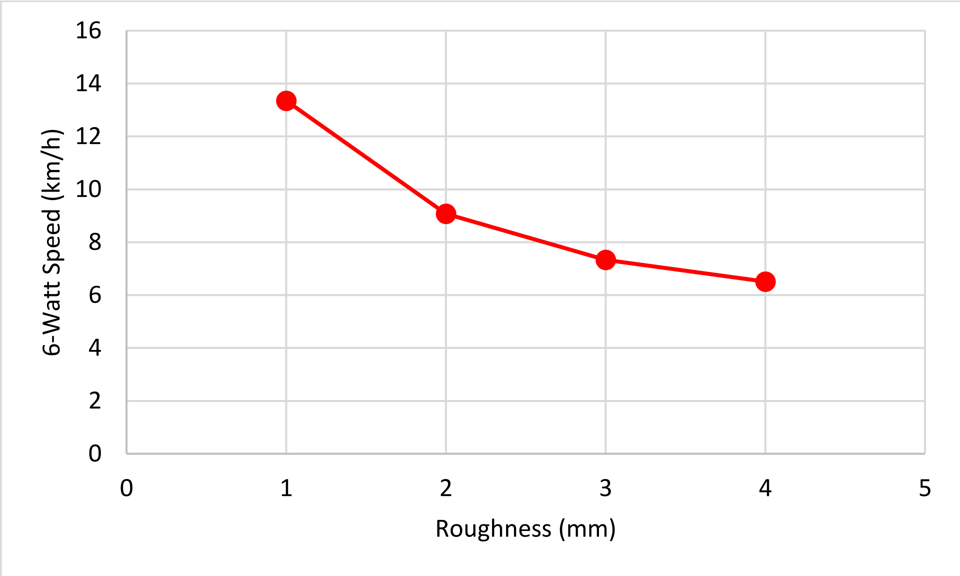

Figure 5.14 : 6-Watt speed on different roughness roads in the z-axis.

It is seen that the ride quality is negatively affected by the increased rms roughness value for the x and y axes. However, the effect of the increasing speed should be evaluated together with the analysis in the frequency domain.

When the variation of the comfort level in the FED-Alpha vehicle is examined, it is seen that the passenger seat has the highest comfort level and the rear passenger has the lowest comfort level.

As the speed increases, it is observed that the vibration evaluation values in the z-axis increase for all evaluation methods. The response of the absorbed power evaluation method against the changing speed is higher than the other evaluation methods. It is seen that time-domain analyzes are not solely sufficient for the x and y axes in the ride quality analysis.

5.2 The Effects of Waviness on Ride Quality

5.2.1 Simulation results of the effects of waviness

Waviness is the negative slope of the PSD curve plotted against spatial frequency in a logarithmic scale. The waviness value of a regular road is accepted as 2. In this study, synthetic roads having a waviness lower and higher than 2 have been created. The acceleration data measured from the seat base of the vehicle from three different positions of the vehicle is used on these roads. The effect of ride quality will be examined by calculating absorbed power, frequency weighted rms acceleration and vibration dose value from the acceleration data.

As the waviness value decreases, it is considered that there is a higher power density in the low-frequency region of the road. In all evaluation methods, the weighting function factors of low-frequency regions are higher. The PSD values in the low waviness graph are in the higher power density region. The power density value of the road with high waviness in the high-frequency region is lower (Figure 5.15).

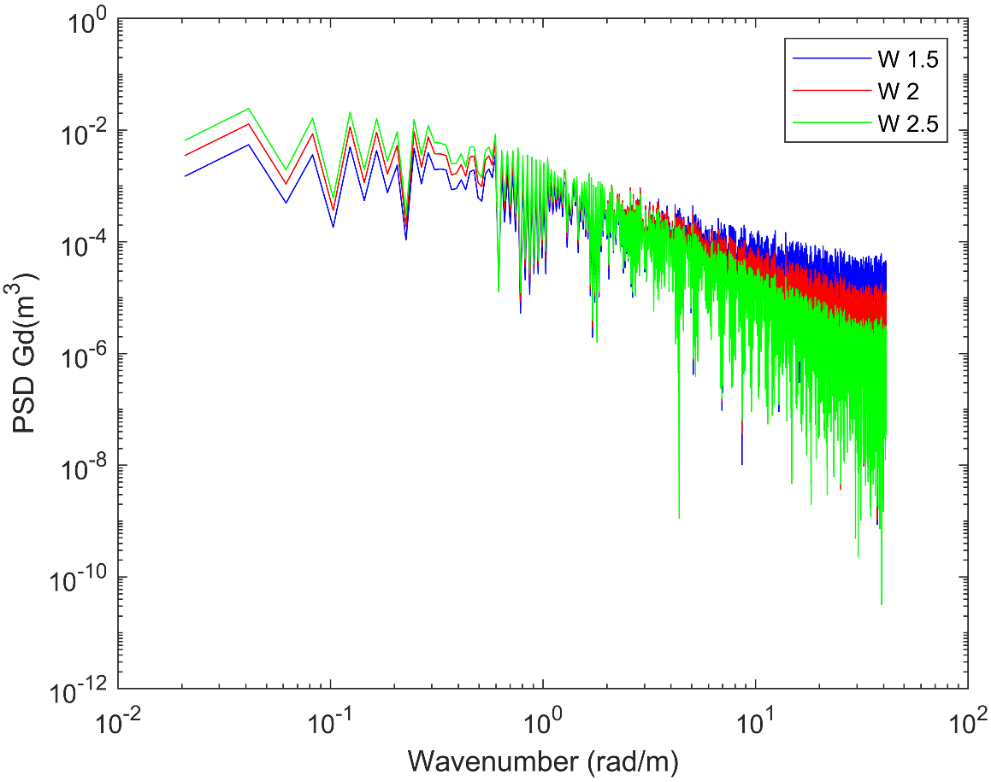

Figure 5.15 : PSD road graph in different waviness as a function of wavenumber.

It is observed that the waviness change gives similar responses in the absorbed power, frequency weighted rms acceleration and vibration dose value values in the z-axis. It is seen that vibration evaluation values in the z-axis increase as waviness decreases. As a result of the increase in the vibration evaluation values, ride quality decreases, with decreasing waviness in the z-axis. The vibration evaluation values increase as the speed increases in all waviness values. It is seen that the evaluation method, which gives the most sensitive results to the increasing speed, is the absorbed power method (Figure 5.16, 5.17, 5.18).

The vibration evaluation values are high in the z-axis on the low waviness road. Because the low waviness road has high PSD values at high wavenumber bandwidth. It is concluded that high wavenumber band PSD values are more effective on ride quality.

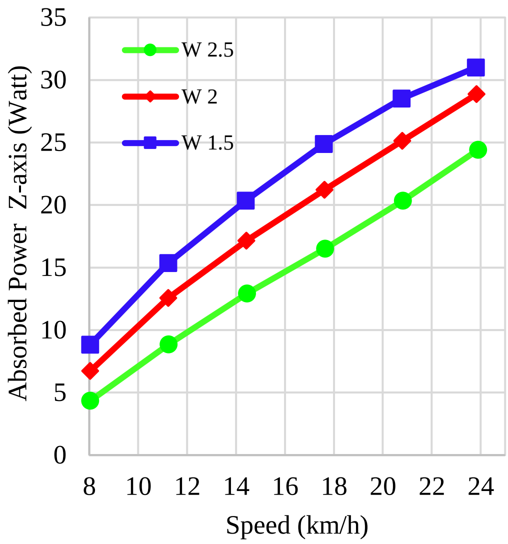

Figure 5.16 : The absorbed power results of the driver seat base as a function of vehicle speed on different waviness roads in the z-axis.

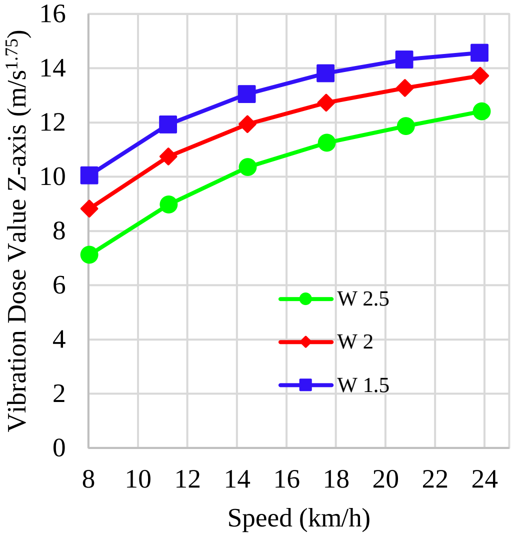

Figure 5.17 : The vibration dose value results of the driver seat base as a function of vehicle speed on different waviness roads in the z-axis.

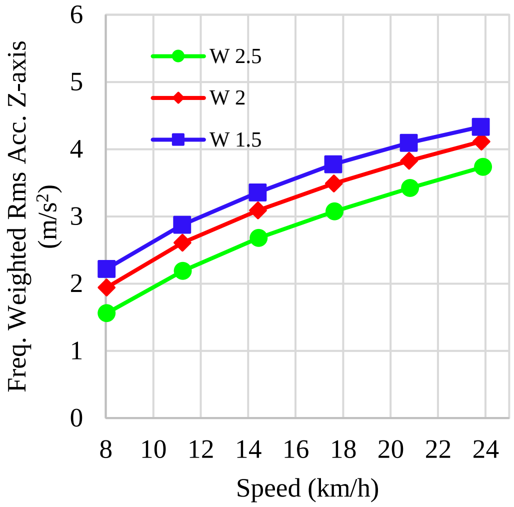

Figure 5.18 : The freq. weighted rms acc. results of the driver seat base as a function of vehicle speed on different waviness roads in the z-axis.

A second-order polynomial curve is set to the driver seat base's absorbed power curve, depending on the speed. According to this polynomial, the vehicle speed corresponding to 6-Watt of absorbed power was calculated. The 6-Watt speed was found at 6,47 km/h for the 1,5 waviness road, 7,33 km/h for the 2 waviness road and 9,19 km/h for the 2,5 waviness road. It is clear that the waviness value of the road is significant in terms of ride quality and should be defined in the analysis and related standards (Figure 5.19).

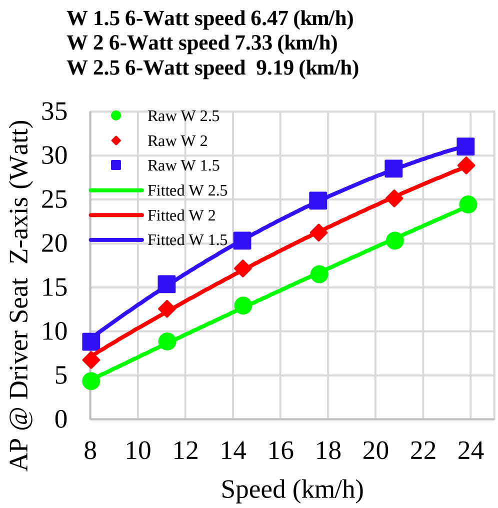

Figure 5.19 : The absorbed power results and the 6-watt speed of the driver seat base as a function of vehicle speed on different waviness roads in the z-axis.

The graphs plotted for the absorbed power, frequency weighted rms acceleration and vibration dose value values in the vehicle speed domain in the y-axis (Figure 5.20, 5.21, 5.22). It is seen that different waviness values do not have much effect on the ride quality of the vehicle on the y-axis. It is assumed that there is no change in the ride quality feeling of the vehicle in the y-axis with the increasing speed. The reason can be considered the lateral motion and lateral force not changing according to waviness.

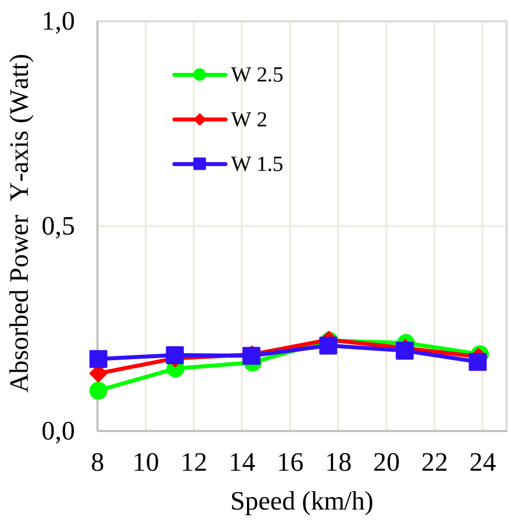

Figure 5.20 : The absorbed power results of the driver seat base as a function of vehicle speed on different waviness roads in the y-axis.

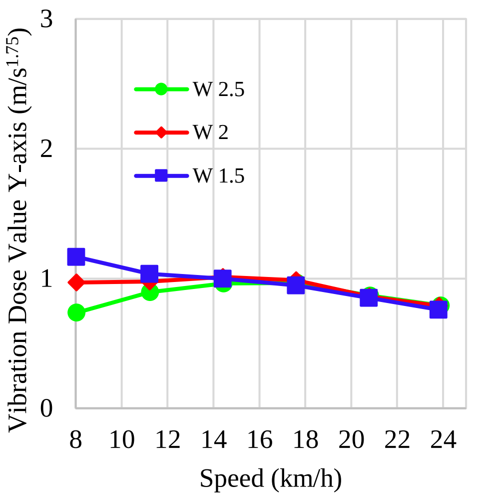

Figure 5.21 : The vibration dose value results of the driver seat base as a function of vehicle speed on different waviness roads in the y-axis.

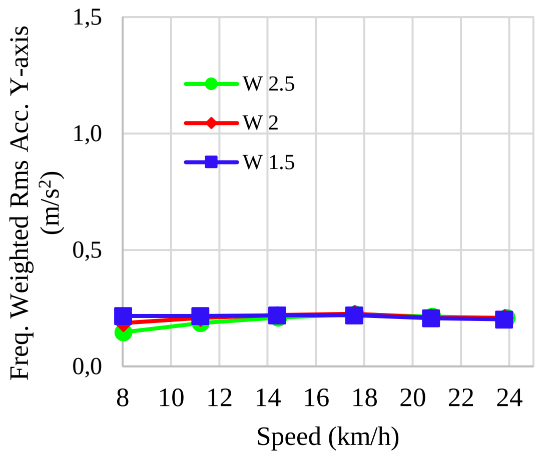

Figure 5.22 : The freq. weighted rms acc. results of the driver seat base as a function of vehicle speed on different waviness roads in the y-axis.

The graphs plotted for the absorbed power, frequency weighted rms acceleration and vibration dose values in the vehicle speed domain plotted for the x-axis (Figure 5.23, 5.24, 5.25). In all evaluation methods, it is seen that as a result of vibration evaluation values increase, ride quality decreases with the waviness decreases. However, it is not enough to explain the vibration evaluation values decrease with vehicle speed increases in the speed domain. It is thought that the decrease in vibration evaluation values in the 20 km/h can be explained by the fact that the pitch and jounce frequencies coincide with the low weighting factor. This decrease also can be explained by a change in the damper function.

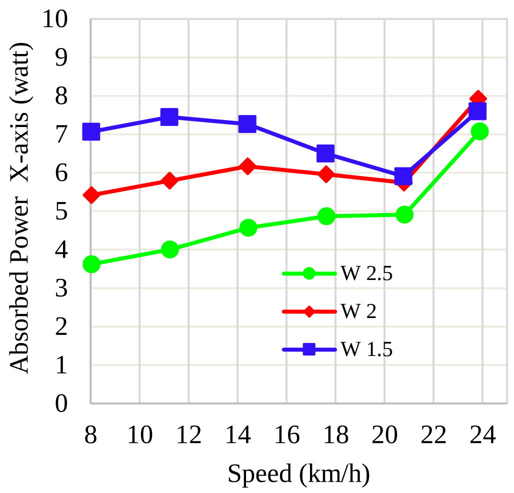

Figure 5.23 : The absorbed power results of the driver seat base as a function of vehicle speed on different waviness roads in the x-axis.

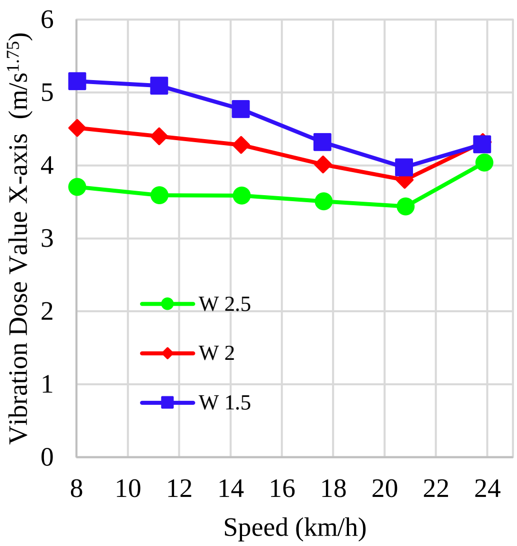

Figure 5.24 : The vibration dose value results of the driver seat base as a function of vehicle speed on different waviness roads in the x-axis.

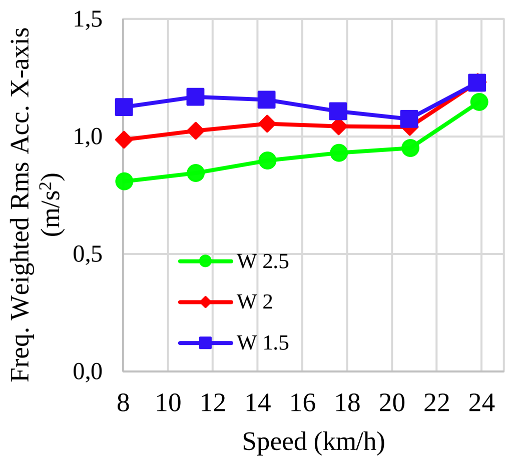

Figure 5.25 : The freq. weighted rms acc. results of the driver seat base as a function of vehicle speed on different waviness roads in the x-axis.

The acceleration in the vehicle was recorded on the seat base at the driver, passenger and rear passenger seat center. When these measurements are examined, it is seen that the highest feeling of discomfort is in the rear passenger. It has been determined that the most comfortable is passenger. When this correlation for FED-Alpha is analyzed on the z-axis in the synthetic road, which is waviness 2, the driver has reached 6-Watt at a speed of 7,33 km/h, the passenger 7,96 km/h and the rear passenger 6,01 km/h. This relation is similar to other evaluation methods and different waviness (Figure 5.26).

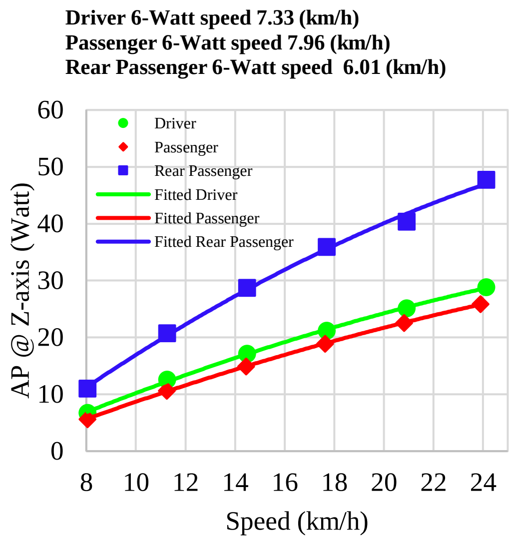

Figure 5.26 : Absorbed power result according to sensors location as a function of 6-Watt speed on waviness 2 road in the z-axis.

5.2.2 Discussion on the effects of rms waviness

The vehicle was driven on synthetic roads with 1,5, 2 and 2,5 waviness. As a result of the analysis, ride quality decreases as the waviness value decreases in all ride quality evaluation methods in the z-axis. In addition, as the test speed increases, all vibration evaluation values increase and the feeling of comfort and ride quality decreases.

As the waviness of the road increases, the 6-Watt speed increase in the z-axis. When the accelerations coming from the driver's seat are examined, 6-Watt speed is 6,47 km/h on 1,5 waviness road, 7,33 km/h on 2 waviness road, 9,19 km/h on 2,5 waviness road (Figure 5.27).

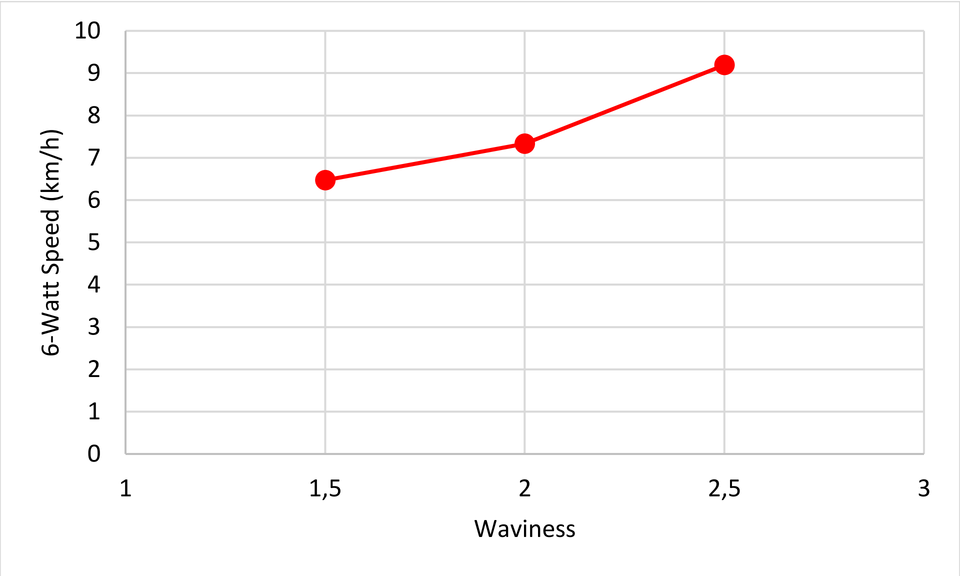

Figure 5.27 : 6-Watt speed on different waviness roads in the z-axis.

When the results on the y-axis are examined, it is seen that there is no change in the ride quality evaluation values of the vehicle under the effect of increasing speed and changing waviness.

When the results in the x-axis are examined, it is determined that the ride quality increase during the waviness value increase. However, no correlation could be detected with the increasing vehicle speed.

When the effect of the location where the acceleration data were recorded, it was determined that the lowest ride quality was in the rear passenger, and the highest ride quality was in the passenger.

It is seen that the absorbed power evaluation method is most affected by the waviness and speed change. For this consideration, it is thought that absorbed power will provide an advantage in examining the effect of change in ride quality.

It is clear from the analyses that the ride quality changes significantly with waviness, especially in the z-axis. Therefore, in all ride quality evaluations, before the test and analyses, road waviness should be defined and the waviness characteristic of the road should be known.

5.3 The Effects of Wavenumber on Ride Quality

5.3.1 Simulation results of the effects of wavenumber

Wavelength can be defined as the width of the wavelength formed by the road, and wavenumber can be defined as wavelengths quantity in the road. These expressions are the opposite of each other.

TOP-01-014 [1] states that the wavelength bandwidth should be in the range of 0,15 to 19,51 meters in ride quality analysis.

Synthetic roads were created wavelength band range between 0,15 - 19,51 meters, 0,15 - 39,01 meters, 0,3 - 39,01 meters, and 0,46 - 39,01 meters. And the vehicle was driven on these roads to observe the wavenumber effect on the vehicle's ride quality.

PSD graphics of the generated synthetic roads are given in Figure 5.28 as below.

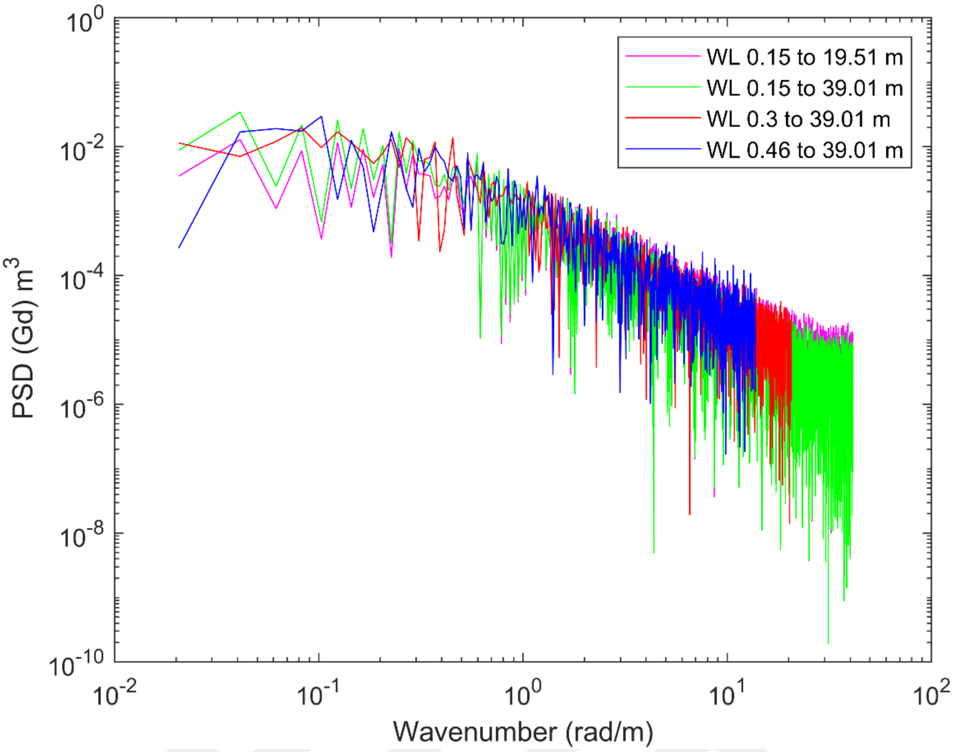

Figure 5.28 : Different wavelength bandwidth.

The ride quality on the z-axis is affected by the change in the wavenumber bandwidth of the road. In the z-axis, all the vibration evaluation values give similar increasing and decreasing trends. The worst ride quality is on the road with a wavelength bandwidth between 0,15 - 19,51 meters. The best ride quality at low speeds on the road with a wavelength bandwidth between 0,46 - 39,01 meters. The best ride quality at high speeds on the road with a wavelength bandwidth between 0,15 - 39,01 meters. Wavelength bandwidth between 0,46 - 39,01 meters has lower vibration evaluation values at low speeds. Therefore, the increasing trend according to vehicle speed is higher than other roads.

As the speed of the vehicle increases, the vibration evaluation values in the z-axis increase in all evaluation methods (Figure 5.29, 5.30, 5.31).

It is necessary to examine the PSD graph of the road and the vibration evaluation values together to understand the reason for the change in ride quality according to wavenumber bandwidth.

When the vibration evaluation values are compared with the 0,15 - 19,51 and 0,15 - 39,01 wavelength bandwidth roads, it is seen that the road with the narrower bandwidth at the low wavenumber range has higher values. According to this result, it can be concluded that the ride quality is lower with the narrower bandwidth at the low wavenumber range. From these results, it can be determined that increasing the bandwidth at low wavenumber reduces the harshness of the road.

The vibration evaluation values increase as the vehicle speed increases. When the effect of the wavelength bandwidth at the high wavenumber range is examined, it can be concluded that the vibration evaluation values of the wider bandwidth road at low speeds are high. However, the vibration evaluation values increase rapidly on the narrower bandwidth road at the high wavenumber range depending on the increasing speed. These results show that if the road has a narrow bandwidth at a high wavenumber range, it is more affected by speed increase. However, the reason for these results can be found by examining the data in the frequency band.

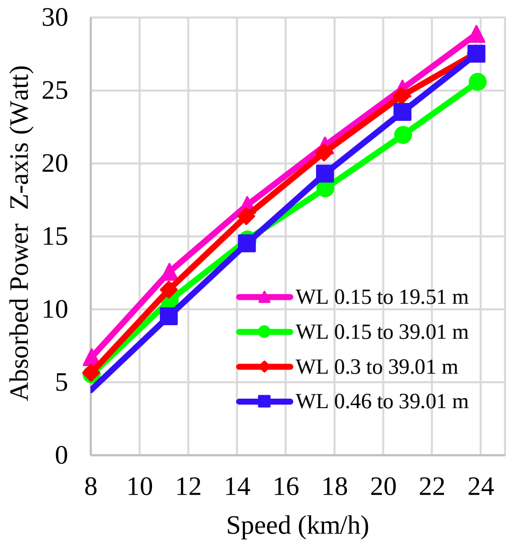

Figure 5.29 : The absorbed power results of the driver seat base as a function of vehicle speed on different wavelength bandwidth roads in the z-axis.

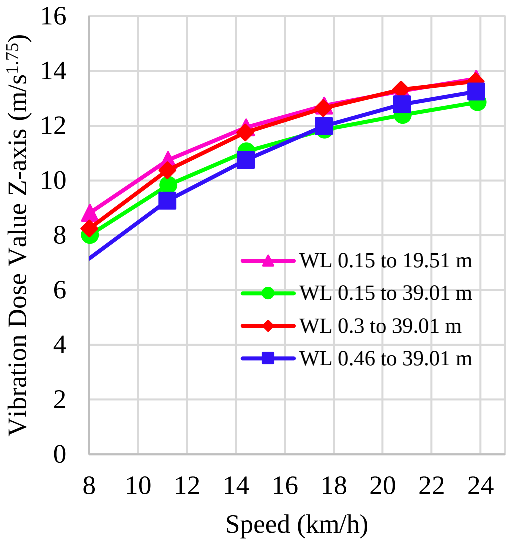

Figure 5.30 : The vibration dose value results of the driver seat base as a function of vehicle speed on different wavelength bandwidth roads in the z-axis.

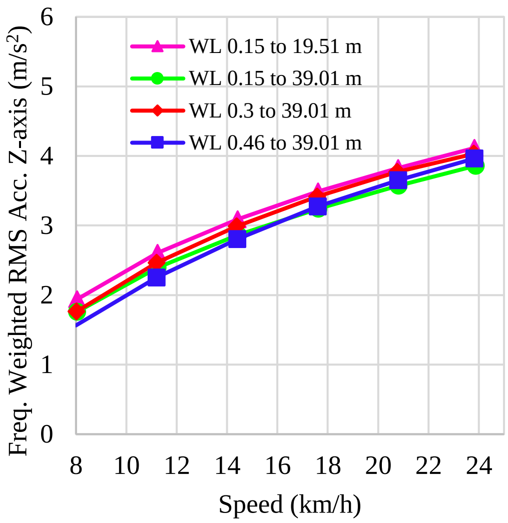

Figure 5.31 : The freq. weighted rms acc. results of the driver seat base as a function of vehicle speed on different wavelength bandwidth roads in the z-axis.

It has been determined that different increasing trends with different wavenumber bandwidths road depending on the speed. The results were evaluated at 11,24 km/h and 17,63 km/h speeds in the frequency domain for the z-axis to understand ride quality change. Weighting factor values have been added to the graphs to understand the effect of the ride quality values. It has been determined that the road with 0,46 - 39,01 meters wavelength bandwidth has higher ride quality at low speeds and lower ride quality at high speeds compared to the road with 0,15 -

39,01 meters wavelength bandwidth. It is determined from the graphs that the maximum acceleration frequency value changes with different wavenumber bandwidth roads at the same speeds. When the results obtained for the speed of 11,24 km/h are examined, it is seen that the maximum acceleration value on the road with 0,46 – 39,01 wavenumber bandwidth is reached in the frequency band with the low weighting factor value. For this reason, vibration evaluation values are lower and ride quality is higher. As the vehicle's speed increased, the frequency value at which the acceleration values were maximum decreased, but the acceleration amplitude values increased. The analyses performed at 17,63 km/h determined that the vibration evaluation values were higher at 0,46- 39,01 wavelength bandwidth road. It is thought that the reason wavelength range of 0,46 - 39,01 wavelength bandwidth road is multiplied by the higher weighting factor. Depending on the increasing speed, the maximum acceleration frequency decreased more at a higher wavenumber bandwidth road. The maximum acceleration frequency value of 0,15 to 39,01 meters of wavelength bandwidth road is approximately 2,8 Hz. The maximum acceleration frequency value of 0,46 to 39,01 meters of wavelength bandwidth road is approximately 1,9 Hz 11,24 km/h. The maximum acceleration frequency value of 0,15 to 39,01 meters of wavelength bandwidth road km/h is approximately 1,4 Hz. The maximum acceleration frequency value of 0,46 to 39,01 meters of wavelength bandwidth road is approximately 1,7 Hz at 17,63. This result may explain why the narrow bandwidth at high wavenumber range road increases with a high trend versus speed.

When 0,3 to 39,01 and 0,46 to 39,01 wavelength bandwidth road are compared, 0,3 to 39,01 wavelength bandwidth road has high acceleration amplitude values in the frequency with high weighting factor at 11,24 km/h (Figure 5.32).

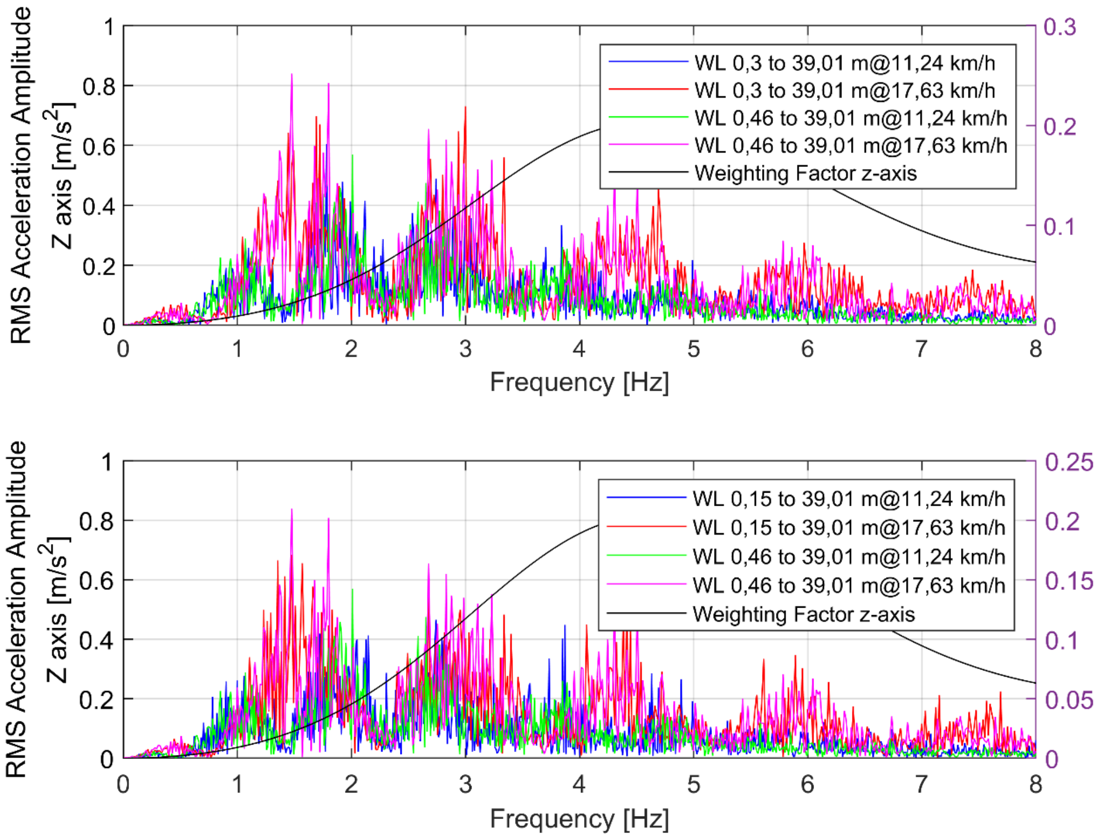

Figure 5.32 : Rms acceleration amplitude results as a function of frequency on different wavenumber roads at 11,24 and 17,63 km/h in the z-axis.

According to the calculations made on roads with different wavenumber bandwidth, 0,15 to 19,51 meters wavelength bandwidth road at 7,33 km/h, 0,15 to 39,01 meters wavelength bandwidth road at 8,21 km/h, 0,3 to 39,01 meters wavelength bandwidth road at 8,21 km/h, 0,46 to 39,01 meter wavelength bandwidth road at 8,96 km/h achieved the 6-Watt speed. These speed values are not far from each other (Figure 5.33).

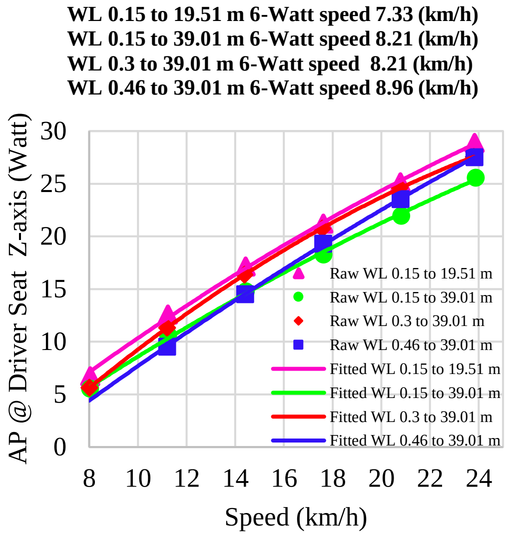

Figure 5.33 : The absorbed power results and the 6-watt speed of the driver seat base as a function of vehicle speed on different wavelength bandwidth roads in the z-axis.

The correlation could not be found according to the wavenumber bandwidth and speed for the y-axis in any evaluation methods (Figure 5.34, 5.35, 5.36). In this situation, it is seen that the relation between the wavelength bandwidth of the road and the lateral motion cannot be analyzed only by ride quality evaluation methods.

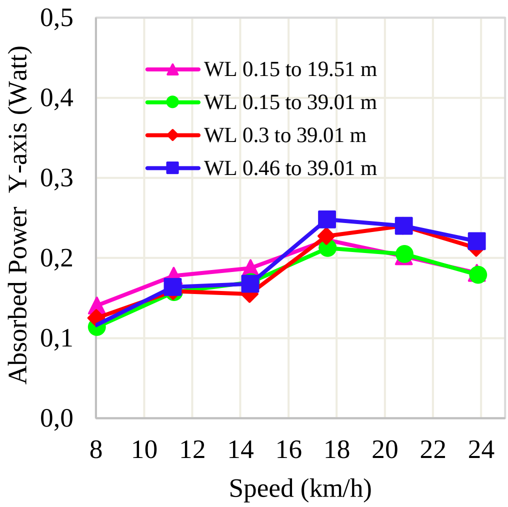

Figure 5.34 : The absorbed power results of the driver seat base as a function of vehicle speed on different wavelength bandwidth roads in the y-axis.

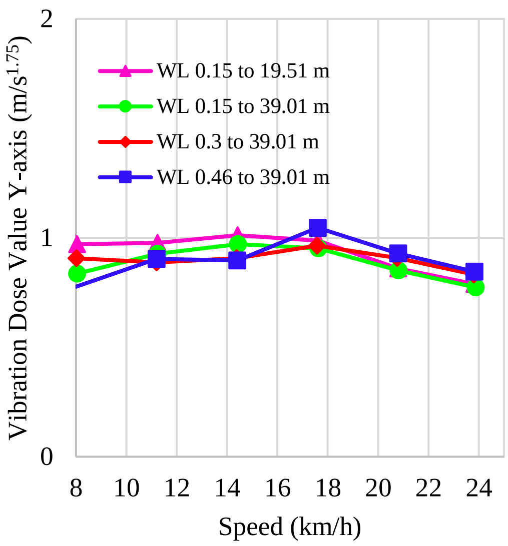

Figure 5.35 : The vibration dose value results of the driver seat base as a function of vehicle speed on different wavelength bandwidth roads in the y-axis.

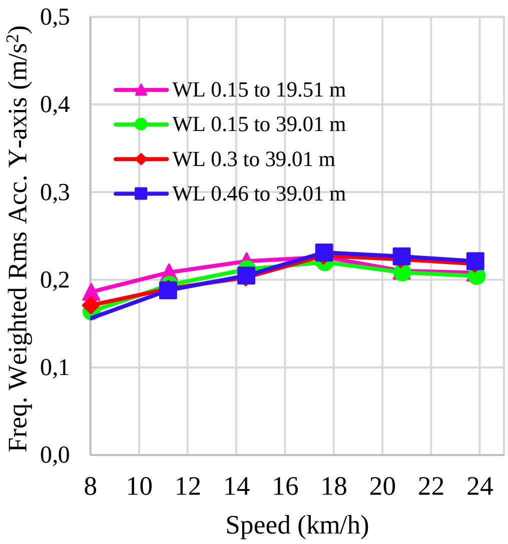

Figure 5.36 : The freq. weighted rms acc. results of the driver seat base as a function of vehicle speed on different wavelength bandwidth roads in the y-axis.

The correlation could not be found according to the wavenumber bandwidth for the x-axis in any evaluation methods. However, it can be concluded that the results on the z-axis affect the x-axis. This correlation changed as the speed of the vehicle increased. This situation is thought to be due to pitch and jounce frequencies changing depending on the speed (Figure 5.37, 5.38, 5.39).

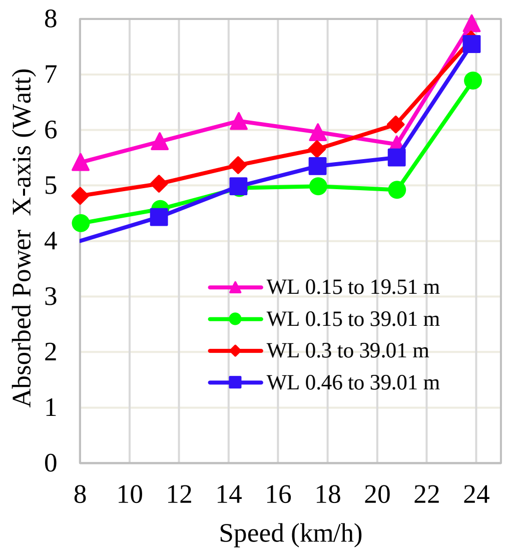

Figure 5.37 : The Absorbed power results of the driver seat base as a function of vehicle speed on different wavelength bandwidth roads in the x-axis.

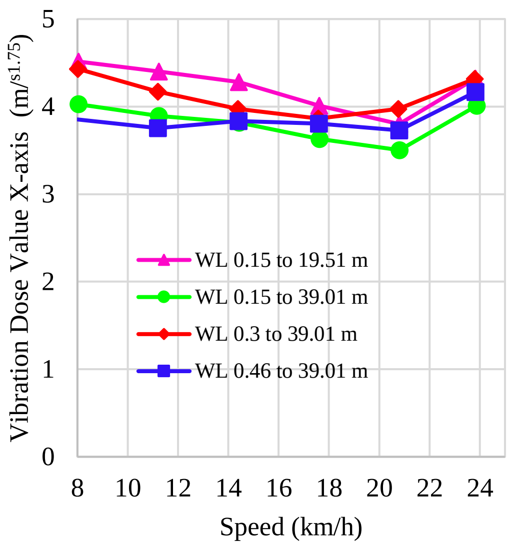

Figure 5.38 : The vibration dose value results of the driver seat base as a function of vehicle speed on different wavelength bandwidth roads in the x-axis.

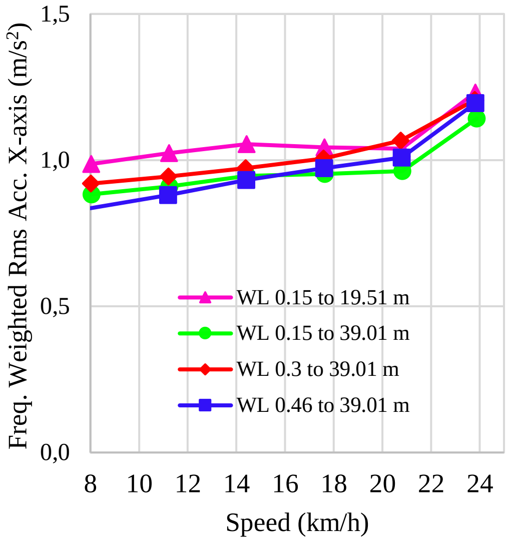

Figure 5.39 : The freq. weighted rms acc. results of the driver seat base as a function of vehicle speed on different wavelength bandwidth roads in the x-axis.

5.3.2 Discussion on the effects of wavenumber

As a result of the analysis, it is seen that the road wavenumber bandwidth effect ride quality values. It is seen that the road with narrow bandwidth at high wavenumber range for the z-axis at low speeds has the highest ride quality. The road with narrow bandwidth at low wavenumber range and wider bandwidth at high wavenumber range for the z-axis has the lowest ride quality. However, analyses should be evaluated in the frequency domain to understand better ride quality change via vehicle speed. The correlation could not be established between wavenumber bandwidth road and ride quality in the x and y-axis.

5.4 The Effects of Phase Angle for Asymmetrical Road on Ride Quality

5.4.1 Simulation results of the effects of phase angle for asymmetrical profiles

The analyses will be created to see the effect of the asymmetric road on the vehicle's ride quality. Creating 45°, 90° and 180° phase angle differences between synthetic roads ensures that the wheels jounce and rebound at different times.

It is seen that the ride quality improves and the feeling of comfort increases with increasing phase angle. The vibration evaluation values increase with the increase in vehicle speed, and the feeling of comfort and ride quality decrease. As a result of the analysis made on the road with no phase angle (phase angle 0°) and 45° phase angle, it is seen that the results converge as the vehicle speed increases. The reason being the time between the jounce and rebound movements of the tires decreases, and the effect of the phase difference of the road decreases as the vehicle speeds up (Figure 5.40, 5.41, 5.42).

The change in chassis pitch angle of the analyzes was made at 8,05 km/h. It has been determined that the pitch angle of the vehicle decreases as the phase difference increases. It can be said that the reduction of the pitch angle of the vehicle improves the ride quality metrics (Figure 5.43).

Although all evaluation methods show similar results, the vibration evaluation values change the most against the increased speed of the absorbed power.

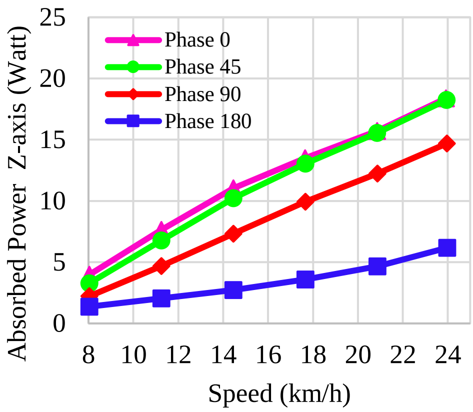

Figure 5.40 : The absorbed power results of the driver seat base as a function of vehicle speed on different phase angle roads in the z-axis.

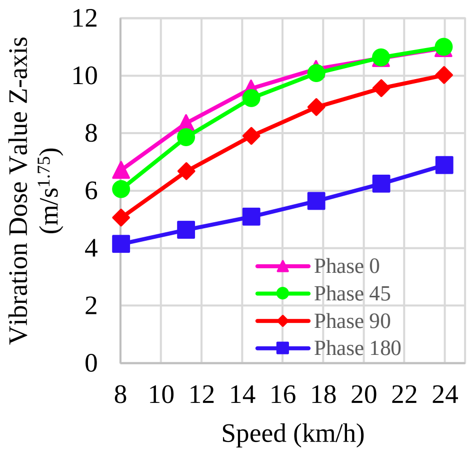

Figure 5.41 : The vibration dose value results of the driver seat base as a function of vehicle speed on different phase angle roads in the z-axis.

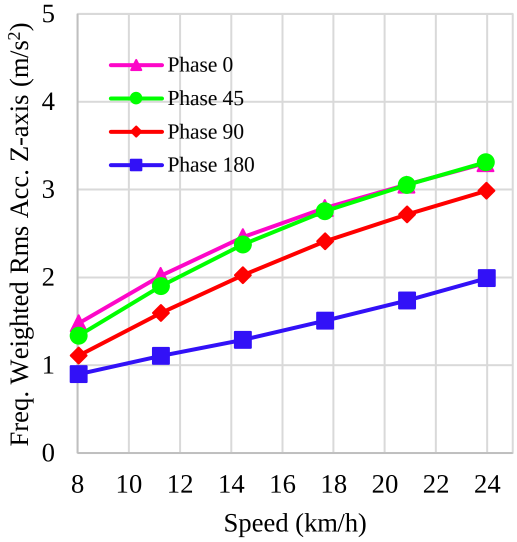

Figure 5.42 : The freq. weighted rms acc. results of the driver seat base as a function of vehicle speed on different phase angle roads in the z-axis.

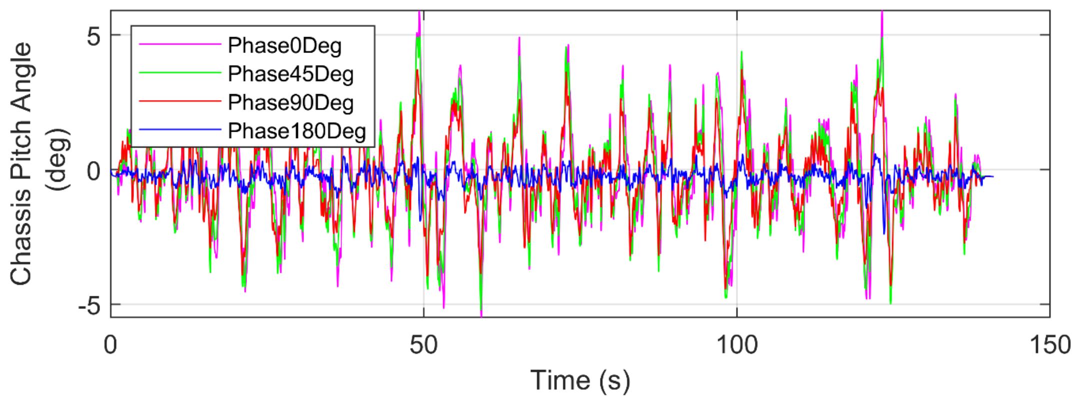

Figure 5.43 : Chassis pitch angle at 8,05 km/h vehicle speed as a function of time on different phase angle roads.

A second-order polynomial curve is set to the absorbed power curve plotted depending on the speed. According to this polynomial, the vehicle speed corresponding to 6-Watt of absorbed power was calculated. 6-Watt speed is; 9,75 km/h on the road with 0° phase angle difference, 10,48 km/h on the road with 45° phase angle difference, 12,78 km/h on the road with 90° phase angle difference and 23,74 in the road with 180 ° phase angle difference. The phase angle of the road should be restricted in the ride quality evaluation standards (Figure 5.45).

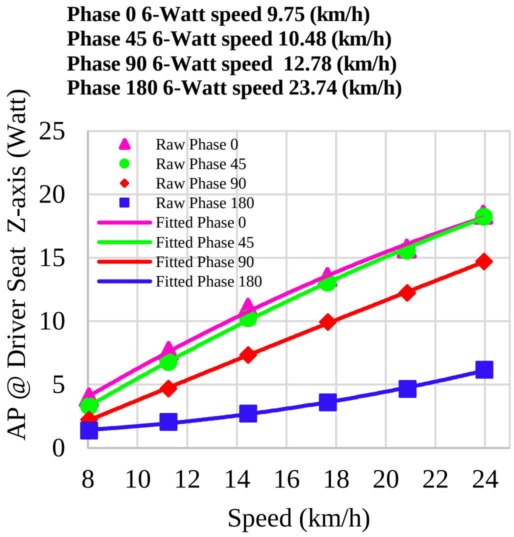

Figure 5.44 : The absorbed power results and the 6-watt speed of the driver seat base as a function of vehicle speed on different phase angle roads in the z-axis.

Change is seen in the absorbed power, vibration dose value and frequency weighted rms acceleration values in the y-axis according to the phase angle difference change (Figure 5.45, 5.46, 5.47). In all evaluation methods, it is seen that the vibration evaluation values increase, ride quality decreases as the phase difference of the road increases in the y-axis. The reason for this is that the steering wheel angle change is seen in the analyzes made at 8,05 km/h (Figure 5.48). As the phase difference increases, the relative movement between the right and left wheels will increase and it will be challenging to move the vehicle with a straight line. As can be seen, the steering wheel angle has changed the most on the road with a 180° phase difference. Changing the steering wheel angle will also increase the generation of forces in the lateral direction. For this reason, the ride quality on the y-axis will decrease.

As the speed increases on the road with a 0° phase difference, the change in the vibration evaluation values in the y-axis is very small. In contrast, the ride quality decreases depending on the speed as the phase difference increases. This change can be evaluated most precisely with the absorbed power method.

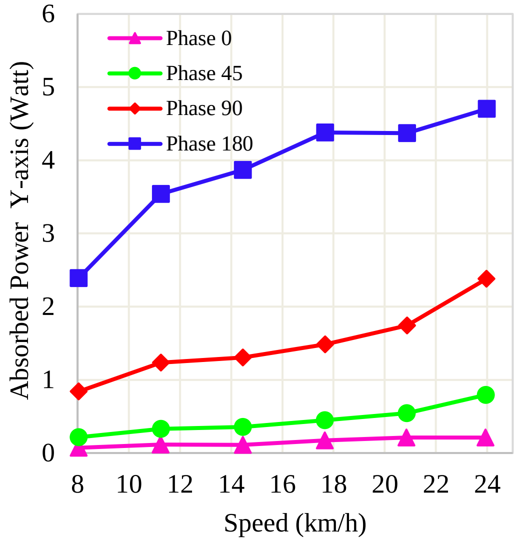

Figure 5.45 : The absorbed power results of the driver seat base as a function of vehicle speed on different phase angle roads in the y-axis.

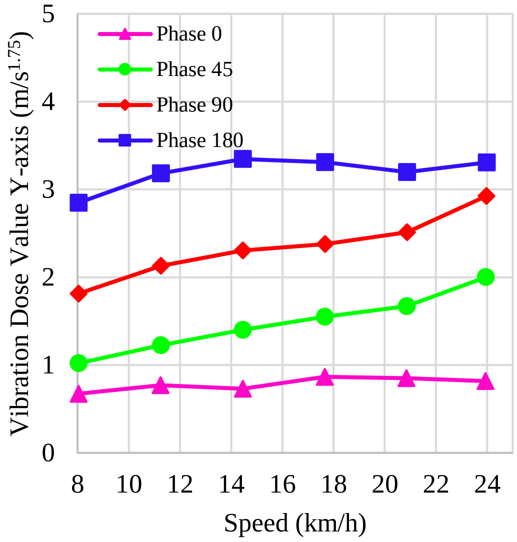

Figure 5.46 : The vibration dose value results of the driver seat base as a function of vehicle speed on different phase angle roads in the y-axis.

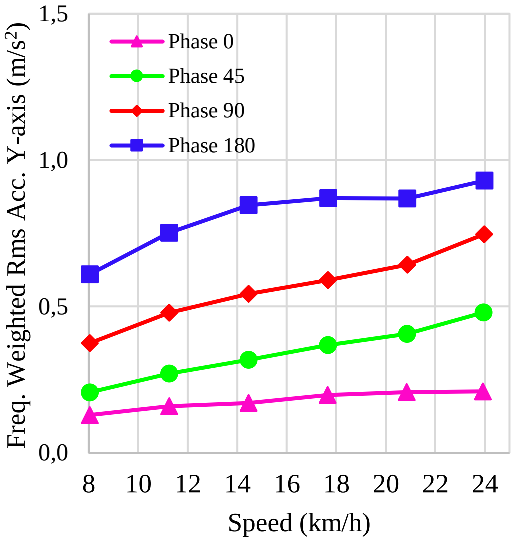

Figure 5.47 : The freq. weighted rms acc. results of the driver seat base as a function of vehicle speed on different phase angle roads in the y-axis.

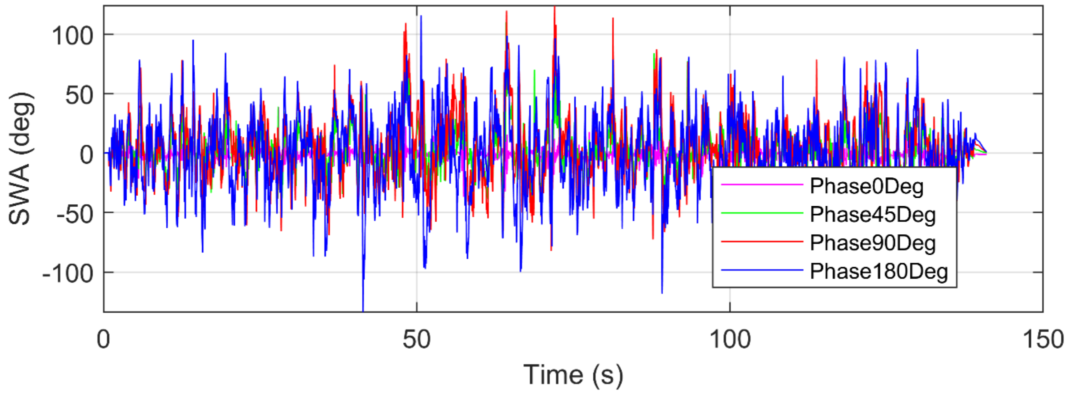

Figure 5.48 : Steering wheel angle as a function of time on different phase angle roads at 8,05 km/h.

The change in the absorbed power, vibration dose value and frequency weighted rms acceleration values in the x-axis according to the phase angle difference (Figure 5.49, 5.50, 5.51). As seen in all evaluation methods, the ride quality in the x-axis increases as the phase angle increases. The acceleration graph in the x-axis of the analysis was made on roads with different phase angles at a speed of 8,05 km/h (Figure 5.52). Acceleration amplitudes decrease on the road with a high phase angle in the graph.

Although it was observed that the absorbed power value in the x-axis increased with increasing speed, this relation could not be detected in the other two evaluation methods. Therefore, this can be considered the more sensitive results of the absorbed power against changing the speed.

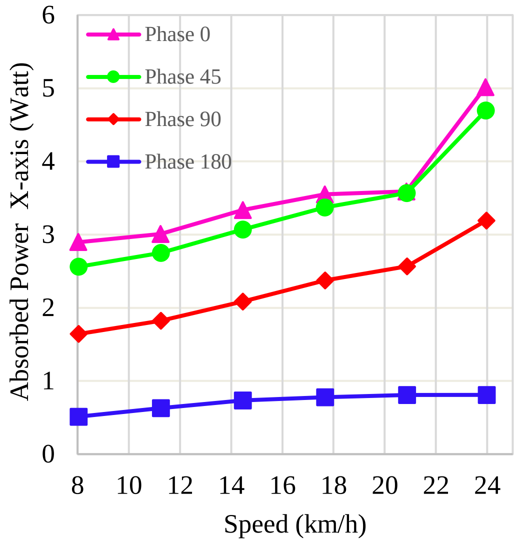

Figure 5.49 : The absorbed power results of the driver seat base as a function of vehicle speed on different phase angle roads in the x-axis.

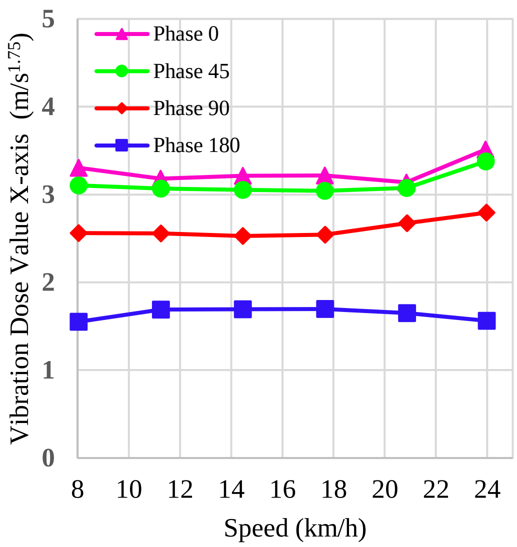

Figure 5.50 : The vibration dose value results of the driver seat base as a function of vehicle speed on different phase angle roads in the x-axis.

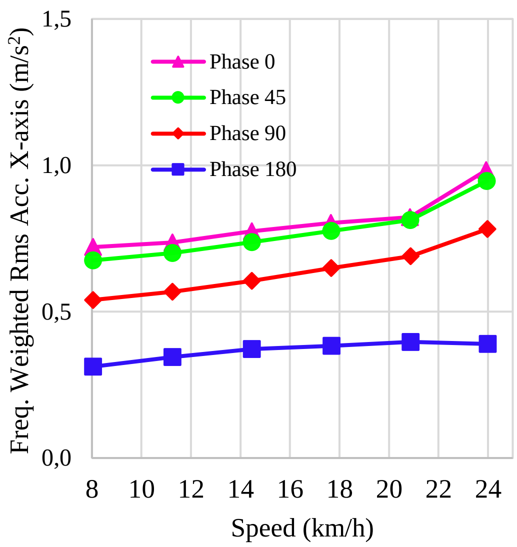

Figure 5.51 : The freq. weighted rms acc. results of the driver seat base as a function of vehicle speed on different phase angle roads in the x-axis.

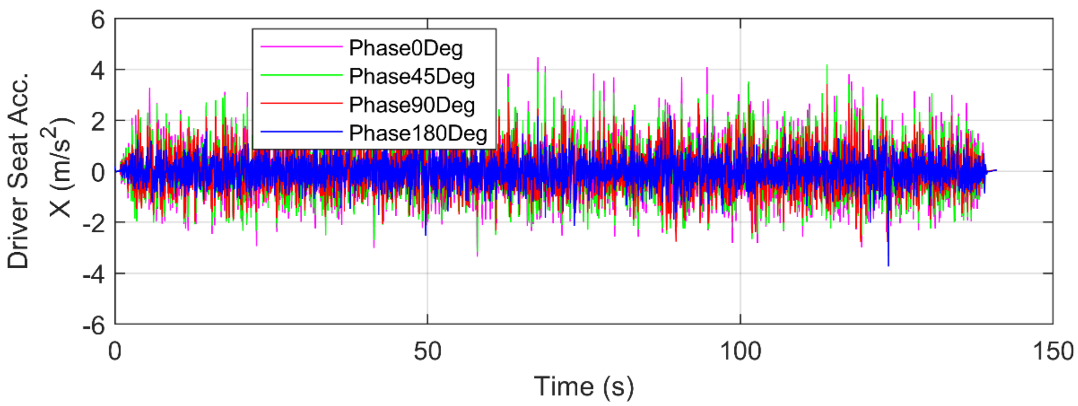

Figure 5.52 : Driver seat acc. as a function of time at 8,05 km/h speed on different phase angle roads.

The acceleration in the vehicle was recorded on the seat base at the driver, passenger and rear passenger seat center locations. The 6-Watt speed values vary according to the sensor locations. If ride quality is interpreted according to the 6-Watt speed value on the 0° phase angle road, the worst ride quality is at the rear passenger and the best ride quality is at the passenger. On the synthetic road with a phase angle of 0°, the driver reached 6-Watt at a speed of 9,75 km/h, the passenger at 10,77 km/h and the rear passenger at 7,60 km/h. It is seen that the ride quality with a road phase angle of 180° is best for the rear passenger and worst for the driver. On the synthetic road with a phase angle of 180°, the driver reached a speed of 6-Watt at 23,74 km/h, the passenger at 25,84 km/h and the rear passenger at 69,94 km/h (Figure 5.53, 5.54). As the phase angle increases, ride quality in the rear passenger increases and vibration evaluation values decrease. This result is different from the results seen for all other road parameters. The reason is that the rear passenger sensor is positioned right in the middle of the vehicle. Since the two wheels move opposite, one wheel makes a rebound movement and the other bump movement. The sensor in this position changes position very little and is under acceleration. The forces from the two sides balance each other and decrease in this position. For this reason, the comfort parameters are very high. These results are similar for all evaluation methods.

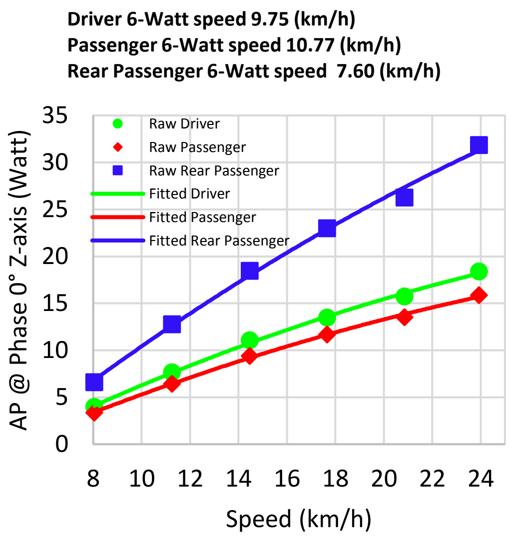

Figure 5.53 : Absorbed power results according to sensor location as a function of the 6-Watt speed at 0° Phase angle road in the z-axis.

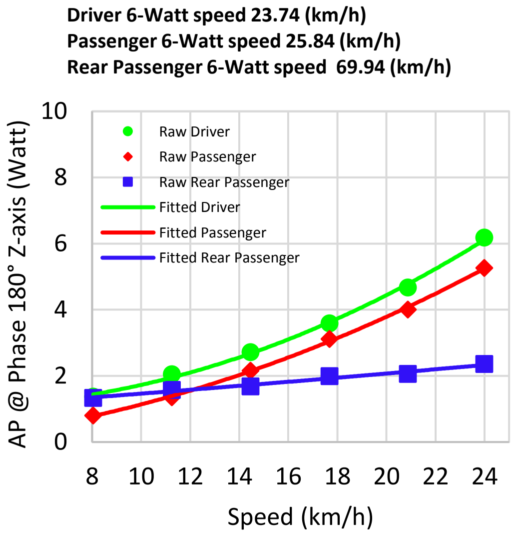

Figure 5.54 : Absorbed power according to sensor location as a function of the 6-Watt speed at 180°phase angle road in the z-axis.

5.4.2 Discussion on the effects of phase angle for asymmetrical profiles

As a result of the analyses, it is observed that the phase angle of the road had a significant effect on the ride quality. Also, it is thought that phase angle should be limited and reported in the test standards.

As the phase angle of the vehicle increases, the absorbed power, vibration dose value, and frequency weighted rms acceleration values in the z-axis decrease. The main reason for this is that when the right and left tires move at a different position, the force and acceleration transmits on the vehicle body are reduced. Opposite movements neutralize each other, and the effect caused by the tires moving together decreases. As the phase difference increases, the pitch movements of the vehicle body decrease, which reduces the loads on the vehicle body. As the speed of the vehicle increases, this effect is more dominant.

As the phase angle of the road increase, the 6-Watt speed increase in the z-axis. When the accelerations coming from the driver's seat are calculated, 6-Watt speed is 9,75 km/h at 0° phase angle, 10,48 km/h at 45° phase angle, 12,78 km/h at 90° phase angle, 23,78 km/h at 180° phase angle road (Figure 5.55).

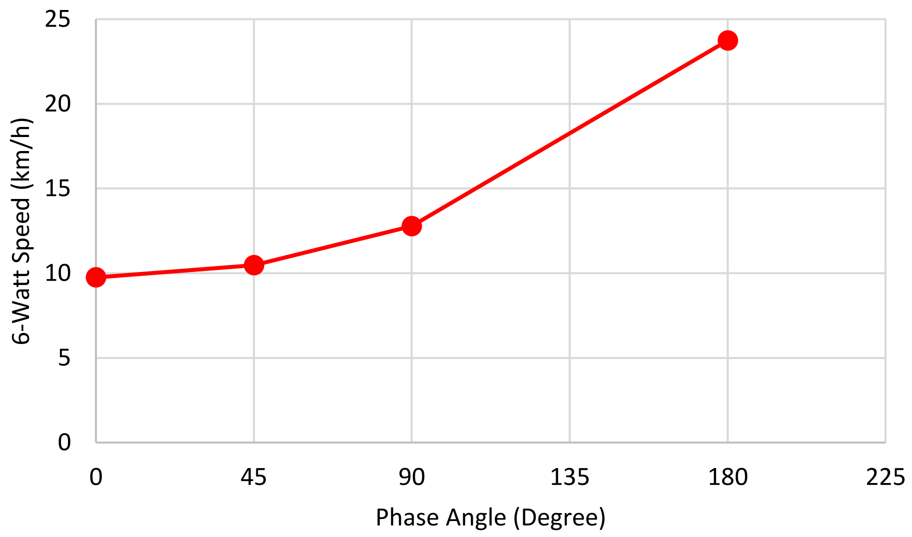

Figure 5.55 : 6-Watt speed on different phase angle roads in the z-axis.

It is observed that as the phase angle of the vehicle increases, the absorbed power, vibration dose value and frequency weighted rms acceleration values in the y-axis increase. Because the two wheels move relative to each other, more steering wheel movements are required to drive the vehicle straight, increasing the lateral forces. Also, due to the relative motion of the wheels increasing, the lateral motion of the vehicle body increase. It is thought that lateral motion is the dominant reason vibration evaluation values increase with phase angle increase. A specific relation cannot be established between the vehicle's speed for the vibration dose value and frequency weighted rms acceleration evaluation methods in the y-axis. In the absorbed power evaluation method, ride quality decreases as the speed increases on roads with a high phase difference.

It is observed that as the phase angle of the vehicle increases, the absorbed power, vibration dose value and frequency weighted rms acceleration formed are not affected in the x-axis. As a result, ride quality is not affected.

The location where the acceleration is recorded on roads with different phase angles is also crucial. As a result of the analysis, it has been determined that the passenger is more comfortable on low phase angle roads. However, there is a very high comfort feeling in the rear passenger positioned in the middle of the vehicle (in the middle of the right and left tires) on high phase angle roads.

5.5 The Effects of Different Speed Profiles on Ride Quality

5.5.1 Simulation results of the effects of different speed profiles

In the TOP-01-1-014 [1] standard, which defines the absorbed power method, the vehicle speed is expected to be kept as constant as possible during the test or analysis. It is defined that the speed coefficient of variation value should be at most 0,1.

In order to examine the effect of the speed profile on the ride quality of the vehicle, analyzes were made on the 5,08 cm rms road in 4 different speed profiles with a speed coefficient of variation of 0,1 and 0,15, and the accelerations received by the driver were recorded. In addition, the effect of ride quality was investigated with the absorbed power evaluation method.

Four different speed profiles were seen in Figure 5.56 and Figure 5.57 were created so that the average speed of 16 km/h would remain constant and the speed coefficient of variation value would be 0,1. Four different speed profiles seen in Figure 5.57 were created to make comparisons. The average speed of 16 km/h remains constant, and the speed coefficient of variation value is 0,15, which is higher than the value stated in the standard [1]. The vehicle is provided to drive in this speed profile by defining this profile to the ADAMS Car driver.

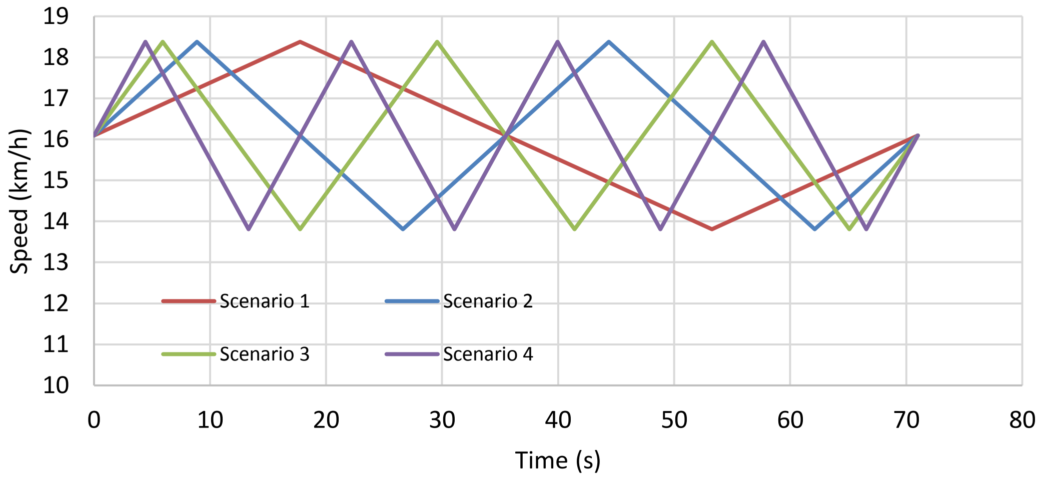

Figure 5.56 : Speed profile at speed coefficient of variation 0,1 at 16 km/h average speed.

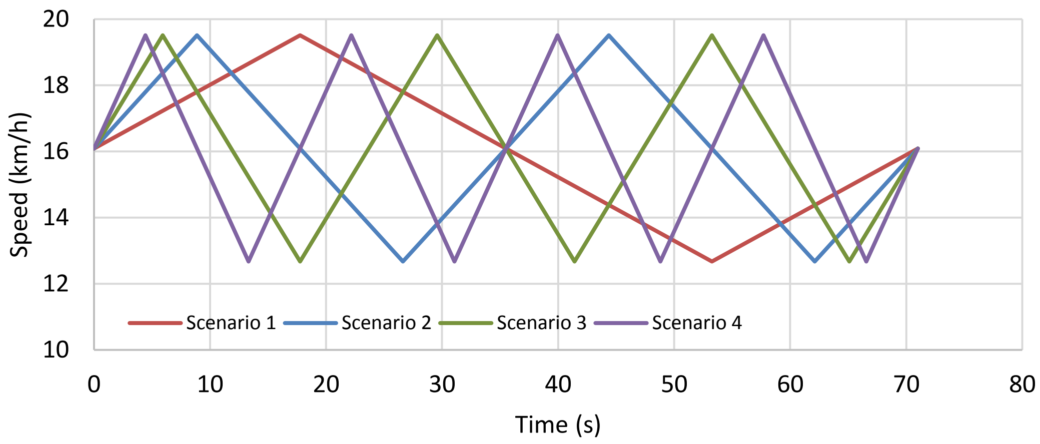

Figure 5.57 : Speed profile at speed coefficient of variation 0,15 at 16 km/h average speed.

When the analyzes with the speed coefficient of variation value of 0,1 were examined, it was concluded that if the vehicle was driven 300 m, the absorbed power values in all axes were approximately the same (Figure 5.58). However, it is considered that this result should be accepted cautiously. Further analysis of different vehicles on different roads needs to support the result.

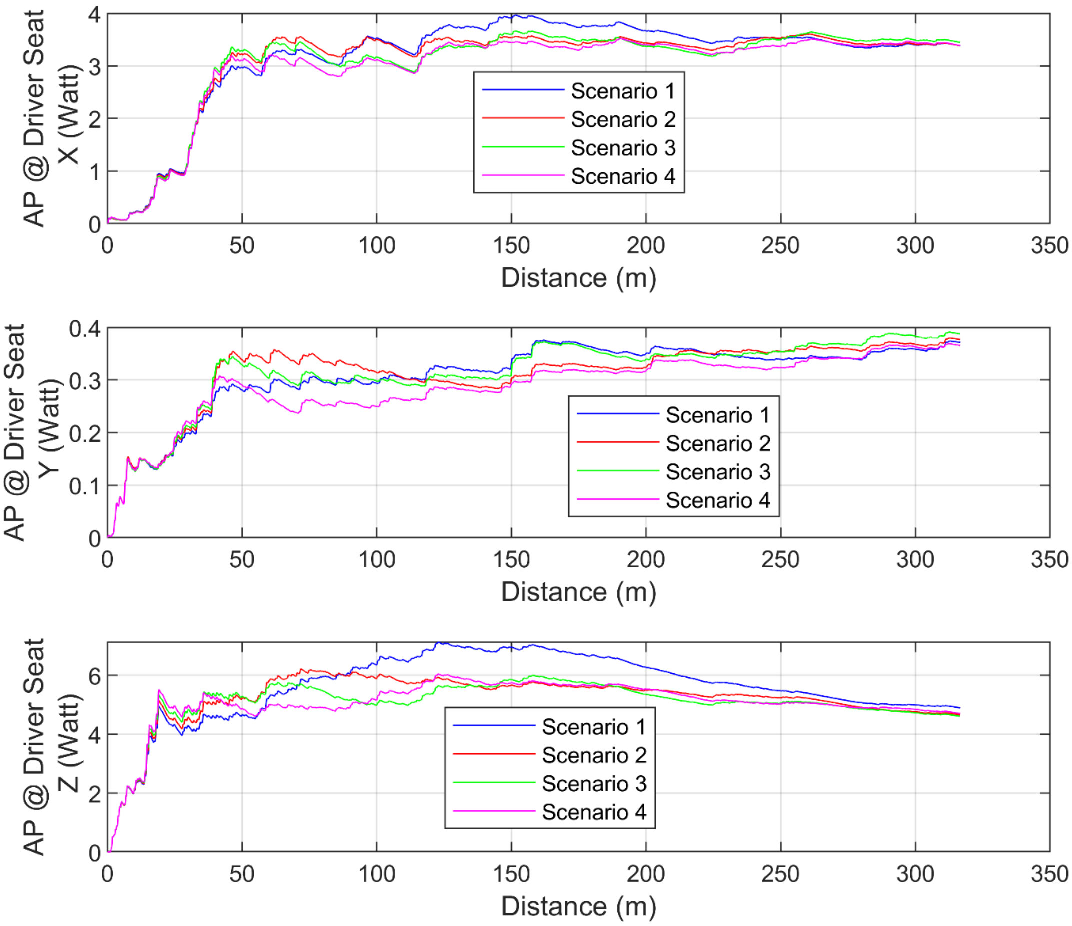

Figure 5.58 : Absorbed power in driver seat base on 5,08 cm rms road different speed profile speed coefficient of variation value of 0,1.

When the analyses with the speed coefficient of variation value of 0,15 were examined, it was concluded that if the vehicle was driven 300 m, the absorbed power value in all axes was approximately the same (Figure 5.60).

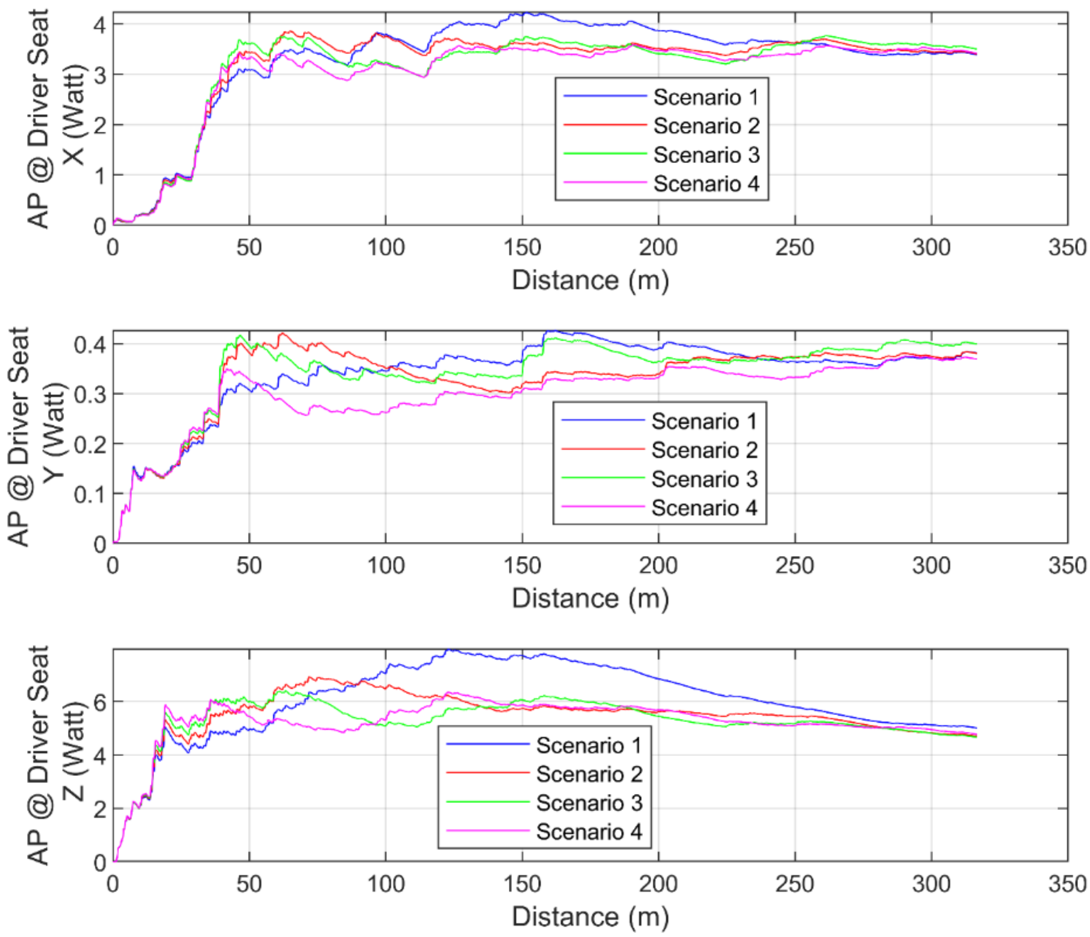

Figure 5.59 : The absorbed power result of driver seat base on 5,08 cm rms road at different speed profile when speed coefficient of variation value is 0,15.

When the speed coefficient of variation values of 0,1 and 0,15 for Scenario 2 are compared, it approaches the same absorbed power values with 300 m road (Figure 5.61).

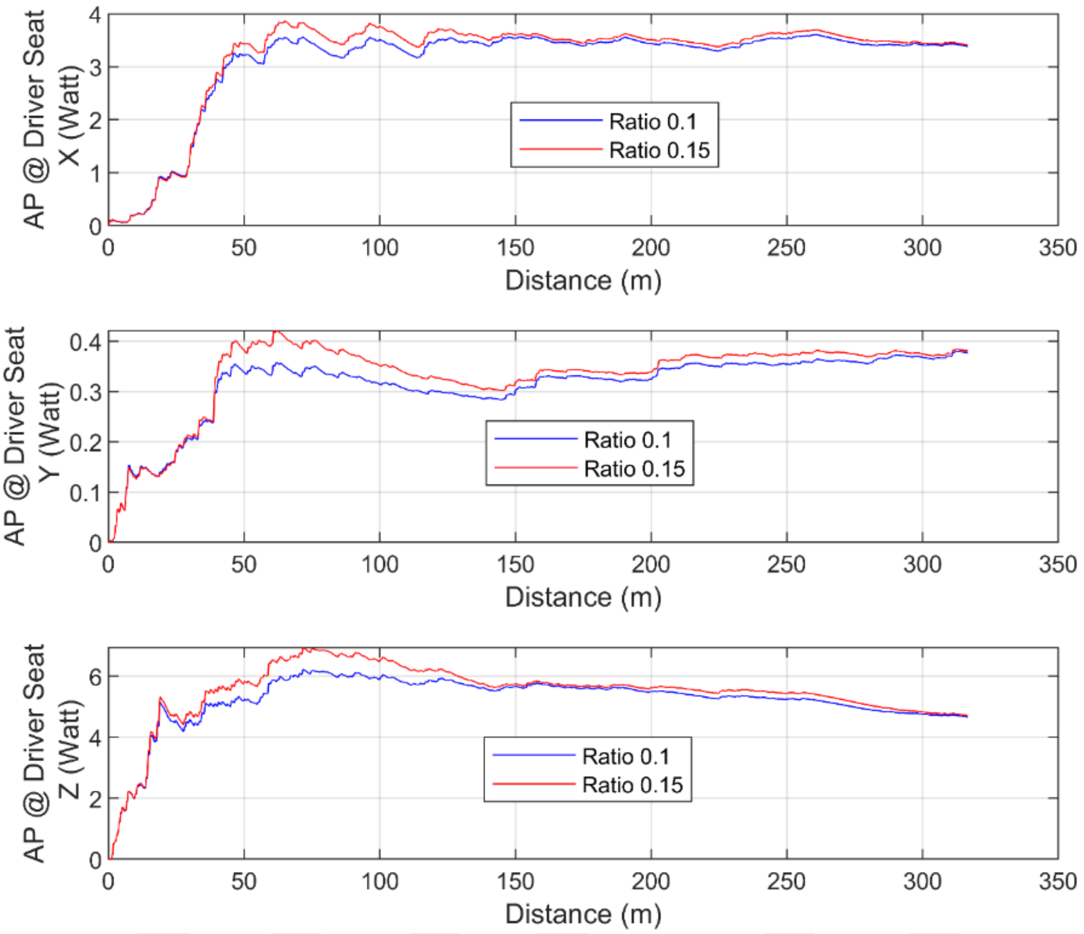

Figure 5.60 : The absorbed power results as a function of driving distance at scenario 2.

When the results are analyzed for vibration dose value and frequency weighted rms acceleration in the whole axis, it can be seen that they are very close to each other (Table 5.1, 5.2).

Table 5.1 : The vibration dose value and frequency weighted rms acc. results in speed coefficient of variation 0,1.

Speed Coefficient of Variation 0,1					
Vibration Dose Value			Frequency Weighted Rms Acc.		
X	Y	Z	X	Y	Z
2,83	1,14	7,21	0,73	0,25	1,86
2,80	1,07	6,94	0,73	0,25	1,85
2,91	1,16	7,01	0,74	0,26	1,83
2,84	1,05	6,94	0,73	0,25	1,84

Table 5.2 : The vibration dose value and frequency weighted rms acc. results in speed coefficient of variation 0,15.

Speed Coefficient of Variation 0.15					
Vibration Dose Value			Frequency Weighted Rms Acc.		
X	Y	Z	X	Y	Z
2,88	1,18	7,38	0,73	0,26	1,87
2,85	1,14	7,05	0,74	0,26	1,84
3,03	1,20	7,14	0,75	0,26	1,84
2,90	1,05	7,04	0,74	0,25	1,85

5.5.2 Discussion on the effects of different speed profiles

In order to examine the effect of the speed profile on the ride quality of the vehicle, analyzes were made on the 5,08 cm rms road at an average speed of 16,09 km/h with a speed coefficient of variation of 0,1 and 0,15, and the results were compared.

According to the analysis results, if the analysis is done at 300 meters in the x, y and z axes and all evaluation methods, it is seen that the results are similar.

Even if the analyzed speed profile deviates by 3 km/h, the profile is defined to maintain the average speed. However, it is not easy to achieve this condition in real life. Because if the driver deviates from the defined average speed, he must keep the average speed constant by increasing or decreasing the speed as he deviates. Also, it is considered that this result should be accepted cautiously. The result needs to be supported by analyses in different vehicles and roads.

5.6 Comparison Evaluation Method 6-Watt Speed Perspective

6-Watt is given as the absorbed power comfort limit in the literature. At the same time, comfort limits are defined for vibration dose value and frequency weighted rms acceleration defined in ISO 2631 [16]. A second-order polynomial was fitted to the vibration dose value and frequency weighted rms acceleration values in the speed domain to determine how close the comfort limits at the 6-Watt speed values were determined in the previous sections. The ride quality parameters were determined by entering the 6-Watt speed value for that road condition in the fitted polynomial (Table 5.3).

Table 5.3 : The vibration dose value and the freq. weighted rms acc. results at the 6-Watt speed on different roads.

Road Type		6-Watt Speed (km/h)	Vibration Dose Value ($m/s^{1.75}$)	Rms Acc. (m/s^2)
Different Roughness Road	2,54 cm rms	13,35	7,08	1,78
	3,81 cm rms	9,08	7,78	1,79
	5,08 cm rms	7,33	8,51	1,68
	6,35 cm rms	6,51	9,30	1,90
Different Waviness Road	W 1,5	6,47	9,20	1,90
	W 2	7,33	8,51	1,82
	W 2,5	9,19	7,83	1,80
Different Wavenumber Road	WL 0,15 to 19,51 m	7,33	8,15	1,74
	WL 0,15 to 39,01 m	8,21	8,19	1,81
	WL 0,3 to 39,01 m	8,21	8,47	1,82
	WL 0,46 to 39,01 m	8,96	7,82	1,78
Different Phase Angle	Phase 0°	9,75	7,63	1,77
	Phase 45°	10,48	7,44	1,77
	Phase 90°	12,78	7,28	1,80
	Phase 180°	23,74	6,83	1,97

When the values corresponding to 6-Watt speed are examined, it is seen that it does not converge to a fixed value. In the frequency weighted rms acceleration evaluation method, values between 1,25 m/s^2 and 2,5 m/s^2 were defined as “very uncomfortable”, and values higher than 2 m/s^2 were defined as “extremely uncomfortable”. Considering that the 6-watt speed value is the comfort limit, it can be deduced that frequency weighted rms acceleration values are also within the comfort limit. It can be observed that there is a consistent relationship between the absorbed power and frequency method in ride quality evaluation. The vibration dose value method values, corresponding to the 6-watt speed, vary over a broader range. For this reason, it can be deduced that there is less correlation between the absorbed power method and the vibration dose value method in the ride quality evaluation.

6. EFFECT OF SUSPENSION PARAMETERS ON RIDE QUALITY

In order to see the effect of suspension parameters on ride quality, analyzes were made in all evaluation methods with on the 90° phase angle and 5,08 cm rms roughness synthetic roads.

In the suspension system of the FED-Alpha vehicle model, called the combined suspension and frequency selected damper were modeled. During the jounce and rebound movement of the suspension model of the FED-Alpha vehicle, the stiffness values corresponding to the suspension speed are given as a look-up table in the ADAMS Car program. In addition, the damper damping function is defined as the transfer function for the low and high-frequency range.

It determines how much the suspension spring stiffness and damping coefficient sprung weight will move in disruptive effect from the road. By changing the k_s and c values, the effect of the values on the ride quality will be examined.

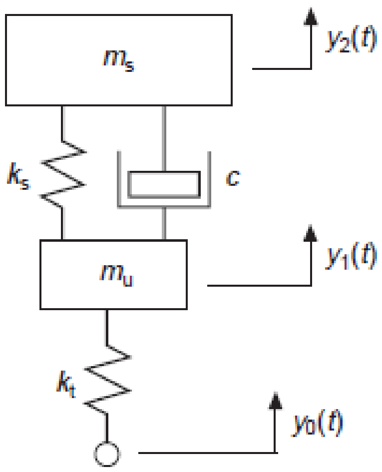

Figure 6.1 : The quarter vehicle model [25].

m_s: Sprung mass

k_s: Suspension stiffness

m_u: Unsprung mass

c: Damping cofficient

k_t: Tire stiffness

$y_0(t)$: Displacement come from ground

$y_1(t)$: Unsprung mass displacement

$y_2(t)$: Sprung mass displacement

6.1 The Effects of Different Spring Stiffness on Ride Quality

6.1.1 Simulation results of the effects of different spring stiffness

Two vehicle models were created with 25% more and less suspension stiffness values. The stiffness value changes the force corresponding to the displacement per unit changes. (Figure 6.2) Vehicle models were analyzed on roads with 90° phase angle and 5,08 cm rms roughness at different speeds, and the accelerations coming to the driver were collected. The accelerations coming to the driver were analyzed in three axes with the help of SIMULINK using the absorbed power, vibration dose value and frequency weighted rms acceleration evaluation methods.

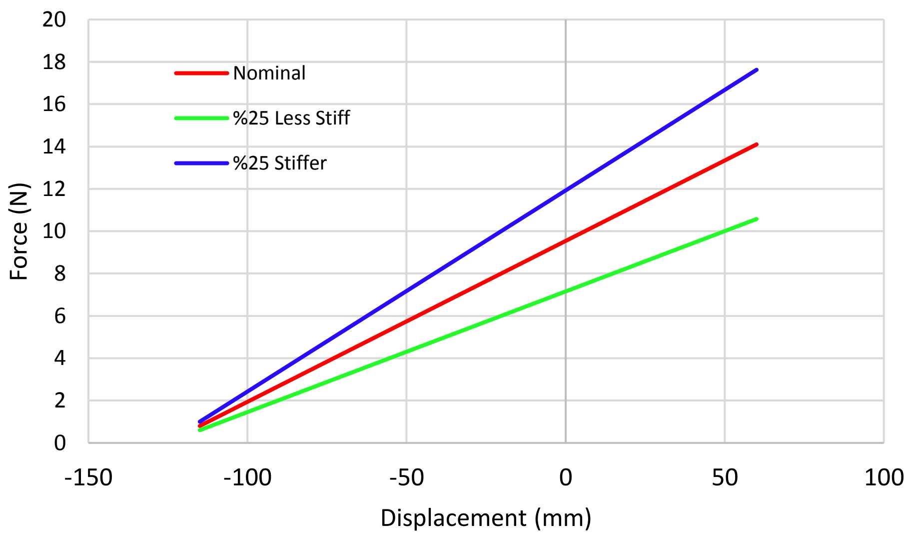

Figure 6.2 : Force-displacement graph for nominal and changed springs.

When the 5,08 cm rms road was examined with all evaluation methods, it was determined that the change in suspension stiffness did not visibly affect the ride quality in the z-axis. Even if there is a difference in the comfort trends of suspensions with different stiffness values in the absorbed power evaluation method, it is not enough to compare (Figure 6.3, 6.4, 6.5). This determination is thought to be related to the FED-Alpha suspension type. It is thought that the air bellows in the FED-Alpha suspension maintain the ride height of the vehicle according to the changing stiffness value and keep the ride quality evaluation values stable by regulating the reaction force against the disruptive effect from the road. The main reason is the suspension of the FED-Alpha vehicle acts like an air suspension, keeping the natural frequency constant. This result will change with different suspension types.

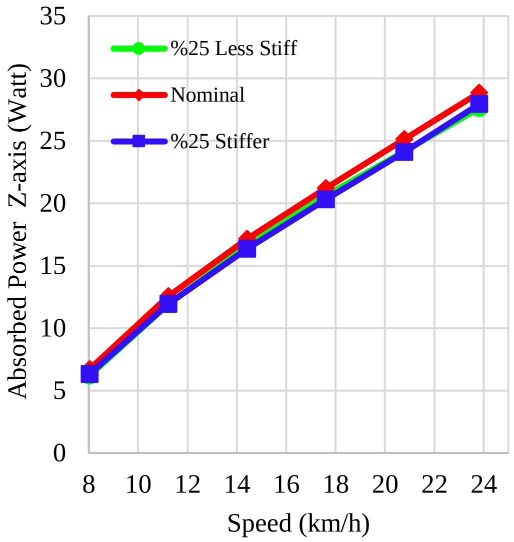

Figure 6.3 : The absorbed power results of the driver seat base as a function of vehicle speed on 5,08 cm rms road in the z-axis with different suspension stiffness.

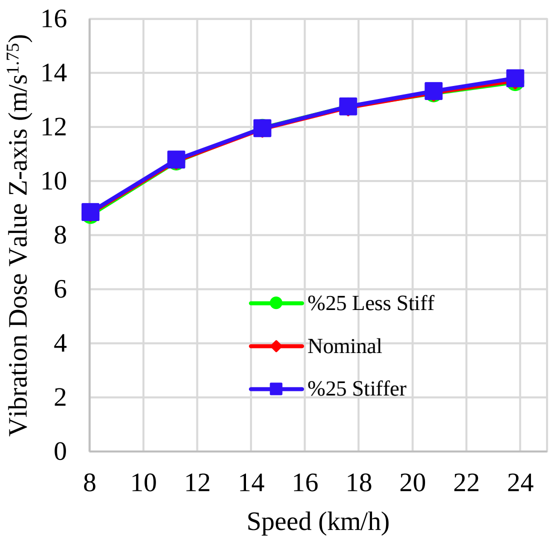

Figure 6.4 : The vibration dose value results of the driver seat base as a function of vehicle speed on 5,08 cm rms road in the z-axis with different suspension stiffness.

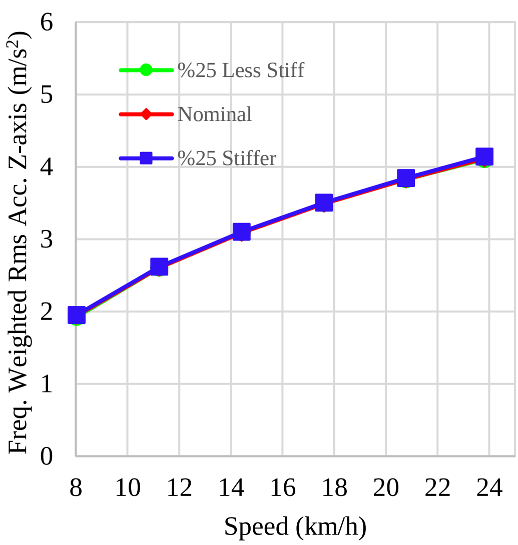

Figure 6.5 : The freq. weighted rms acc. results of the driver seat base as a function of vehicle speed on 5,08 cm rms road in the z-axis with different suspension stiffness.

When the 5,08 cm rms road was examined with all evaluation methods, it was determined that the change in suspension stiffness did not visibly affect the ride quality in the y-axis. It is seen that the value in the absorbed power evaluation method is lower than the nominal value. This result may be due to the deterioration of the vehicle's balance due to increased lateral forces and lateral motion in the y-axis. The suspension stiffness value increases or decreases, lateral acceleration values increase. However, when the effect of the change is minimal, it is difficult to interpret (Figure 6.6, 6.7, 6.8).

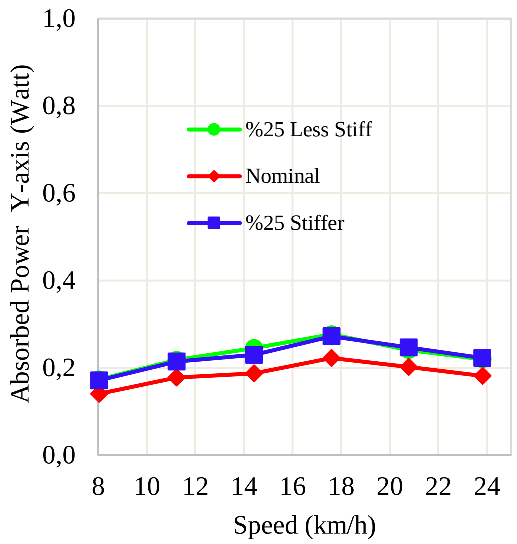

Figure 6.6 : The absorbed power results of the driver seat base as a function of vehicle speed on 5,08 cm rms road in the y-axis with different suspension stiffness.

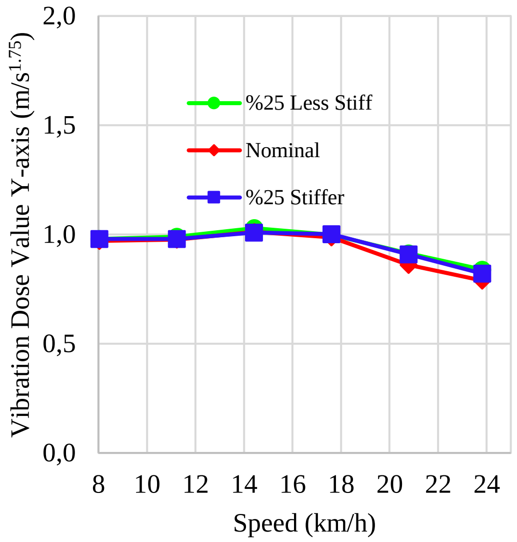

Figure 6.7 : The vibration dose value results of the driver seat base as a function of vehicle speed on 5,08 cm rms road in the y-axis with different suspension stiffness.

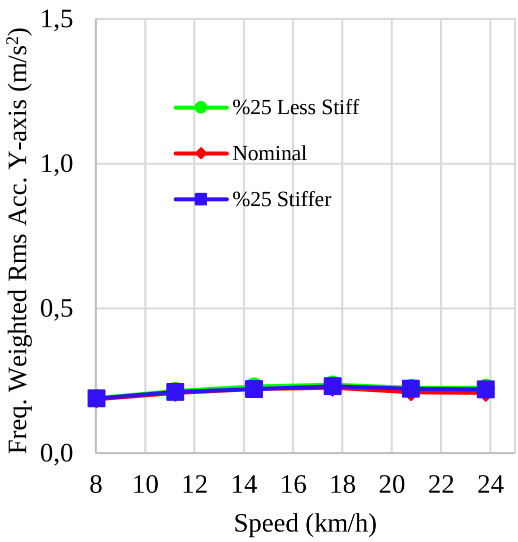

Figure 6.8 : The freq. weighted rms acc. results of the driver seat base as a function of vehicle speed on 5,08 cm rms road in the y-axis with different suspension stiffness.

When the 5,08 cm rms road was examined with all evaluation methods, it was determined that the change in suspension stiffness affected the ride quality in the x-axis. The ride quality decreases as the stiffness of the suspension increases. This effect can be observed clearly in the absorbed power evaluation method (Figure 6.9, 6.10, 6.11).

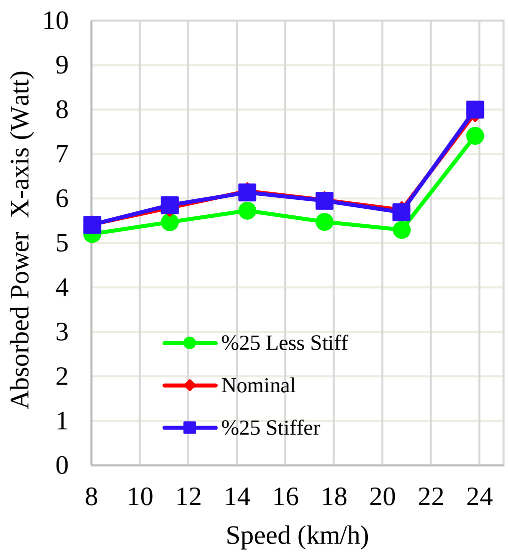

Figure 6.9 : The absorbed power results of the driver seat base as a function of vehicle speed on 5,08 cm rms road in the x-axis with different suspension stiffness.

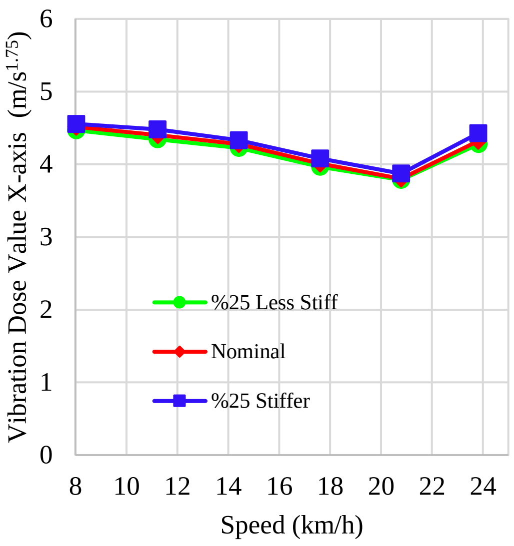

Figure 6.10 : The vibration dose value results of the driver seat base as a function of vehicle speed on 5,08 cm rms road in the x-axis with different suspension stiffness.

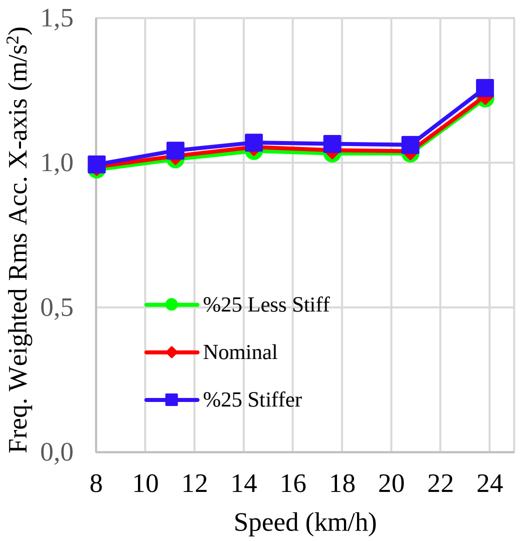

Figure 6.11 : The freq. weighted rms acc. results of the driver seat base as a function of vehicle speed on 5,08 cm rms road in the x-axis with different suspension stiffness.

When the absorbed power values in the z-axis are examined on the 90° phase difference road, different results are obtained from the 5,08 cm rms road. It is seen that the ride quality of the stiffer suspension is lower. The less stiff suspension has low vibration evaluation values. As the analyzed vehicle speed increases, the difference between the absorbed power values of the vehicles belonging to different stiffness values decreases. Similar results are obtained with the frequency weighted rms acceleration and vibration dose value methods. However, the stiffness effect is more visible with the absorbed power method (Figure 6.12, 6.13, 6.14).

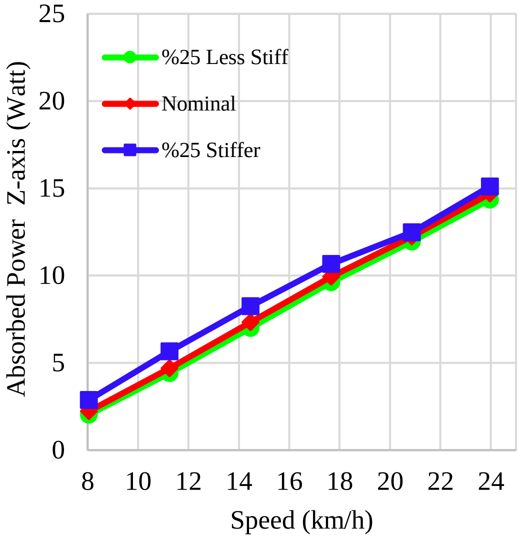

Figure 6.12 : The absorbed power results of the driver seat base as a function of vehicle speed on phase angle 90° road in the z-axis with different suspension stiffness.

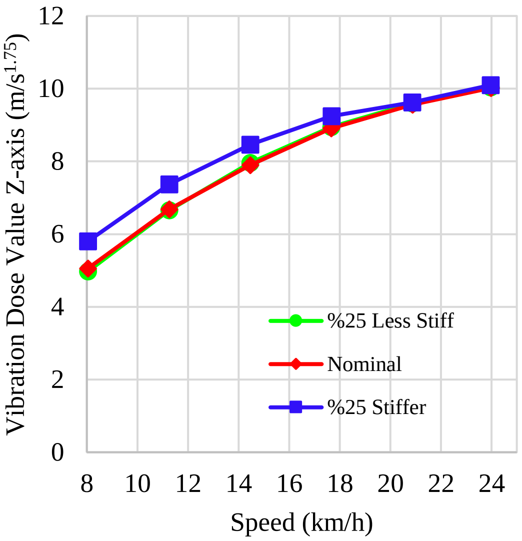

Figure 6.13 : The vibration dose value results of the driver seat base as a function of vehicle speed on phase angle 90° road in the z-axis with different suspension stiffness.

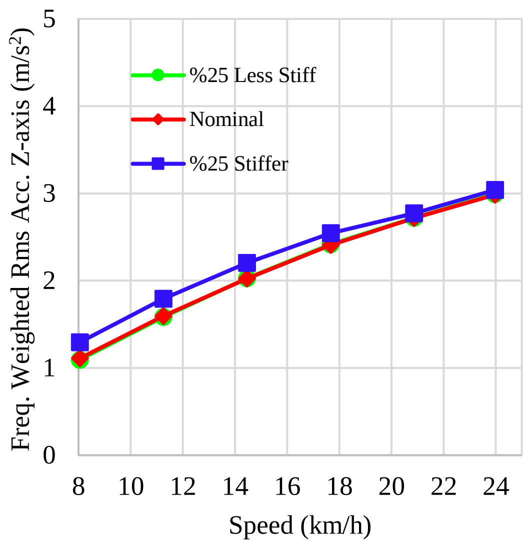

Figure 6.14 : The freq. weighted rms acc. results of the driver seat base as a function of vehicle speed on phase angle 90° road in the z-axis with different suspension stiffness.

When the phase angle is 90° on the road, it has been determined that the change in suspension stiffness affects the ride quality in the y-axis when examined with all evaluation methods. Since the right and left wheels of the road move at different phase angles, the lateral forces are high on these roads. The change made to the suspension has affected the stability of the vehicle. When examining the absorbed power evaluation method, the worst ride quality appears to be on stiffer suspension, and the best ride quality appears to be on less stiff suspension. It is estimated that increasing the suspension stiffness causes an increase in the lateral force and motion in the y-axis. Nevertheless, it is not correct to form a general judgment based on this result. This result might be based on the suspension modeling and type of the FED-Alpha vehicle (Figure 6.15, 6.16, 6.17).

In the frequency weighted rms acceleration and vibration dose value evaluation methods, the changing trend against the increase in speed is the same. However, when those evaluation methods are examined, it is impossible to make a definite judgment like the absorbed power evaluation method.

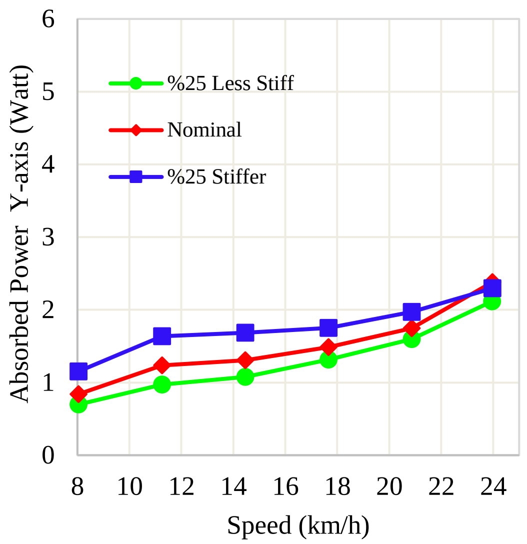

Figure 6.15 : The absorbed power results of the driver seat base as a function of vehicle speed on phase angle 90° road in the y-axis with different suspension stiffness.

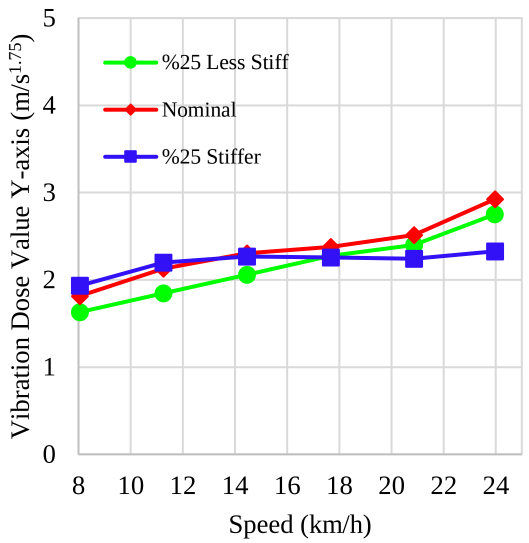

Figure 6.16 : The vibration dose value results of the driver seat base as a function of vehicle speed on phase angle 90° road in the y-axis with different suspension stiffness.

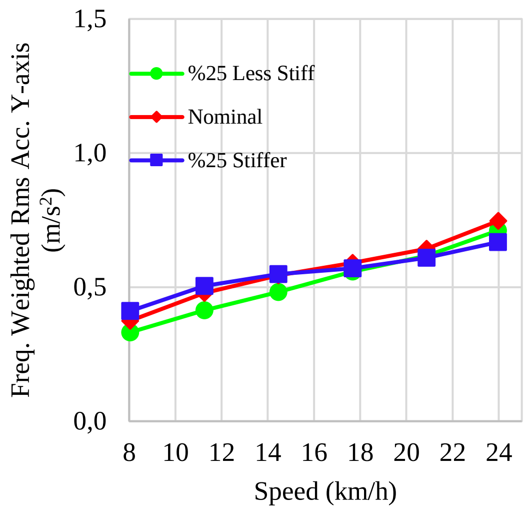

Figure 6.17 : The freq. weighted rms acc. results of the driver seat base as a function of vehicle speed on phase angle 90° road in the y-axis with different suspension stiffness.

It has been observed that the change in suspension stiffness affects the ride quality in the x-axis on the 90° phase angle road when examined with all evaluation methods. The vibration evaluation values increase with increasing speed. The absorbed power method shows an increasing trend with a higher slope depending on the increase in speed. The lowest evaluation values in the x-axis are seen in the vehicle with the %25 stiff suspension. The highest values are seen in the vehicle with the nominal suspension (Figure 6.18, 6.19, 6.20).

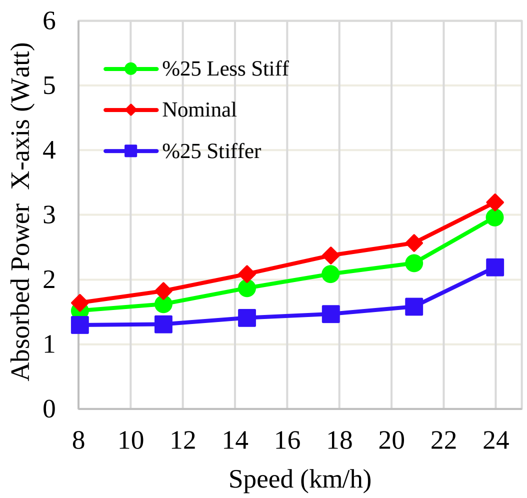

Figure 6.18 : The absorbed power results of the driver seat base as a function of vehicle speed on phase angle 90° road in the x-axis with different suspension stiffness.

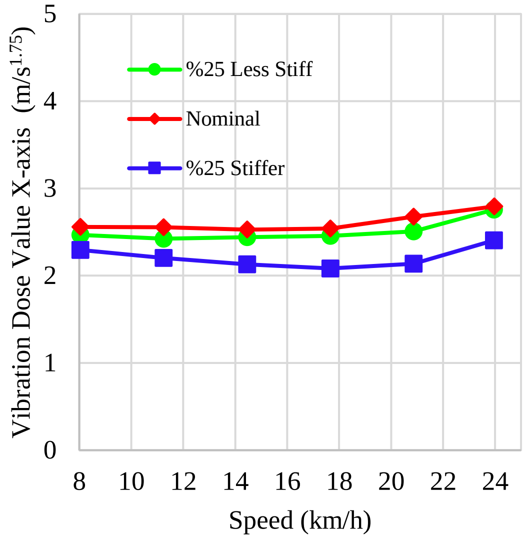

Figure 6.19 : The vibration dose value results of the driver seat base as a function of vehicle speed on phase angle 90° road in the x-axis with different suspension stiffness.

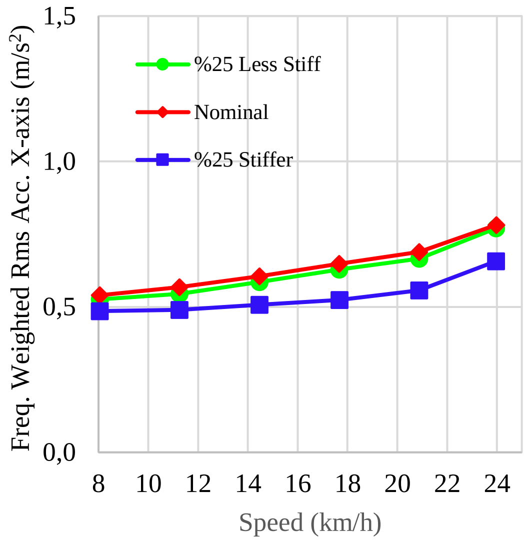

Figure 6.20 : The freq. weighted rms acc. results of the driver seat base as a function of vehicle speed on phase angle 90° road in the x-axis with different suspension stiffness.

6.1.2 Discussion on effects of different spring stiffness

As a result of the analysis, it was determined that the suspension change showed different results on the ride quality on symmetrical and asymmetrical roads. Since the ride height does not change in the symmetrical road, the suspension stiffness change effect is not observed in the z-axis. While the vibration evaluation values increase and the comfort and ride quality decrease as the suspension stiffness value increases on the asymmetrical road. It is thought that the reason for this is that the vehicle's suspension system can adjust the ride height via the air bellows. It is considered that this effect varies in different suspension types.

When the analysis results are examined on the y-axis, the effect caused by the change in the suspension stiffness value on the 5,08 cm rms rough road could not be detected. On the road with a phase angle of 90°, the lateral force and motion between the two wheels are high due to the coherence function. Since the lateral force effect is high, the suspension stiffness change’s effect is visible on the road with the 90° phase angle. Here, this effect increases linearly depending on the speed in the absorbed power evaluation method, but different results are obtained at low and high speeds in other evaluation methods.

When the analysis results are examined on the x-axis, the change effect in the suspension stiffness value was observed on the 5,08 cm rms rough road. The higher suspension stiffness value means lower ride quality. On the road with a phase angle of 90°, an effect was detected due to the change in the suspension stiffness value different from a 5,08 cm rms rough road. It is seen that the vehicle with nominal suspension stiffness has the lowest ride quality in all evaluation methods.

The most sensitive suspension stiffness change is observed with the absorbed power evaluation method when the evaluation methods are examined.

Vehicle suspension types should be considered when observing the spring stiffness changes in ride quality evaluation. While making these judgments for the spring characteristic's effect on ride quality, it will be necessary to repeat the analysis for other suspension types.

6.2 The Effects of Different Damping Coefficient on Ride Quality

6.2.1 Simulation results of the effects of the different damping coefficient

Two vehicle models were created with high and low damping coefficient values. The FED-Alpha vehicle model is modeled as a transfer function in ADAMS Car software. The damping force value is changed by doubling the coefficient of the transfer function and reducing it by half. Vehicle models were analyzed on roads with 90° phase angle and 5,08 cm rms roughness at different speeds, and the driver accelerations were collected. The accelerations affecting the driver were analyzed in three axes with the help of SIMULINK using the absorbed power, vibration dose value and frequency weighted rms acceleration evaluation methods.

The relationship between damper force and damper speed is not linear in the FED-Alpha vehicle, especially at rebound low-frequency characteristics. However, the damper has a different characteristic during the compression and rebound movement. The damper used in the FED-Alpha vehicle has different force-velocity graphs at high and low frequencies (Figure 6.21).

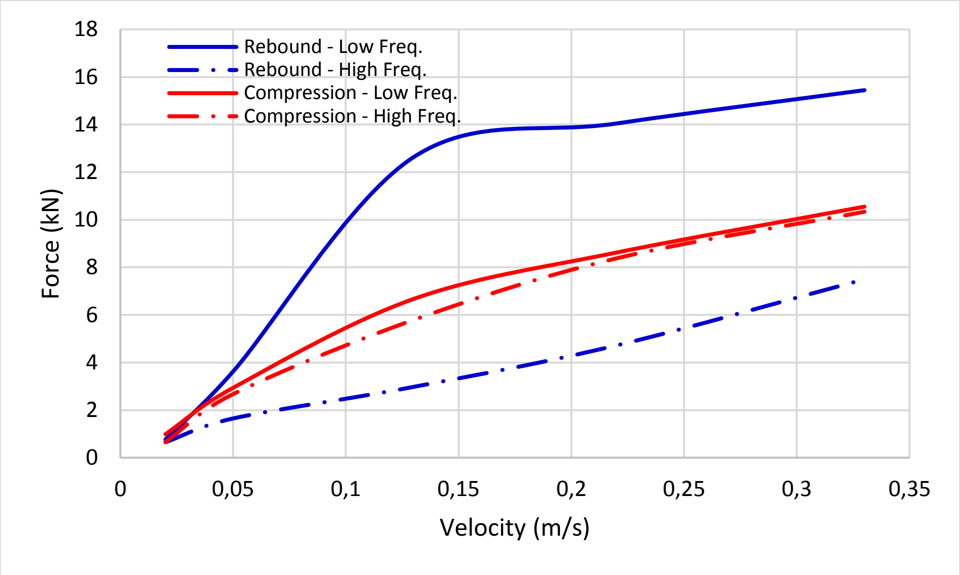

Figure 6.21 : Rebound and compression damper force-velocity graph at low and high frequency for the nominal damper.

The vibration evaluation values in the z-axis increase and the ride quality decrease with the vehicle speed increase in all evaluation methods. Despite the increase in speed, the results of the absorbed power values increased with higher acceleration than the other evaluation methods. Therefore, it can be concluded that the absorbed power method is a more suitable method for examining the ride quality values compared to the speed increase.

In all evaluation methods, growth in the increased speed was observed at around 18 km/h in the less damping curve. The reason is expected to be the transition of the damper curve from the low-frequency characteristic to the high-frequency characteristic.

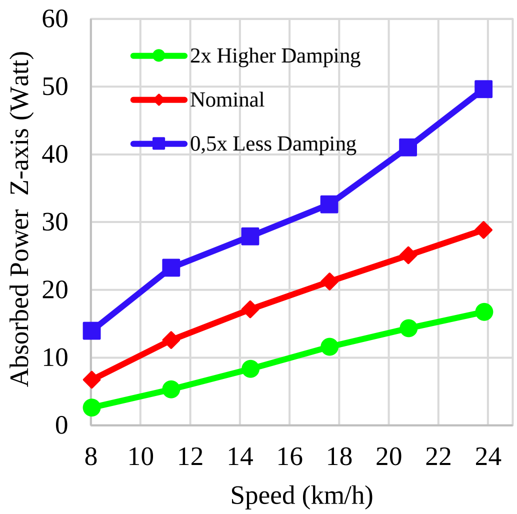

Figure 6.22 : The absorbed power results of the driver seat base as a function of vehicle speed on 5,08 cm rms road in the z-axis with different damping coefficients.

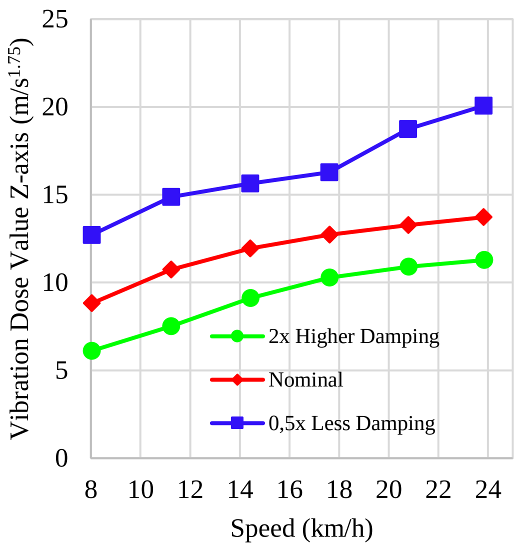

Figure 6.23 : The vibration dose value results of the driver seat base as a function of vehicle speed on 5,08 cm rms road in the z-axis with different damping coefficients.

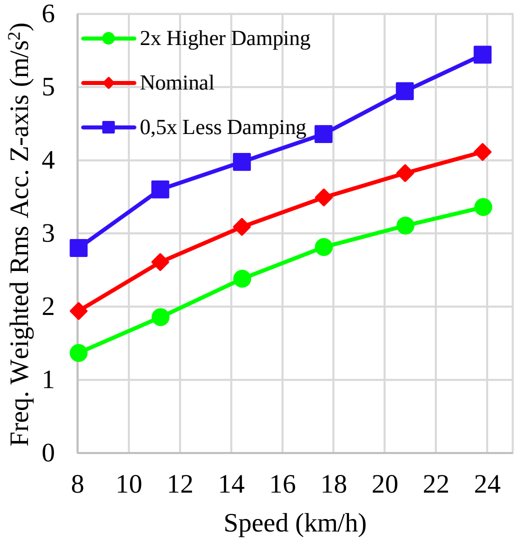

Figure 6.24 : The freq. weighted rms acc. results of the driver seat base as a function of vehicle speed on 5,08 cm rms road in the z-axis with different damping coefficients.

When the acceleration values in the z-axis are examined in the frequency domain, it is seen that the sprung mass acceleration values of the vehicle with less damping are maximum at high frequency. Since the damping coefficient is low, it is thought that the acceleration amplitude values are higher in the less damping characteristic (Figure 6.25).

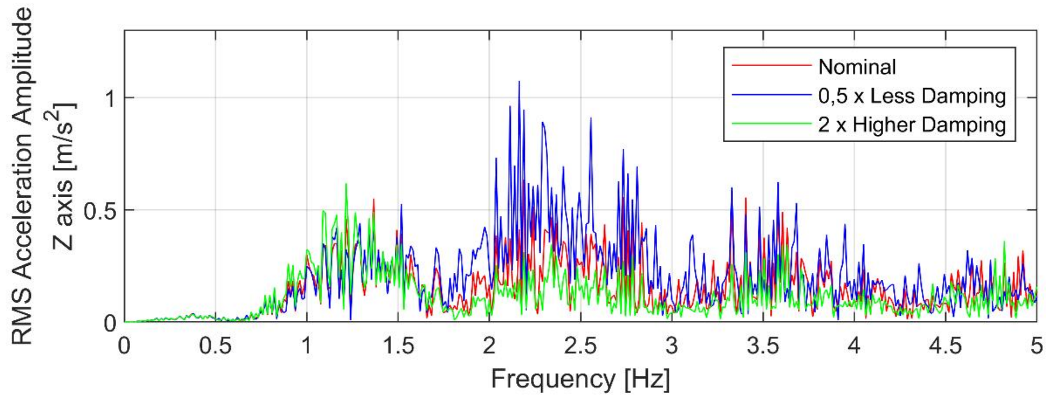

Figure 6.25 : Rms Acceleration graph on 5,08 cm rms different damping coefficients at 14,43 km/h.

As a result of the analyzes on the y-axis on the road with 5,08 cm rms roughness, the same results came up in all evaluation methods. It has been determined that the ride quality is lower with the less damping characteristic, and the ride quality is higher with the higher damping characteristic. There is no difference in all vibration evaluation values for vehicles with nominal and higher damping depending on vehicle speed. As the vehicle's speed increases with the less damping characteristic, the ride quality decreases, and the comfort decreases (Figure 6.26, 6.27, 6.28). When looking at the analysis results on the y-axis, it can be said that the lateral forces increase in the vehicle with the less damping characteristic. It can be shown that the reason the damping decreases and the lateral body movements of the vehicle increase against the disturbing effect from the road.

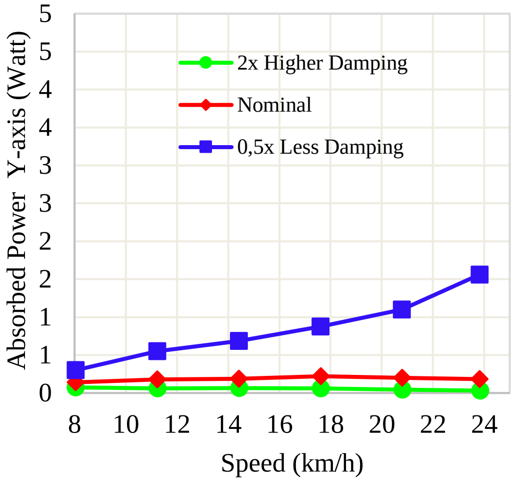

Figure 6.26 : The absorbed power results of the driver seat base as a function of vehicle speed on 5,08 cm rms road in the y-axis with different damping coefficients.

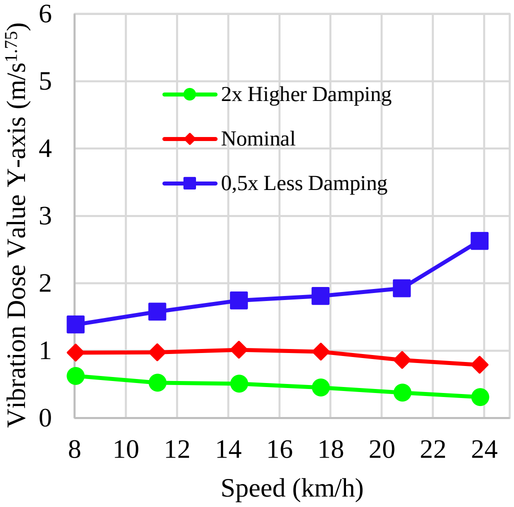

Figure 6.27 : The vibration dose value results of the driver seat base as a function of vehicle speed on 5,08 cm rms road in the y-axis with different damping coefficients.

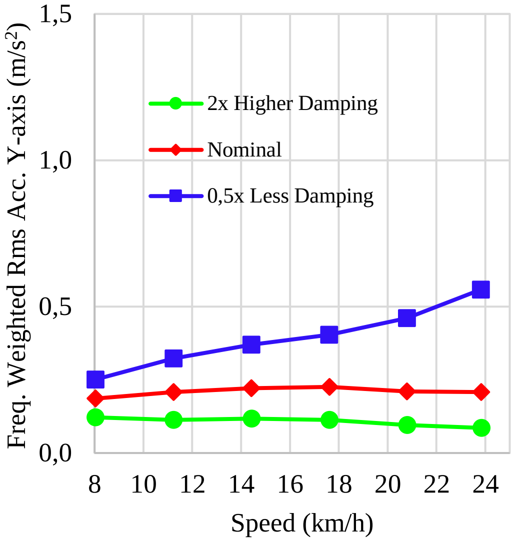

Figure 6.28 : The freq. weighted rms acc. results of the driver seat base as a function of vehicle speed on 5,08 cm rms road in the y-axis with different damping coefficients.

As a result of the analyzes made on the x-axis, it was determined that the vibration evaluation values of the vehicle with the less damping characteristic were the highest, so the ride quality was the lowest. Ride quality evaluation metrics show the same results in all methods. However, the absorbed power method has the highest response to increasing speed. It is seen that there is a change in the vibration evaluation values of the vehicle at 21 km/h speeds. While the vibration evaluation values decrease to 21 km/h with nominal and high damping characteristics, it increases after 21 km/h. Opposite this conclusion, while the vibration evaluation values with the less damping characteristic tend to increase up to 21 km/h, it tends to decrease after this speed. It is thought that the reason for this is that the defined damper characteristic with the function that carries the different force-speed graph after this speed (Figure 6.29, 6.30, 6.31).

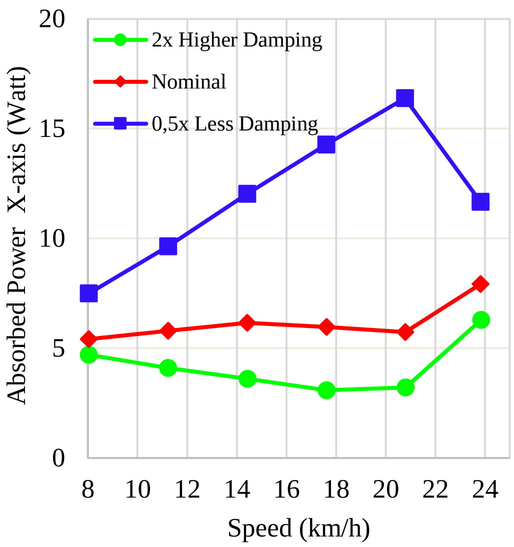

Figure 6.29 : The absorbed power results of the driver seat base as a function of vehicle speed on 5,08 cm rms road in the x-axis with different damping coefficients.

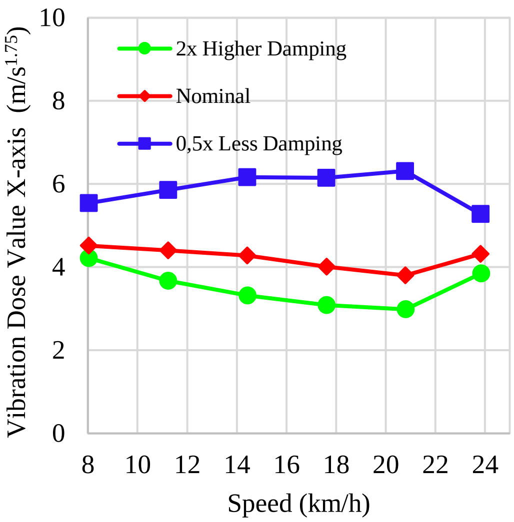

Figure 6.30 : The vibration dose value results of the driver seat base as a function of vehicle speed on 5,08 cm rms road in the x-axis with different damping coefficients.

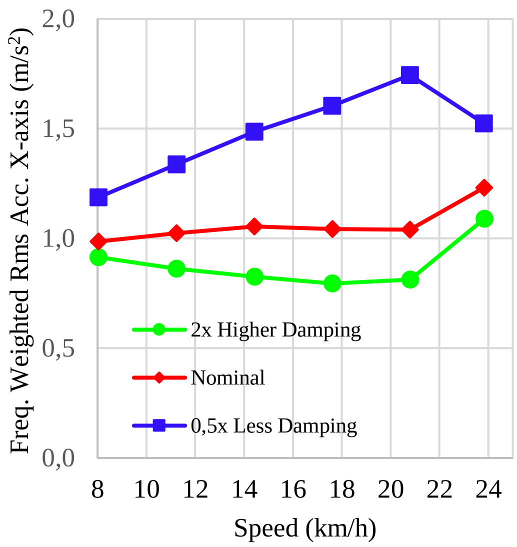

Figure 6.31 : The freq. weighted rms acc. results of the driver seat base as a function of vehicle speed on 5,08 cm rms road in the x-axis with different damping coefficients.

Analysis results for the roads with a phase angle of 90° are the same as the roads with 5,08 cm rms roughness for the z-axis. The vibration evaluation values are higher with less damping characteristics. As the speed of the vehicle increases, the vibration evaluation values increase in all damper types. Similar results are found in all evaluation methods according to increased speed. It is found that the absorbed power method is the method that showed the most response to the speed increase (Figure 6.32, 6.33, 6.34).

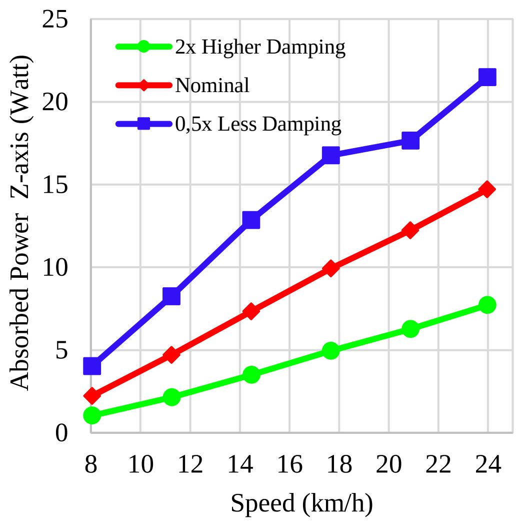

Figure 6.32 : The absorbed power results of the driver seat base as a function of vehicle speed on phase angle 90° road in the z-axis with different damping coefficients.

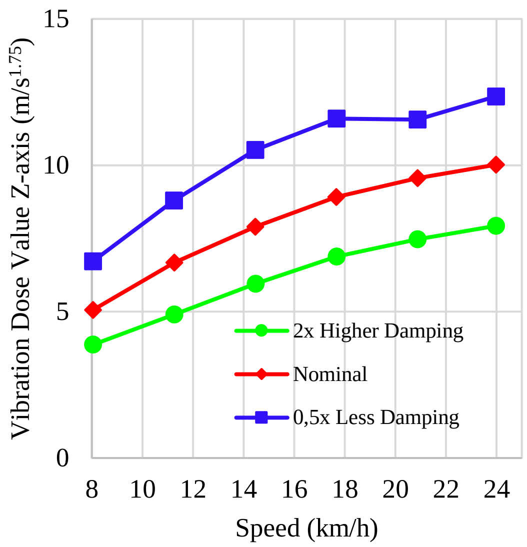

Figure 6.33 : The vibration dose value results of the driver seat base as a function of vehicle speed on phase angle 90° road in the z-axis with different damping coefficients.

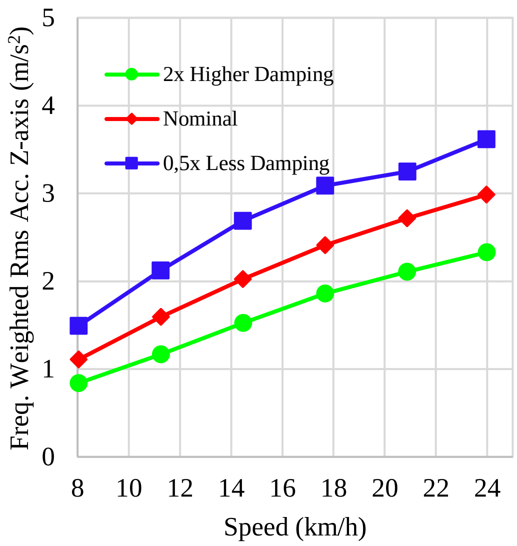

Figure 6.34 : The freq. weighted rms acc. results of the driver seat base as a function of vehicle speed on phase angle 90° road in the z-axis with different damping coefficients.

When we examine the rms acceleration amplitude values in the z-axis in the frequency domain, it is seen that the acceleration amplitude values affecting the driver are the highest in the vehicle with the less damping characteristic. It has been determined that the maximum amplitude values are in the 2,5 Hz region for the less damping characteristic and 1,2 Hz for the higher damping characteristic (Figure 6.35).

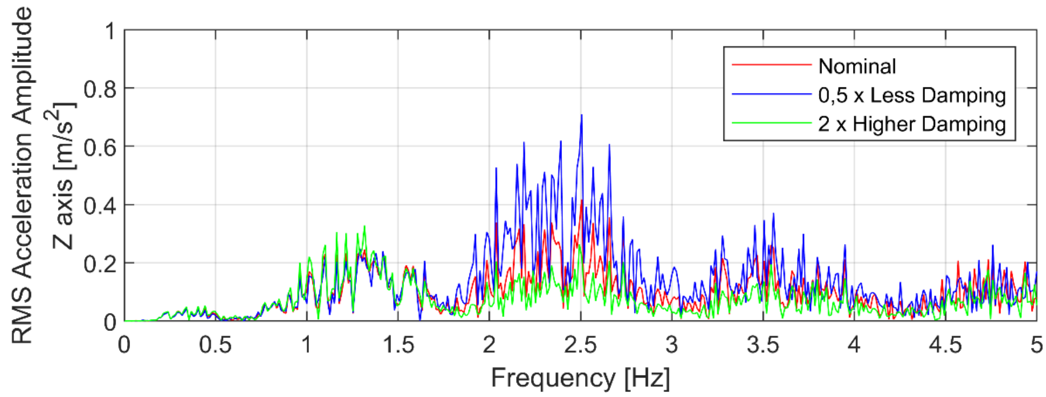

Figure 6.35 : Rms Acceleration graph on phase 90° different damping coefficients at 14,43 km/h.

As a result of the analyses on the y-axis, it is deduced that the vehicle with a less damping characteristic has the lowest ride quality. Depending on the increase in the vehicle's speed, there is an increase in the vibration evaluation values. But vibration evaluation values have different increase trends at different speed ranges. The reason for the trend difference can be defined as the damper function behaving differently at different frequencies (Figure 6.36, 6.37, 6.38).

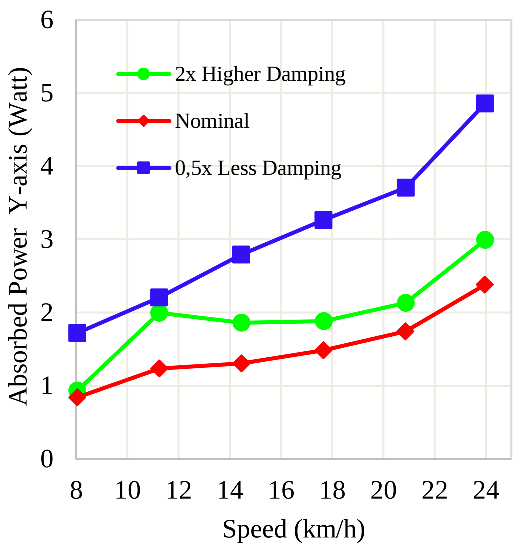

Figure 6.36 : The absorbed power results of the driver seat base as a function of vehicle speed on phase angle 90° road in the y-axis with different damping coefficients.

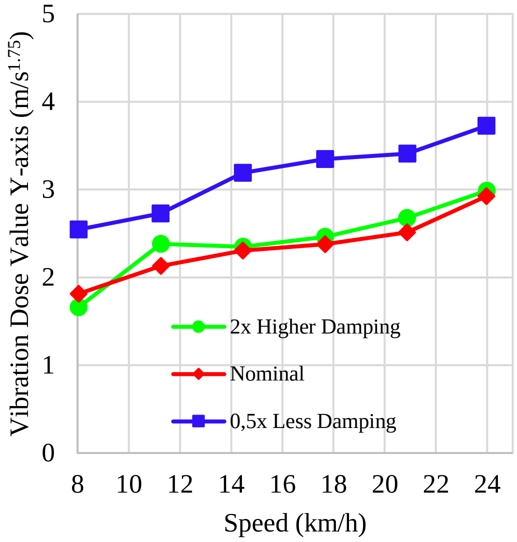

Figure 6.37 : The vibration dose value results of the driver seat base as a function of vehicle speed on phase angle 90° road in the y-axis with different damping coefficients.

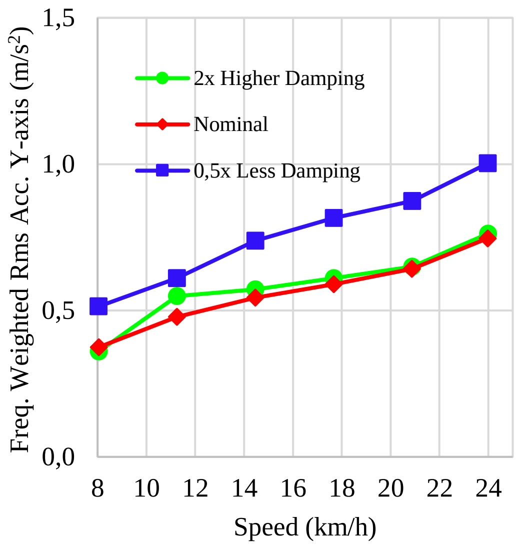

Figure 6.38 : The freq. weighted rms acc. results of the driver seat base as a function of vehicle speed on phase angle 90° road in the y-axis with different damping coefficients.

It can be deduced that the lateral forces increase when the damper transfer function is changed, so the handling characteristics deteriorate. Roads with a large phase angle result in large body lateral motion and lateral load transfer. According to the analysis results, it is predicted that the higher damping characteristic is the best before the deterioration.

As a result of the analysis studies carried out on the x-axis, it was determined that the less damping characteristic had the highest values in the vibration evaluation. The higher damping characteristic had the lowest values in the vibration evaluation. Considering the increase in the vibration evaluation values depending on the vehicle's speed, the increase in the speed of the frequency weighted rms acceleration and vibration dose value methods is too small can be ignored. Especially in nominal and higher damping, no effect is observed depending on the speed. However, in the absorbed power evaluation method, an increase is observed according to the speed. A change was observed in the damper ride quality trend in the 21 km/h speed region. While the less damping started to decrease, the nominal and higher damping increased the upward trend. It has been evaluated that the change is occurred on the damper function according to the frequency. This change will be examined in detail in the frequency domain (Figure 6.39, 6.40, 6.41).

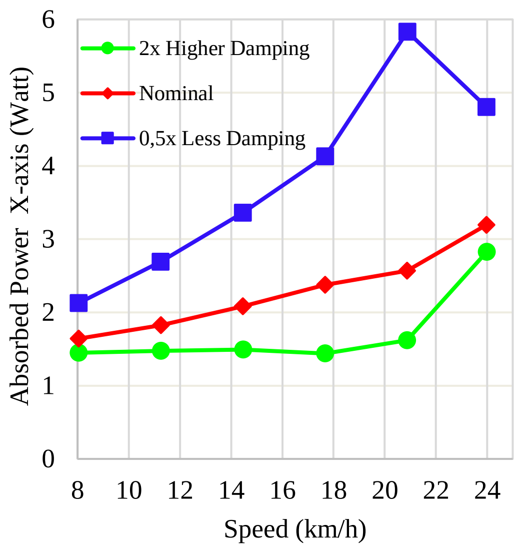

Figure 6.39 : The absorbed power results of the driver seat base as a function of vehicle speed on phase angle 90° road in the x-axis with different damping coefficients.

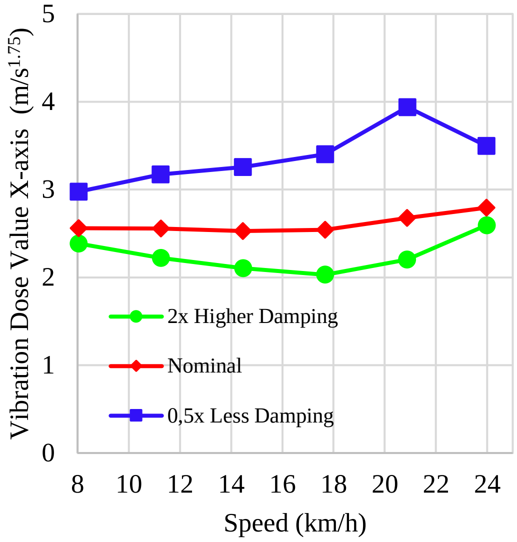

Figure 6.40 : The vibration dose value results of the driver seat base as a function of vehicle speed on phase angle 90° road in the x-axis with different damping coefficients.

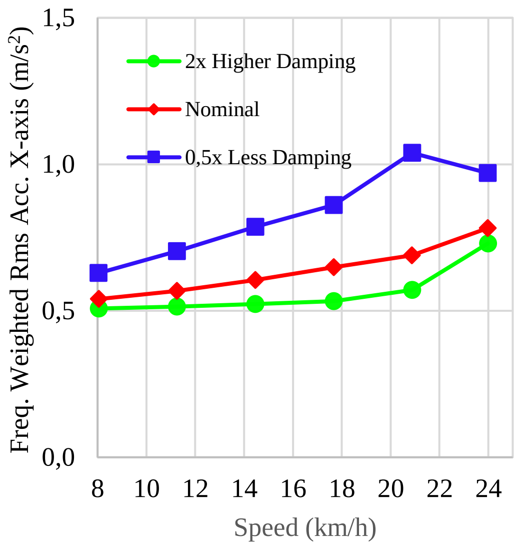

Figure 6.41 : The freq. weighted rms acc. results of the driver seat base as a function of vehicle speed on phase angle 90° road in the x-axis with different damping coefficients.

6.2.2 Discussion on effects of the different damping coefficient

As a result of the analysis, it was determined that changing the damping force-velocity graph of the damper affects the ride quality in all axes. As the damping force increases, the amplitudes of the accelerations to the driver increase, which increases the vibration evaluation values and negatively affects the ride quality. This effect was primarily seen in the z-axis.

It has been determined that the change in ride quality caused by changing the damper function on the road with the 90° phase angle and the road with 5,08 cm roughness is similar for the x and z axes. On the road with the 90° phase angle, the lateral motion are higher due to the road characteristics, so the ride quality in the y-axis is lower. With the change of the damper transfer function, the handling behavior of the vehicle is impaired. This effect is felt more on the road with a high phase angle. For this reason, the 90° phase difference was determined on the road in the vehicle with the highest ride quality with nominal damper.

Studies have shown that the damper force parameter is directly related to the ride quality.

7. CONCLUSION AND RECOMMENDATIONS

Within the scope of the thesis, absorbed power, vibration dose value and frequency weighted rms acceleration values were calculated to examine the ride quality effect of the roughness, waviness, wavenumber, phase angle on the three axes. Eventually, it was determined that changing these road characteristics resulted in the vibration evaluation value changes and ride quality being affected.

When the relationship between the absorbed power, vibration dose value, frequency weighted rms acceleration methods and vehicle speed was examined, it was determined that the vibration evaluation values in the z-axis had the same trend depending on the speed. However, this relation could not be observed for the x and y axes. This result is thought to be due to the difference in weighting function between the methods.

It is seen that the ride quality is most affected by the speed change while using the absorbed power evaluation method. The absorbed power values in the z-axis show a more significant increase with increasing vehicle speed.

A single evaluation method will be sufficient when it is desired to determine the ride quality in the z-axis. However, a single method is not sufficient when it is desired to detect the ride quality on the x and y-axis. Therefore, analyses in the frequency domain should be done and examined with ride quality evaluation methods.

Sufficient road length must be used to stabilize the ride quality metrics. In the speed profile analyses made within the scope of the thesis, it is seen that the vibration evaluation values stabilize at approximately 300 meters. Therefore, it is thought that shorter analyses will cause wrong evaluation results.

As the roughness of the road increases, the ride quality gets worse in all evaluation methods. Likewise, as the speed of the vehicle increases, the ride quality decrease at the z-axis in all evaluation methods.

It has been determined that the ride quality in the z-axis is affected by the wavenumber bandwidth change. The ride quality increases when the road has a wider bandwidth at low wavenumber range. Because road harshness decreases with bandwidth increase at low wavenumber. The road with narrow bandwidth at low wavenumber range and wider bandwidth at high wavenumber range for the z-axis has the lowest ride quality. Because the vibration evaluation values increase with a higher trend as the vehicle's speed rises on narrow bandwidth at high wavenumber road. Also, ride quality metrics in the x-axis are affected by wavelength bandwidth change. In line with these determinations, it is thought that the wavenumber bandwidth of the road should be restricted in standards or reported in analyses and tests.

The inverse slope of the PSD plot of the road is defined as waviness. As the waviness increases, the power density values of the high wavenumber components of the road decrease. For this reason, as the waviness increases in the z-axis, the ride quality increases. Likewise, it has been determined that the waviness value of the road should be restricted in the standards.

The phase angle of the road affects the ride quality in the all axes. Therefore, when the roads with phase angle between the right and left tires are compared, the ride quality values will be very different even if they have the same roughness, waviness and wavenumber values. For this reason, it is necessary to report the phase angle when defining the road to be analyzed.

The speed deviation from the mean speed is restricted in the absorbed power evaluation standard. The speed deviation changed more than the speed coefficient of variation value defined in the standard to examine the effect of speed deviation. As a result of the analyses made, it was determined that there was no change in the absorbed power values as long as the vehicle's average speed was maintained. However, this determination needs to be supported in different vehicle models. Unfortunately, it is thought that this determination will not make the test easier. Even if it is thought that the deviation from the average speed is not essential, it is necessary to provide the average speed. Yet it is still difficult for the driver to achieve.

7.1 Practical Application of This Study

Within the scope of the studies, it has been determined that the absorbed power, vibration dose value or frequency weighted rms acceleration calculations defined in the standards are sufficient to evaluate the ride quality in the z-axis. In addition, it is seen that the ride quality analyses made with the ADAMS Car model, which is confirmed by the test results, will be sufficient for optimization.

7.2 Future Recommendations

The studies carried out within this thesis gave satisfactory results only for the ride quality in the z-axis. However, it was concluded that the ride quality evaluation methods are not sufficient to determine the ride quality in the x and y axes. The ride quality effects on these axes should be analyzed in the frequency domain.

It was concluded that the road length analyzed should be at least 300 meters for stabilizing the ride quality evaluation values. It is considered beneficial to conduct analyses with roads of different lengths to support this result.

It has been determined that the deviation in speed does not affect the absorbed power values in the z-axis as long as the average speed is kept constant. However, analyses of other vehicles are needed to support this finding.

Within the scope of the thesis, all analyzes were made with a light class wheeled vehicle. However, analyses should be made with vehicles with a higher weight class and a longer wheelbase, and the results should be supported.

REFERENCES

[1] **Aberdeen Test Operations Procedure,** (2011). 01-1-014A Ride Dynamics and Evaluation of Human Exposure to Whole Body Vibration, 29 November 2011

[2] **SAE J1060,** (2014). Subjective Rating Scale for Evaluation of Noise and Ride Comfort Characteristics Related to Motor Vehicle Tires, May

[3] **BS ISO 8606,** (2016). Mechanical vibration — Road surface profiles — Reporting of measured data, 01 November 2016

[4] **Deusen, Van, D., Bruce,** (1974). Human Response to Vehicle Vibration

[5] **Metha, N., C.,** (1981). Subjective and Objective Ride Evaluations of Commercial Vehicles, International Congress and Exposition Cobo Hall, February 23-24

[6] **Mansfields, N., J., Lundström, R., Holmlund, P.,** (2000). Comparison Of Subjective Responses To Vibration And Shock With Standard Analysis Methods And Absorbed Power, *Journal of Sound and Vibration* ,230(3), 477-491

[7] **Stephens, G., David,** (1974). Development and Application of Ride Quality Criteria, NASA-Langley Research Center, NASA TM X-72008

[8] **Kumar, K., Senthill, Pal, S., Sethi, R., C.,** (1999). Objective Evaluation of Ride Quality of Road Vehicles, Symposium on International Automotive Technology

[9] **Holmlund, P.,** (1999). Absorbed Power and Mechanical Impedance of the Seated Human Measured Within a Real Vehicle Environment Compared with Single Axis Laboratory Data, *Journal of Low Frequency Noise, Vibration and Active Control*, Vol. 18 No.3

[10] **Healey, J., Anthony, McGehee, Y. David, Smith, C., Craigh,** (1976). The Prediction of Passenger Riding Comfort from Acceleration Data, Department of Transportation Office of University Research Washington

[11] **Strandemar, Katrin,** (2005). On Objective Measures for Ride Comfort Evaluation, Automatic Control Department of Signals, Sensors and Systems Royal Institute of Technology (KTH)

[12] **Keenan, E., Robert,** (1973). Effects of Terrain Power Spectral Density Shaping and Measurement Interval On A Vehicle Ride Simulator, National Technical Information Center, (Report No: OAAE-O7-69-O356), Department of Defence

[13] **Pradko, Fred, and Lee, A., Richard,** (1966). Vibration Comfort Criteria, Society of Automotive Engineers, January 10-14

[14] **Pradko, Fred, and Lee, Richard, A.,** (1968). Analytical Analysis of Human Vibration, *SAE Transactions*, Vol. 77, Section 1: Papers 680005–680246 (1968), pp. 346-370

[15] **Pradko, Fred, Lee, A., Richard., Kaluza, V.,** (1966). Theory of Human Vibration Response, DTIC document, U.S. Army-Tank Automotive Center, Warren, MI, USA, 1966.

[16] **BS ISO 2631-1** (1997). Mechanical Vibration and Shock Evaluation of human exposure to whole-body vibration, 15 July 1997

[17] **Dell, J., Grote, P., Handrickx, P., Mergay, M., Little., E.,** (1999). Ride Comfort Analysis : Practice and Procedures, Symposium on International Automotive Technology

[18] **Bao, C., Deng, G., Tang, A. Tian, J.,** (2011). The Analysis of Applicability of Ride Comfort Standards to Vehicles, M. Zhou and H. Tan (Eds.): CSE 2011, Part II, CCIS 202, pp.269-275

[19] **Els, P., S.,** (2004). The applicability of ride comfort standards to off-road vehicles, *Journal of Terramechanics*, 42,47–64

[20] **Durst, J., Phillip, Baylot, A., Mason, L., George, McKinley, Burney,** (2015). A General Model For Inferring Terrain Surface Roughness As A Root-Mean-Square To Predict Vehicle Off-Road Ride Quality, Int. J. Vehicle Design, Vol. 64, Nos. 2/3/4

[21] **Mucka Peter** (2009). Effects Of Longitudinal Road Waviness On Vehicle Vibration Response, Vehicle System Dynamics, Vol. 47, No. 2, pp. 135-153

[22] **Cenek, P., D., Fonk, S., Mcların, W., M.,** (1968). Wavelength Analysis Of State Highway Longitudinal Profiles, *Transfund New Zealand Research Report* (Report No: 153), pp. 44

[23] **Elmann, A., Mill, T., Uueküla, K., Joala, V.,** (2011). Road Surface Surveying Usıng Terrestrial Laser Scanner And Total Station Technologies, The 8th International National Environmental Conference, May 19-20

[24] **Lee, A., Richard., Cumbow, J.,** (1978). Absorbed Power Ride Measurement Instrument, Taradcom Laboratory Technical Report, (Report No: 12415)

[25] **Smith, Julian, Happian,** (2002). An Introduction to Modern Vehicle Design, Oxford: Reed Educational and Professional Publishing Ltd.

CURRICULUM VITAE

Name Surname **:** Hande Tütüncü Çalkan

EDUCATION **:**

- **B.Sc.** **:** 2015, Marmara University, Mechanical Engineer

PROFESSIONAL EXPERIENCE AND REWARDS:

- 2015-2018 TÜMOSAN Motor Sanayi A.Ş.
- 2018-2020 Anadolu Isuzu A.Ş.
- 2020 FNSS Defence Company